MPHIL

Structured Catalyst Support Systems

Zhao, Chen

Award date:
2013

Awarding institution:
University of Bath

Structured Catalyst Support Systems

Chen Zhao

A thesis submitted for the degree of Master of Philosophy

University of Bath

Department of Chemical Engineering

September 2013

Abstract

By coating supports with an alumina sol-gel, which is then immersed in liquid nitrogen, freeze-dried and subsequently calcined, it has been confirmed (with scanning electron microscopy) that leaf-like structures with nano-thin walls can be formed from alumina. This work confirms that similar structures can be formed to the KK leaves described in the literature. By exploring different preparation techniques, it is confirmed that to form such leaf-like structures, the steps consisting of: immersion in liquid nitrogen, freeze-drying and calcination, are all essential.

Using these techniques, coating methods with a silica sol-gel are also explored, and when cordierite ceramic monoliths were coated, some exciting structures consisting of plates, leaves and tunnels with nano-thin walls were formed which could have commercial applications.

Adopting these novel coating procedures, 3.2 mm wire-mesh Dixon rings (used as a packing in a gas scrubbing column) were also successfully coated with sol-gels made from alumina and also silica. These coated 3.2 mm rings were then impregnated with a carbonic anhydrase enzyme, to test if the presence of the enzyme (acting as a catalyst) could increase the overall rate of CO_2 removal from a gaseous stream in a small gas scrubber. A very small improvement was observed but this requires further work to confirm its viability.

Chapter 1 Introduction

Chapter 2 Freeze-drying techniques

Chapter 3 Preparation of freeze dried structures

Chapter 4 Enzyme immobilization on Dixon rings

Chapter 5 Conclusions and recommendations

Chapter 1 Introduction

1.1: Background

1.1.1 Introduction to freeze-drying

Freeze-drying is a well-established process, which is already used in many commercial applications. For example in:

(a) Pharmaceutical and biotechnology industries: to increase the shelf life of products such as vaccines and other injectables (Mellor (1978)).

(b) Food industry: products used by the military or by campers as they can be preserved and kept very light (King (1971)).

(c) Technical applications: products can be made more stable, and can also be more easily dissolved in water. Heat sensitive materials may be preserved, for example, proteins, enzymes, micro organs and blood plasma (Mellor (1978)).

Freeze-drying is also known (e.g. Oetjen and Haseley, 2004, p.1) as lyophilisation, which is a drying process in which the solvent and /or the suspension medium is crystallized at low temperatures, and thereafter sublimed from the solid state directly into the vapour phase. In a number of applications water is used as a solvent, and in Figure 1.1 a phase diagram is presented, to illustrate areas where the transfer from the solid to the vapour phase is possible. The drying transforms the ice or water in an amorphous phase into vapour. Owing to the low vapour pressure of the ice, the vapour volumes become large, as can be seen in Figure 1.2. During the second step of the drying, the water adsorbed on the solids is desorbed.

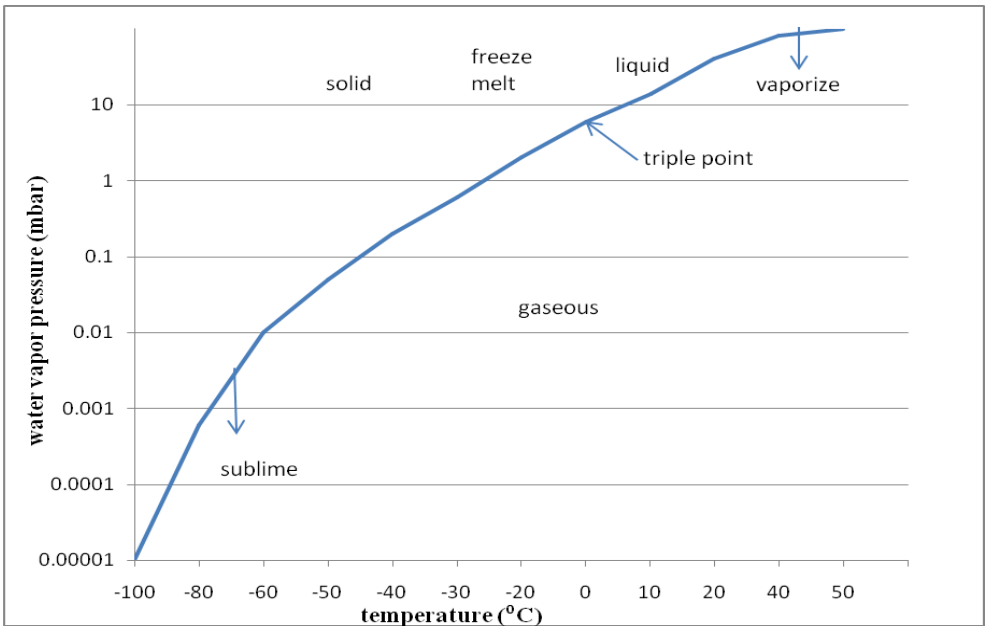

Figure 1.1 Phase diagram for water (adapted from Oetjen and Haseley, 2004, p.1).

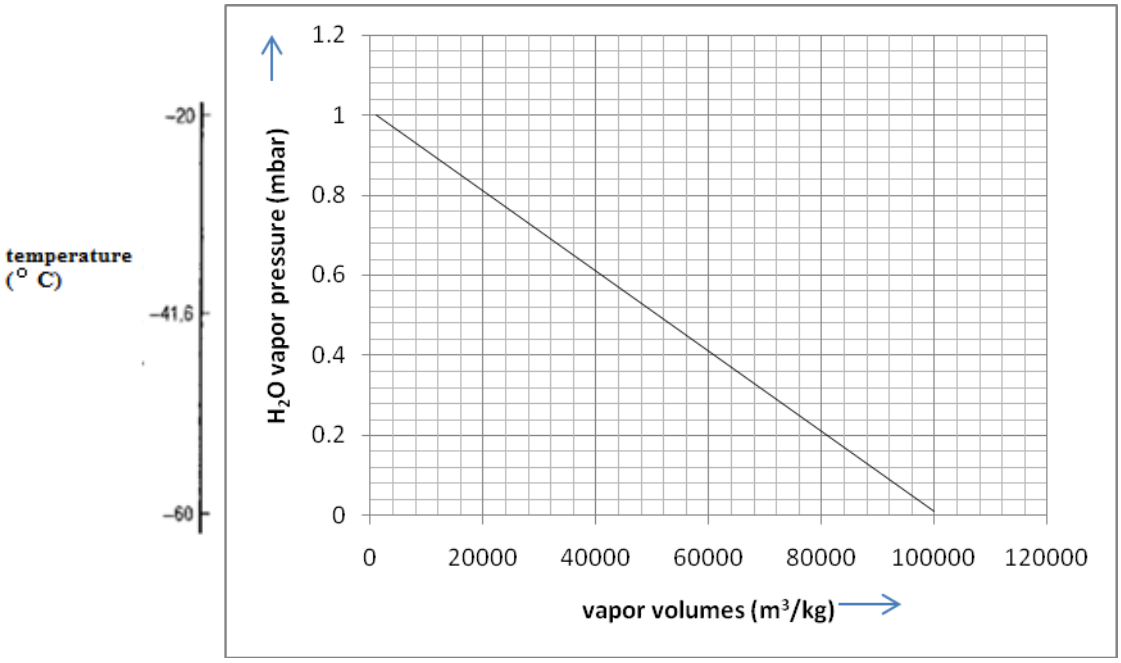

Figure 1.2 Specific volume of water vapour as a function of the water vapour pressure. The temperature of the vapour in this diagram is that of ice (adapted from Oetjen and Haseley, 2004, p.2).

Based on information presented in Chen and Wang (2007), the three main steps in a freeze-drying process consist of:

Step 1 Freezing: An aqueous solution or slurry is frozen to a solid state. The freezing can be carried out by immersing in liquid nitrogen, placing on a cold plate of regulated temperature, or spraying into a flow of chilly gas. The freezing rate would influence the sublimation rate and the final quality of the dried product. In general a slow freezing rate shortens the sublimation of large ice crystals, whereas a fast freezing rate avoids aggregation and recombination of nanoparticles.

Step 2 Primary Drying: In this step the frozen solvent, mostly ice, is sublimated. This sublimation can be achieved by reducing the pressure to a value below the triple point, or by using an ultra-dry gas with a vapour pressure below the value of the triple point. The key parameter to monitor is the collapse temperature, which is the upper value of operation during sublimation.

Step 3 Secondary Drying: In this step the bound water or solvent that was not frozen is desorbed. This part of drying is similar to the last stage of an ordinary drying process. The drying temperature can be higher than the freezing point of the solvent but has to be below the glass transition temperature of the matrix. The vacuum level can be even lower than that of the primary drying step.

The following were listed (Oetjen and Haseley, 2004, pp. 2) as advantages of freeze-drying:

- Drying at low temperatures reduces degradation of heat sensitive products.
- The liquid product can be accurately dosed.

- The moisture content of the final product can be controlled during the drying process.
- The dry product formed can have an appealing physical form.
- The dry product with a high specific surface area can be rapidly reconstituted.

The following disadvantages were highlighted:

- Investment, operating and maintenance costs can be high.
- The complexity of the process and the equipment requires a team of skilled individuals.

According to Chen and Wang (2007): over 100 years ago, Bordas and d'Arsonval demonstrated for the first time that a delicate material can be dried under vacuum conditions in its frozen state. In their literature review, they state:

> Freeze-drying is known for its slow drying rate, high operating cost, and low energy efficiency in comparison with other ordinary drying technologies such as spray drying, fluid bed drying, rotary drying, etc. Because of these disadvantages, freeze-drying was applied mainly in the dehydration of high value products such as pharmaceuticals and bio-products. In drying of food-related products, freeze drying is more often than not referred to as a benchmark for quality comparison. This scenario has witnessed some changes in the past decade with the rapid development of nanotechnology. Freeze-drying has become a simple and economical operation to produce nano-sized materials.

1.1.2 Freeze drying in catalytic applications

The technique has been used in a number of applications to catalyst systems. For example: Vargas *et al*. (2004) studied the textural properties of Al_2O_3-TiO_2 mixed oxides which had been synthesized by the aqueous sol method. They found that the porous properties of Al_2O_3-TiO_2 depend on the drying procedure. In a conventional air static oven this led to a multimodal pore size distribution (PSD), whereas the freeze drying method gave rise to samples with a uni-modal PSD. Freeze-drying can be advantageously used in catalysis since it allows the preparation of mixed oxides with specific pore size distributions and larger surface areas. In the case of Al_2O_3-TiO_2 mixed oxides, they obtained mesoporous materials with a narrow single mode PSD which is an important feature to be taken into consideration for the preparation of catalytic supports.

According to Mamchik *et al.* (1998), aluminium oxide powders are widely used in various solid-state materials such as adsorbents and catalysts. One of the main methods for the preparation of these materials is thermal decomposition of aluminium hydroxides. Depending on the conditions of precipitation and further decomposition (see Figure 1.3), various mechanisms of dehydration can be observed.

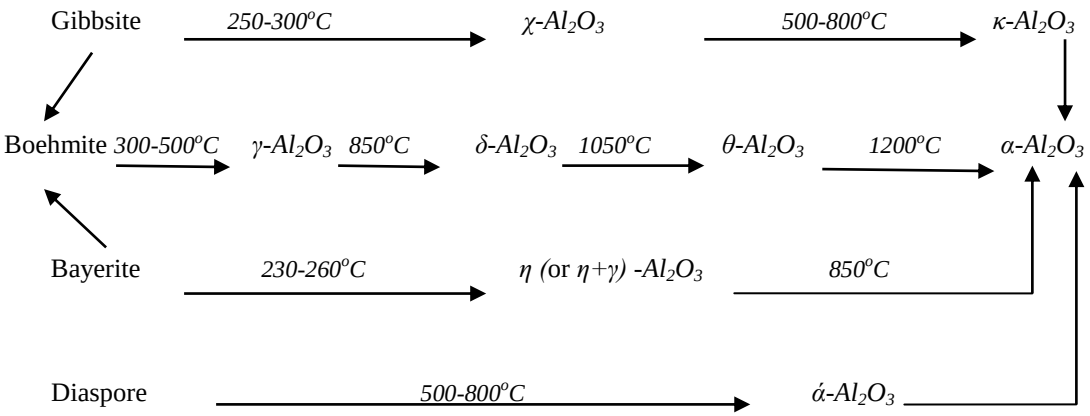

Figure 1.3 Transformations of aluminium oxides (adapted from Mamchik *et al.*, 1998).

Mamchik *et al.* (1998) studied cryosol synthesis of nanocrystalline alumina. They found that the freeze-drying process led to high uniformity of the particle sizes, which was due to the thermal stability of the freeze-drying process. The uniformity of the particles' size was predetermined by the method of the synthesis. The freeze-drying fixed the structures prepared in a colloid solution and converted them into the solid state without significant change.

Su *et al.* (2000) investigated the synthesis of isobutene from synthesis gas over nanosize zirconia catalyst. They found that the surface properties of the acid-base sites depend on the preparation method. Freeze-drying technology was one of the techniques that they studied. Their results showed that the crystal phases, acidic and basic properties of nanosize zirconia depend to a remarkable extent on the drying conditions. .

Nishihara *et al.* (2006) studied the preparation of monolithic SiO_2-Al_2O_3 cryogels with inter-connected macropores through ice templating. They said that, "forming mico/mesoporous materials into desirable shapes is extremely effective to enhance their performance in practical applications". Macropores were generated by using ice crystals as the template, while the walls which surround the macropores were tailored as porous cryogels by freeze-drying. Macropores and walls formed honeycomb-like structures, which were confirmed from scanning electron microscopy images of cross-sections of the samples. Forming micro/mescoporous materials into desirable shapes is extremely effective to enhance their performance in practical applications.

Kolaczkowski and Kim (2006), whilst exploring different methods of coating ceramic monoliths with a γ-alumina washcoat (in which a catalyst could be dispersed), discovered that by using a freeze-drying technique, they were able to produce a distinct leaf-like structure

consisting of γ-alumina, which was at a nano-scale, and could be beneficial in many applications (e.g. as a catalyst support). They described these structures as 'KK leaves' and these are compared with conventional washcoated structures in Figure 1.4.

As can be seen in the above examples, typical literature shows that freeze-drying technology could be a topic to study in order to understand the mechanism of forming nano-sized structures, and also to investigate applications where such structures could act as catalytic supports.

From this section, it is clear that freeze-drying methods have been used to create nano-sized structures (particles and leaves), which in turn leads to a number of interesting new applications.

1.1.3 Preparation of gamma alumina (γ-Al_2O_3) using a sol-gel method

In many catalytic applications, γ-Al_2O_3 is often encountered as a catalyst support. For example:

(a) Selective catalytic reduction of NO_X with NH_3 applied to reduce the emission of nitrogen oxides from mobiles or stationary sources (e.g. Cao *et al.* 2012).

(b) Catalytic converters to control exhaust emissions from vehicles (e.g. Irani *et al*. 2005).

(c) Catalytic methane cracking in a fluidized bed reactor for hydrogen production (e.g. Amin *et al.* 2012),

When used as a catalyst support, γ-Al_2O_3 can be formed *via* a sol-gel process (and other methods). A sol is a colloidal suspension of solid particles in a liquid phase. Sol-gel chemistry

is based on inorganic polymerization reactions. Two routes can be considered, depending on whether the precursor is an aqueous solution, or an alkoxide in an organic solvent. According to Edward *et al.* (1995), the reaction can be described as follows (where M represents a metal cation):

1) Hydroxylation of anionic oxo-ions:

$$MO_n^{x-} + H^+ \rightarrow H\ MO_n^{\{x-1\}-}$$

The hydroxylation of alkoxides is simply performed via hydrolysis by adding water.

$$M(OR)_n + H_2O \rightarrow M(OH)(OR)_{n-1} + ROH$$

2) Condensation then follows olation and oxolation:

Olation:

$$M\text{-}OH + M\text{-}OH_2 \rightarrow M\text{-}O\text{-}M + H_2O$$

Oxolation:

$$M\text{-}OH + HO\text{-}M \rightarrow M\text{-}OM + H_2O$$

$$M\text{-}OH + RO\text{-}M \rightarrow M\text{-}O\text{-}M + ROH$$

In both cases hydroxyl and oxygen bridges are formed leading to condensed species. At the end all oxygen atoms are bridging oxygen and a hydrated oxide network is formed.

Kolaczkowski and Kim (2006): described a method of preparing alumina sol gel to make 'KK leaves'. The methodology is based on the advice offered in Yoldas (1975). The sol was prepared by hydrolysing an aluminium alkoxide and then it was transformed into a sol gel.

1.2 Motivation for the research

This arose from the discovery by Kolaczkowski and Kim (2006) at the University of Bath, (UK), that γ-Al_2O_3 leaf-like structures (which were named KK leaves) can be formed using the freeze-drying method. Having made that discovery, they proposed that this technique could be beneficial in the following range of applications:

(a) When coated onto the surface of a porous support, as the multi-layered structure has the ability to penetrate the larger pores in the support, it could be exploited as a surface that acts as an interface, e.g. acting as a membrane, or a support for a membrane such as palladium.

(b) A coated ceramic monolith could be used to support a wide range of different types of catalysts, e.g., auto-catalyst application.

(c) The catalyst could be incorporated into gel, and then formed onto the mechanical support.

(d) The leaf-like structure could be used as a filter to trap small particles between the leaves.

(e) The thermal inertia of this structure would be less than that of a wash-coated monolith of equivalent thickness.

(f) The thin layers of the leaf would offer less resistance to diffusion than a more conventionally formed catalytic monolith. This could result in applications where a small quantity of catalyst is used to achieve the same outcome.

(g) These fine leaf structures may find applications in the field of nanotechnology.

(h) The method of preparation (with slightly different conditions), may also produce leaf shaped structures for other materials that undergo a transition from sol to gel.

(i) The leaf like structure could be use as a filter to trap the small particles between the leaves to develop a deeper understanding of the catalyst supports and their applications.

This therefore provided the motivation to explore such prospects further.

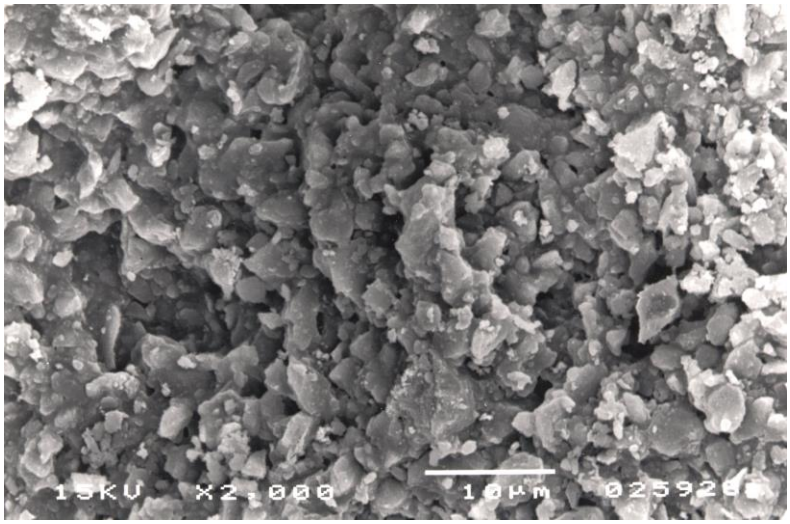

(a) An SEM image showing a magnified view of the corner of a washcoated monolith, with γ-alumina. This is typical of γ-alumina washcoats used for diesel oxidation catalysts. Because of the way in which the washcoat is prepared, the γ-alumina is in the forms of tightly packed grains.

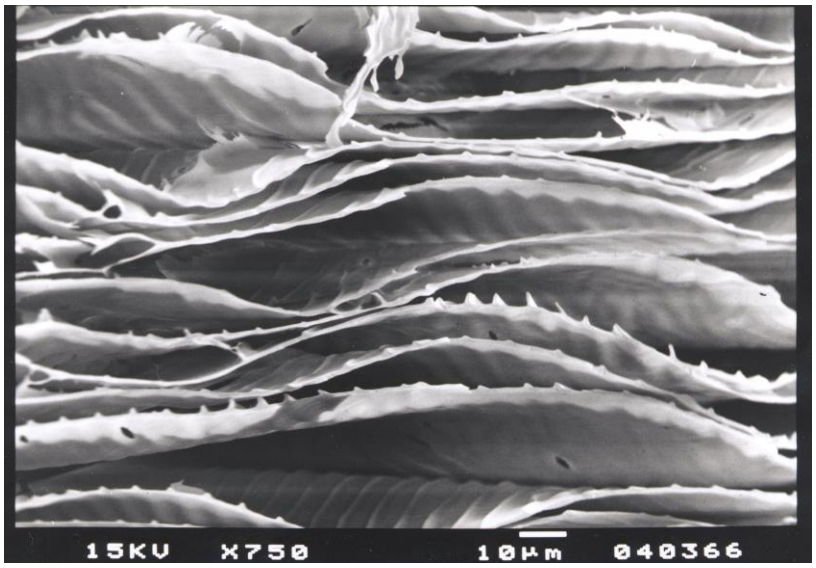

(b) An SEM image showing the KK leaves formed on the surface of a sample formed in a dish. The novelty and difference between this and the grain-like structures in Figure 1.4(a) are very clear.

Figure 1.4 Images presented in Kolaczkowski and Kim (2006), supplied for this thesis courtesy of Kolaczkowski, University of Bath.

1.3 Structure of the Thesis

At the start of this research, three key questions were posed:

(a) How were these leaf-like structures formed?

(b) What conditions are necessary for the preparation of these leaf-like structures that could be used as catalyst supports?

(c) In what other applications could these leaf-like structures be used?

The thesis is divided into five chapters. Figure 1.5 presents a road map to the thesis. Having introduced the topic, **Chapter 2** consists of a literature review which looks more closely at: freeze-drying techniques; catalytic monoliths; the sol-gel process; coating techniques; and the modelling of vacuum desorption in freeze-drying processes. This then leads to the selection of conditions, which are then studied in **Chapter 3**. In that chapter alumina sol-gel is freeze-dried, using a variety of different techniques, leading to a number of interesting structures being formed. Structures are also formed using silica slurry as a starting material. Freeze dried structures are formed inside honeycomb monolith structures, and also on flat and wire metal surfaces (making them easier to inspect). Making structures at the nano-scale, means that Scanning Electron Microscopy (SEM) needs to be used, so as to visualize these structures, and to measure important dimensions.

In **Chapter 4**, in collaboration with another research activity taking place in the department, the application of an enzyme coating onto wire meshes that could be used in a packed bed gas absorption tower for CO_2 removal in a submersible habitat is explored.

Finally, in **Chapter 5** conclusions are presented with recommendations for further work.

Figure 1.5 Outline structure of the thesis.

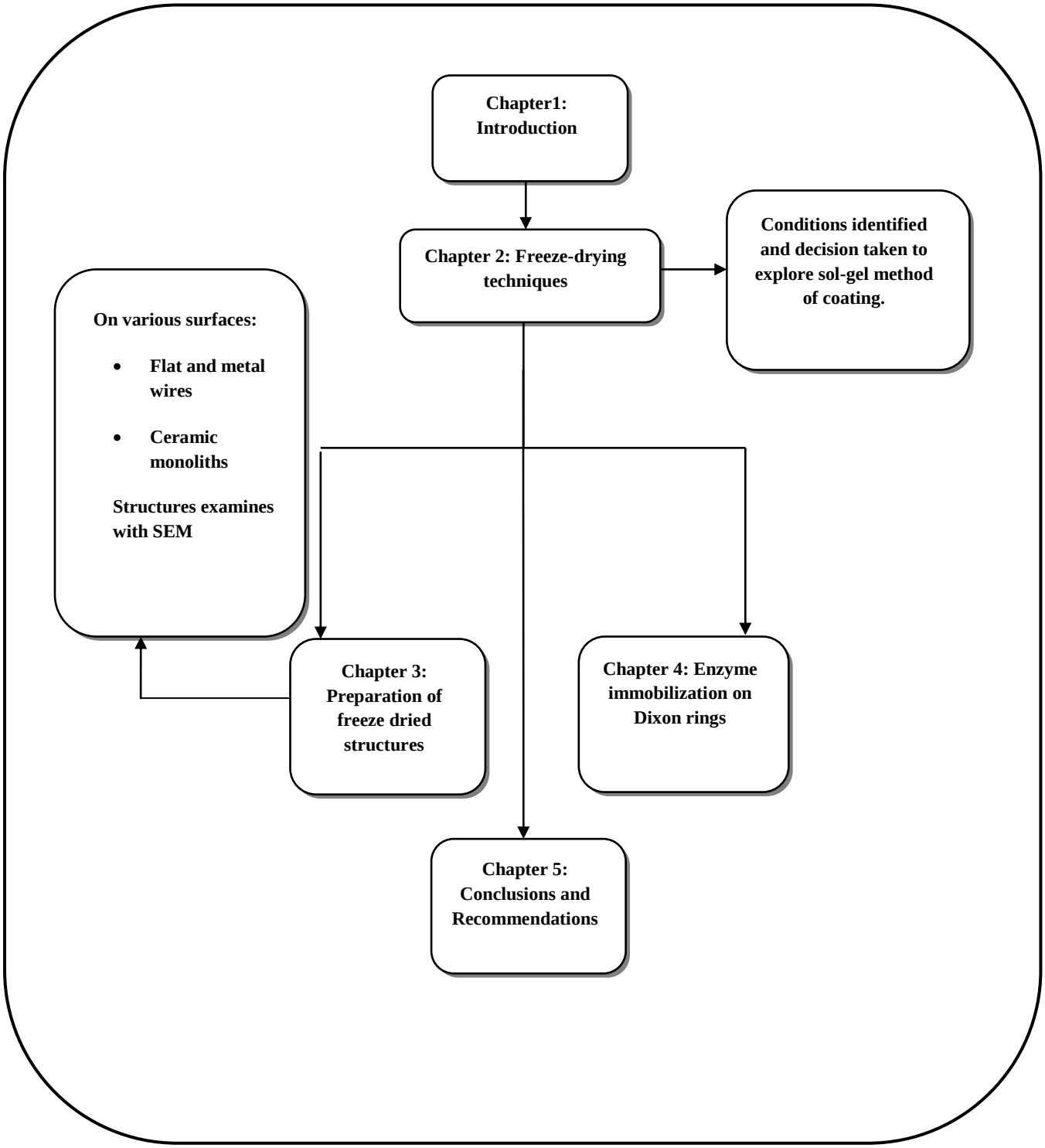

References:

1. Amin, A. M., Croiset, E., Malaibari, Z., Epling, W., 2012. Hydrogen production by methane cracking using Ni-supported catalysis in a fluidized bed. *International journal of hydrogen energy,* Vol. 37, pp. 10690-10701.
2. Cao, F., Su, S., Sun, L., Zhao, Q., Wang, P., Lei, S., 2012. Density functional study of adsorption properties of NO and NH_3 over CuO/ gamma Al_2O_3 catalyst. *Applied surface science,* Vol. 261, pp. 659-664.
3. Chen, G., Wang, W., 2007. Role of freeze drying in nanotechnology. *Drying Technology,* Vol. 25, pp. 29-35.
4. Edward, J., Pope, A., Sakka, S., Klein, L., 1995. *Sol-gel science and technology,* Ohio; American ceramic society.
5. Irani,M., Soltanieh,M., and Rashidzadeh, 2005. Monolithic three-way palladium catalytic converters for automobile exhaust emission control. *Iranian journal of chemical engineering,* Vol. 2, pp. 61-70.
6. Kim, D.Y., Yoo, J.B, Berdinsky, A.B., Park, C.Y., .Han, I.T., Jung, J.E., Jin, Y.W., Kim, J.M, 2005. Preparation of uniformly dispersed iron-acetate nanoparticles using freeze-drying method for the growth of carbon nanotubes. *Diamond & Related Materials,* Vol. 14, pp. 810-814.
7. King, C.J., 1971. *Freeze-drying of foods,* Ohio: The chemical rubber Co.
8. Kolaczkowski, S.T., Kim, S., 2006. Novel alumina 'KK Leaf Structures' as catalyst supports. *Catalysis Today,* Vol.117, pp. 554-558.
9. Mamchik, A.L., Kalinin,S.V., Vertege, A.A., 1998. Cryosol synthesis of manocrystalline alumina. *Chemistry of materials,* Vol. 10, pp. 3548-3554.

10. Mellor, J.D., 1978. *Fundamentals of freeze drying*, London: Academic press Inc. Ltd.
11. Nishihara, H., Mukai,S.R., Fujii, Y., Tago, T., Masuda, T., Tamon, H., 2006. Preparation of monolithic SiO_2-Al_2O_3 cryogels with inter-connected macropores through ice templating. *Journal of materials Chemistry,* Vol.16, pp. 3231-3236.
12. Oetjen, G.W., Aseley, P.H., 2004. *Freeze –Drying, Wenham*: WILEY-VCH Veriag GmbH & Co. KGaA.
13. Su, C., Li, J., He, D., Cheng, Z., Zhu, Q., 2001. Synthesis of isobutene from synthesis gas over nanosize zirconia catalysts. *Applied Catalysis A: General,* Vol. 202, pp. 81-89.
14. Vargas, A., Montoya, J.A., Maldonado, C., Hernandez-Perez, I., Acosta, D.R., Morales, J., 2004. Textural properties of Al_2O_3-TiO_2 mixed oxides synthesized by the aqueous sol method. *Microporous and Mesoporous Materials,* Vol.74, pp. 1-10.
15. Yoldas, B.E., 1975. Alumina jells that from porous transparent Al_2O_3. *Journal of material science,* Vol.10, pp. 1856-1860.

Chapter 2 Freeze-Drying Techniques

In this chapter a literature review is provided of freeze-drying techniques and their potential in applications relating to catalysis.

2.1 Freeze-drying to produce different materials

In the sub-sections that follow, examples have been selected from the literature, which illustrate the way in which freeze-drying techniques could be used advantageously in catalytic systems.

2.1.1 Freeze-drying to form titanium oxide particles

In a review paper by Chen and Wang (2007), they report that freeze-drying has found applications in the production of nanoparticles for: electrochemical and environmental applications, engineering materials, and in the pharmaceutical industries. They also highlight possible applications in the field of catalysis, and the freeze-drying of sol-gel materials as a method of obtaining high surface areas. In one example the production of titanium oxide (TiO_2) nanoparticles from the hydrolysis of titanium isopropoxide is discussed. TiO_2 can be used in advanced oxidation or photo-oxidation reactors. The anatase TiO_2 form has been found to be responsible for the photo-reactivity of this material, and the freeze-dried form gives a complete anatase phase with a larger surface area compared with that obtained either from supercritical fluid extraction, or oven dried forms of the material. In their review the emphasis was very much on the formation of nanoparticles, rather than the use of this technique to coat a surface.

Izutsu *et al.* (1997) provided evidence that the anatase (TiO_2) phase provides a higher surface area. They report that after calcinations at 700^oC for 8 h, then:

- freeze-dried samples showed more than 97% anatase phase with a surface area of 29 m^2g^{-1}, and porosity of 37%,
- whereas, the oven-dried samples showed a surface area of 5 m^2g^{-1}, and a porosity of 10%.

Boiadjieva *et al. (*2003), studied the formation of nano TiO_2 particles by the sol-gel method, and explore the role of the solvent removal step. Titanium isopropoxide was the starting compound, and HCl (at constant ionic strength) was employed as the catalyst for the polycondensation reaction in the gel formation at 25^oC. Three different types of dried precursors were obtained:

(i) xerogels: by evaporating the solvent in an oven at 80^oC ,

(ii) aerogels: formed by reaching supercritical conditions for the fluid, and

(iii) cryogels formed by freeze-drying.

All of the samples were calcined at 300 and 600^oC for the same length of time (6h). The powders were characterized for phase composition crystallinity (using XRD), surface area porosity (using BET), water and solvent content (using TGA). The dried cryogels showed very large surface areas and were amorphous, compared with particles obtained from supercritical fluid extraction, or oven drying processes. After calcinations the powders were:

- composed of pure anatase, except for traces of brookite at 300^oC,

and their specific surface areas remained large:

- at 300^{o}C the cryogel showed a surface area which was almost twice the one of the xero and areogel, and
- at 600^{o}C it is still larger especially with respect to the xerogel.

Ma *et al*. (2003), reports on the use of freeze-drying to make TiO_2 microtubes which are about 1 µm in diameter, with lengths ranging from several to over 100 µm. Some sheets were also observed to be formed with the microtubes. They proposed that this formation occurs through the physical rearrangement or self-organization of nanoparticles, most likely driven by capillarity and aided by hydrogen bonding between nanoparticles and solvent molecules during freeze-drying. They also found that Al_2O_3, and ZnO nanoparticles can self-assemble in the same way.

Vargas et *al.* (2004) explore the textural properties of Al_2O_3-TiO_2 mixed oxides synthesized by the aqueous sol method. The resulting hydroxides were dried either in a conventional air static oven or by the freeze-drying method. The hydroxides were transformed into their corresponding oxides by calcinations at 600^{o}C. The resulting mixture oxides were thermally stable up to 900^{o}C. The crystallite size of the hydroxides and the mixed oxides were affected by the incorporation of TiO_2 into the alumina structure. The mixture oxides obtained by both drying methods presented a greater surface area than the corresponding pure alumina structure. The mixed oxide dried by the freeze-drying methods presented a greater surface area than the corresponding mixed oxides dried by the conventional method. The oxides dried by freeze-drying developed a smaller pore size with a narrower, unimodal pore size distribution (PSD) if compared to the corresponding oxides dried by the conventional method, which showed a bimodal and broad PSD.

2.1.2 Freeze-drying of alumina

Mamchik *et al.* (1998), explore freeze-drying of alumina sols. They start by stating that aluminium oxide powers are widely used in various materials such as adsorbents and catalysts, and one of the main methods for preparation is thermal decomposition of aluminium hydroxide. The reaction path of the system during heating is primarily governed by the phase composition and morphology of initial aluminium hydroxide particles. The latter also influences the microstructural properties of the resulting materials. By using freeze-drying techniques, aluminium hydroxide powders with extremely low density and small particle size are formed. Then, after thermal decomposition highly dispersed powders of aluminium oxide are formed with a wide temperature interval of stability at the nanocrystalline phase. The crystallization is supposed to take place within particles forming colloidal aggregates. Thermal stability is due to the high uniformity of the particle size distribution, a direct result of the freeze-drying process.

2.1.3 Freeze-drying to form carbon nanotubes

The production of carbon nanotubes has been studied by many researchers. For example, Kim *et al.* (2005) studied the growth characteristics of carbon nanotubes grown from uniformly dispersed iron nanoparticles prepared from iron-acetate. In summary, the procedure consisted of the following steps:

- The iron acetate solution was prepared using ethylene glycol to create a solution that was low in vapour pressure and viscosity.
- The solution was then spin coated onto a glass substrate.

- The substrate was then quickly frozen in liquid nitrogen, and then moved into a vacuum chamber.
- The chamber was then evacuated to $1x10^{-2}$ Torr and the substrate was heated to 100 ºC for 20 min.
- It was then placed in a vacuum oven, and heated at 300 ºC for 20 minutes to achieve thermal decomposition.
- The decomposed iron acetate was then placed into a carbon nanotube growth chamber, where it was subsequently heated up to 550 ºC which was sustained for 40 minutes in the presence of CO and H_2.

Mehn *et al.* (2004), made a comparison of different methods of preparing $Fe/Mo/Al_2O_3$ sol-gel catalysts, which could be used for the synthesis of single wall carbon nanotubes. They explored the use of: different solvents, metal salts and different drying processes including the application of chelating agent or freeze-drying. They concluded that by using the freeze-drying method, they were able to prepare a sol-gel alumina catalyst "with favourable texture and, in consequence, with enhanced activity" in single wall nanotube synthesis.

2.1.4 Freeze-drying to form nanosize zirconia catalysts

Su *et al.* (2001), describe the preparation of nanosize zirconium oxides prepared by: precipitation, supercritical fluid drying, and freeze-drying methods. Then for the selective synthesis of isobutene ($i\text{-}C_4H_8$) from synthesis gas, they compared the performance of the catalysts made. The crystal structure, particle size and specific surface area were measured by XRD, TEM and BET. The acidic and basic properties of the catalysts were studied by NH_3

and CO_2-TPD, respectively. The results showed that the crystal phases, acidic and basic properties of nanosize zirconia depend remarkably on the drying conditions. Freeze-drying gave a lower number of base site in comparison with that obtained by conventional solvent evaporation. Higher ratios of basic to acidic sites lead to higher selectivity for i-C_4H_8. The acidic sites are responsible for the activation of the reactant molecules, while the basic sites were said to be responsible for the chain propagation to form i-C_4H_8.

2.1.5 Freeze-drying to form vanadium-molybdenum oxynitrides as catalysts

El-Himri *et al.* (1999), demonstrate that vanadium-molybdenum oxynitrides can be successfully synthesized by direct ammonolysis of freeze-dried precursors with the stoichiometric metal ratio precisely controlled. Such catalysts were considered to be promising materials in processes involving hydrogen transfer reactions, such as dehydrodenitrogenation and hydrodesulphurization. The procedure started with the preparation of V, and Mo containing solutions (by dissolving the salts in distilled water), then combining to obtain the V-Mo source solution with the required cationinc concentration. The droplets of this solution were flash frozen by contact with liquid nitrogen, and then freeze-dried at a pressure of 1-10 Pa. This technique produced solid precursors in the form of amorphous loose powders.

2.1.6 Freeze-drying to form Pt-Al_2O_3 catalysts

In response to the knowledge that at high temperatures Pt agglomerates and sinters easily, Osaki *et al.* (2007) explored the use of a Pt catalyst formed via a freeze-drying process (cryogel), and how its thermal stability and catalytic combustion activity compared with other

xerogel forms. The cryogel catalyst was prepared from aluminium sec-butoxide and H_2PtCl_6 through the sol-gel technique and subsequent freeze-drying. The cryogel catalyst showed higher thermal stability of platinum than the corresponding xeroel, or impregnation catalysts. This was attributed to the more intimate platinum-alumina interaction accompanied by the encapsulation of the metal into the alumina cryogel. It was also shown that platinum accessibility was higher on the cryogel than on the xerogel despite the higher thermal stability of the metal on xerogel and impregnation catalysts. When the catalytic combustion of methane was studied, then the cryogel showed higher activity, although it showed lower activity than the impregnation catalysts above 600^{o}C. When ceria was added to the cryogel catalysts, the CH_4 combustion activity was improved especially in the temperature region above 600^{o}C.

2.1.7 Freeze-drying applications for catalytic foam-like structures

Nishihara *et al.* (2006), describe the use of an 'ice-templating method', for the preparation of macroporous foam-like structures, with micro-honeycomb shape. This they made from SiO_2-Al_2O_3. The macropores were generated by using ice crystals as the template, while the walls which surround the macropores were tailored as porous cryogels by freeze-drying. The macropores and walls formed honeycomb-like structures. The macropores ranged from 10-20 μm and the wall thickness ranged from 200-500 nm. Mapping analysis by energy dispersive X-ray diffractometry showed that Al atoms were homogeneously dispersed throughout the samples without local aggregation. It was also confirmed:

- that the macropores were highly interconnected and passed through the whole of the foam structure;

- that in the SiO_2-Al_2O_3 cryogel Al atoms were incorporated into the silica framework by forming an Al-O-Si polymeric network, therefore these structures were expected to show Bronsted acidity;

- from nitrogen adsorption-desorption measurements that the walls were micro/mesoporous with high BET surface areas (>700 m^2g^{-1}) and large pore volumes;

- that the freezing of the SiO_2-Al_2O_3 hydrogels does not deteriorate the dispersion of Al atoms, which was achieved during the sol-gel synthesis.

Choi *et al.* (2004), observe that the pore structure of freeze-dried silica gel can be changed during calcination. The silica gel was formed by the hydrolysis of ethyl silicate. They found that the colloidal particles derived from tetraethyl orthosilicate hydrolysis with an average particle size of 31 nm formed porous microsized agglomerates with high specific surface area 9435 m^2/g via the freeze-drying route. The nonocrystalline freeze dried gel consisted mainly of mesopores (4-6 nm).

2.2 Catalytic monoliths

There are many papers and a few textbooks, where the general structure of catalytic monoliths is well described. For example in Hayes and Kolaczkowski (1997), a catalytic monolith is described as consisting of a number of parallel passageways through which the gas flows, with the catalyst being located on the channel walls. The monolith channels can have various cross-sectional shapes, e.g. square, hexagonal. The surface of the monolith support may be coated with a layer of high surface area material, commonly known as the washcoat, in which the catalyst is dispersed. The washcoat thickness may vary from 10 to 50 μm and may not have a uniform thickness around the perimeter of the cell.

When a monolith is washcoated, by a wet process, then that structure needs to be dried. So in the section that follows, drying is discussed in more detail, as it is an important part in the overall process.

2.2.1 Drying the washcoated monolith support

Vergust *et al. (*2001) provide a detailed description of the various steps that occur during a drying process, and they draw an interesting analogy with the process of drying a bed of sand. They state that drying is a combined mass and heat transfer problem, in which the evaporation and heat transfer rates are coupled by the heat of evaporation. The way in which the drying process occurs depends very much on the extent of contact between the liquid and the support. This leads to important conclusions about the role that evacuation of air from the sample prior to impregnation plays on the overall drying process, and they provide the following key points:

Case A - If the support prior to wetting had been evacuated then:

- the liquid is present throughout the porous network, and initially, the liquid is evaporated from the exterior of the support;
- the amount of liquid in both the large and small pores at the exterior of the support reduces, and menisci at the pore mouths develop;
- because of the larger curvature of their menisci, these pores attract liquid from larger pores located at the interior of the catalyst particle, which will progressively be emptied.
- This situation is maintained as long as the exterior of the particle is connected to the interior via a continuous liquid film, and this is characterized by a constant drying rate.
- When this connectivity is lost, wet regions become isolated and evaporation occurs from the interior of the particles, characterized by a decreasing drying rate.

Case B - If the support particle prior to impregnation had not been evacuated, then:

- it is likely that there is gas trapped under pressure inside the particle, compressed by capillary forces;
- in addition to the processes described in Case A, the occluded gas is heated as well by the surrounding air during drying and expands, pushing the impregnation solution outward.

Vergust *et al. (*2001) finally conclude that drying causes an outward flow of liquid, from the interior of a particle to the exterior. In cases of weak interaction between the catalyst precursor and the catalyst support material, this can lead to the transport of catalyst precursors to the exterior of the support. This aspect was of interest to them as they explored

why there were variations in the distribution of the active phase in catalyst supports, and how this was influenced by the choice of drying method. When they studied the use of freeze-drying, they found that this technique prevented the liquid from flowing, and was considered one of three preferred methods (others were microwave drying, and deposition-precipitation).

2.2.2 Sol-gel coating of the monolith support

As described in Klein (1991, p.502)**:** The sol-gel coating process involves a solution or sol that undergoes a sol-gel transition. A solution is a single phase liquid, while a sol is a stable suspension of colloidal particles. At the transition, the solution or sol becomes a rigid, porous mass by destabilization, or supersaturation. The coating can be applied by spinning, dipping and draining. The advantages of the sol-gel process are high purity, homogeneity and low temperature. Also the material use is efficient; any excess material is recovered to leave little waste. The only disadvantage is the cost of raw material. Costs are prohibitive when the process is considered for bulk ceramics, but are acceptable for the applications where conventional technology fails.

A schematic of a film coating (washcoating) process is shown in Figure 2.1. A thin layer can be formed on the support from a solution using a dipping method. During this process, the viscosity of the solution, surface tension, and time to gel, all need to be carefully monitored.

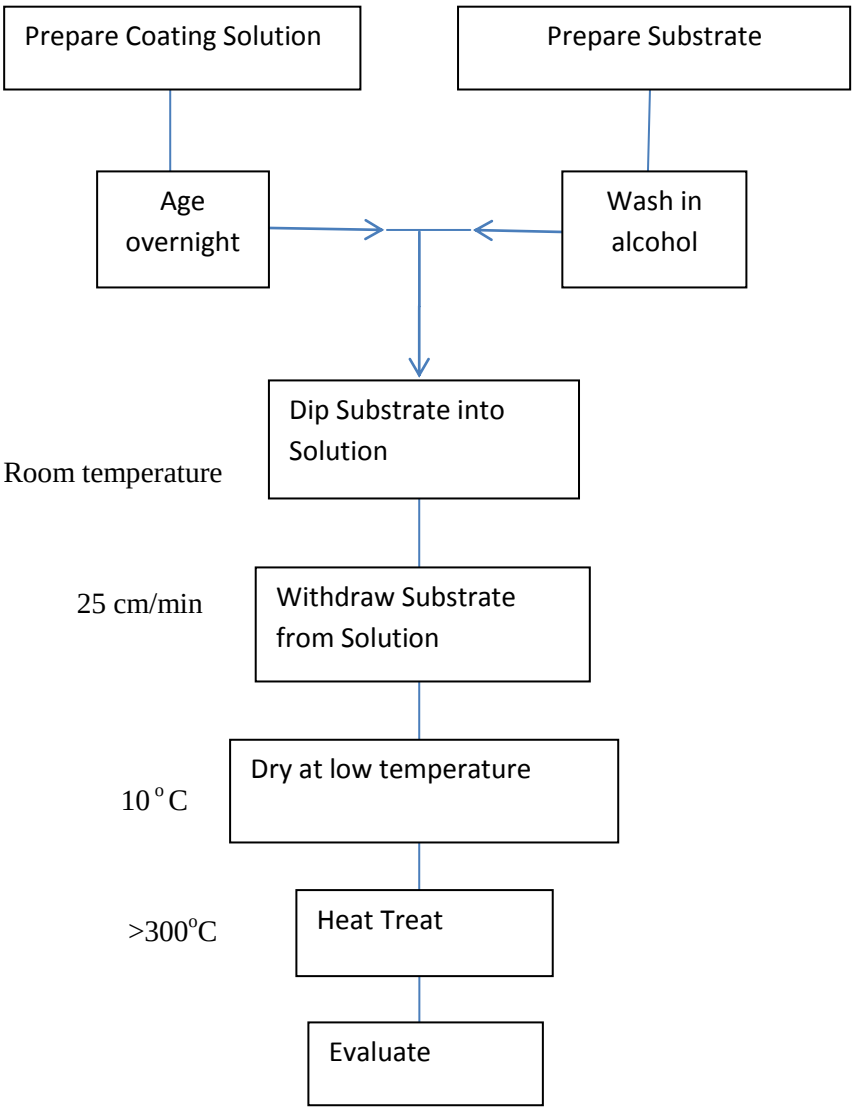

Figure 2.1: Flow diagram indicating the key steps in the coating process (adapted from Klein, 1991, p.508).

In the literature there are many examples describing recipes for the sol-gel process. For example:

Example 1 In Osaki *et al.* (2007), the cryogel catalyst was prepared from aluminium sec-butoxide and H_2PtCl_6 through the sol-gel technique and freeze drying:

(i) Aluminum sec-butoxide (0.029 mol) was hydrolyzed with ultra-pure water (20 mL) in a flask at 86^{o}C, and the resultant mixture was kept stirring.

(ii) Then 1.0 mol L^{-1}nitic acid (4.0 ml) was added to the sol for peptization and the sol was refluxed for a few hours with stirring to obtain a clear boehmite solution.

(iii) In a separate vessel, 0.37g of H_2PtCl_6 aqueous solution (2.0 wt. %) was mixed with the aqueous solution (4.8 ml) containing oxalic acid (0.088 mol L^{-1}) and ammonia (0.60 mol L^{-1}), and the solution was kept at 86^{o}C for 30 min.

(iv) The platinum solution was added to the boehmite sol and the mixture was refluxed at 86^{o}C with vigorous stirring.

(v) For gelation, urea (0.2g) was added to the sol, and the sol was then allowed to stand for one night at 86^{o}C.

(vi) The gel obtained was frozen at a liquid nitrogen temperature without the solvent exchange, and then subsequently dried under vacuum on a laboratory freeze-drier equipped with a vacuum pump.

(vii) The dried gel was then calcined in air in the temperature range of 500 to 800 ºC.

(viii) The final platinum content was 0.5 wt% on a weight base.

Example 2 In Nijhuis *et al.* (2001), the procedure for coating with alumina using the sol method consists of the following steps:

(i) A sol is prepared from pseudo-boehmite (AlOOH), urea, and 0.3 M nitric acid in weight ratio of 2:1:5. They are mixed using a stirrer.

(ii) A dried monolith is dipped in this sol and the dipping time does not influence the coating process.

(iii) The monolith is emptied by shaking and by pressurized air and then dried horizontally while continuously being rotated around its axis.

(iv) The monolith is calcined at 723K to produce a γ-alumina coating, the carbon dioxide and nitric oxide produced from the oxidation of the urea will help in the formation of microspores in the alumina coat layer.

2.2.3 Sol-gel coating of the monolith support and freeze-drying forming KK leaves

The formation of leaf-like structures of alumina, attached to a ceramic monolith support structure and with a leaf thickness at the nano-scale, was first reported by Kolaczkowski and Kim (2006). This has already been discussed in Chapter 1, and a more comprehensive description of the sol-gel preparation, monolith support washcoating, and freeze-drying processes will be presented in Chapter 3.

2.3 Modelling of vacuum desorption in freeze-drying process

There have been a number of papers published on the subject of mathematical modelling of the freeze drying processes (e.g. Fey *et al*.1988, Liapis *et al.*1987, Liapis *et al.*1995; Sadikoglu and Liapis 1997). In these publications, various theoretical and practical problems were also discussed.

To illustrate some of the factors that are considered, the following information has been obtained from a paper by Nastaj and Ambrozek (2005) on modelling:

(a) The motivation for their work arose from an interest in the freeze-drying of porous biomaterials and pharmaceuticals.

The resulting set of equations in the model was solved using the numerical method of lines, and they were able to predict the moisture content and temperature distributions within the drying material as a function of drying time.

(b) The freeze–drying process was assumed to consist of the following steps:

(i) pre-freezing,

(ii) sublimation drying under vacuum (primary drying) resulting in a moisture content of approximately 7 wt%,

(iii) followed by desorption (secondary drying), aiming for a moisture content of between 0.5 to 2.0 wt%. A schematic of this step is shown in Figure 2.2.

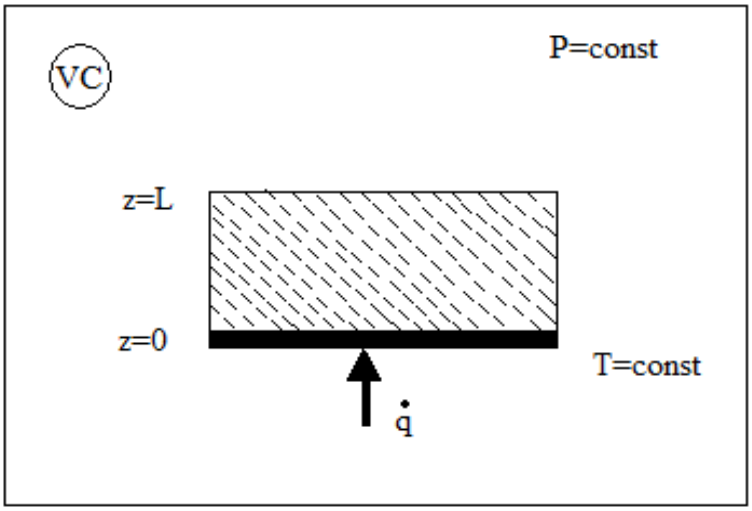

Figure 2.2 A physical model of vacuum desorption in the secondary freeze–drying step (adapted from Nastaj and Ambrozek 2005).

Nastaj and Ambrozek (2005) applied the following assumptions in their model:

- All inert gases are evacuated rapidly and therefore it is possible to ignore their presence.
- The pressure drop in the material is neglected because of the thin thickness of the material layer in vacuum freeze-drying and low vapour mass flux densities.
- The vacuum pump removes vapours coming from the material immediately, then vapour concentration of the components in interparticle voids is practically equal to zero.

They presented the following set of equations for multicomponent vacuum desorption:

The gas phase material balance equation for component, *i*:

$$\frac{\partial C_i}{\partial t}+\frac{\partial(y_i \cdot J_z)}{\partial z}+\frac{1-\varepsilon}{\varepsilon}\frac{\rho_b}{M_i}\frac{\partial \bar{X}_i}{\partial t}=0 \tag{2.1a}$$

$$\frac{\partial(y_i \cdot C)}{\partial t}+\frac{\partial(y_i \cdot J_z)}{\partial z}+\frac{1-\varepsilon}{\varepsilon}\frac{\rho_b}{M_i}\frac{\partial X_i}{\partial t}=0 \tag{2.1b}$$

where C=P/RT, is the sum of the molar concentrations of all components in the gas phase.

The mass transfer is formulated by a linear driving force approximation:

$$\frac{\partial X_i}{\partial t}=K_i(X_i^*-X_i) \tag{2.2}$$

The equilibrium relationship is given by a function:

$$X_i^*=f(C_1,C_2,\ldots,C_S,T) \tag{2.3}$$

in which C_1, C_2… are the molar concentrations of the components in the mixture. The energy balance equation is:

$$-k\frac{\partial^2 T}{\partial Z^2}+(1-\varepsilon)\rho_b c_S\frac{\partial T}{\partial t}+\sum_{i=1}^{S}\Delta H_i\frac{\rho_b}{M_i}(1-\varepsilon)\frac{\partial X_i}{\partial t}=0 \tag{2.4}$$

The pressure drop equation was given by:

$$\frac{\partial P}{\partial Z}=-\frac{150\,\mu}{d_p^2\cdot C}\frac{(1-\varepsilon)^2}{\varepsilon^3}J_z-\frac{1.75\sum_{i=1}^{s}y_i M_i}{d_p\cdot C}\frac{(1-\varepsilon)}{\varepsilon^3}J_z^2 \tag{2.5}$$

The boundary and initial conditions were as follows:

$$\frac{\partial C_i}{\partial z}=0;\ \frac{\partial P}{\partial z}=0;\ T=T_0=\text{const}\quad \text{for } z=0 \tag{2.6a, b, c}$$

$$\frac{\partial T}{\partial z}=0;\ P=P(t)\quad \text{for } z=L \tag{2.6d, e}$$

$$X_i=X_i(z,0);\ T=T(z,0);\ P=P(z,0)\quad \text{for } t=0 \tag{2.7a, b, c}$$

2.4 Research questions providing direction

Following on from Chapter 1, the literature review with the summary of applications presented in Table 2.1 helps to formulate a number of questions which provide a direction for the work that follows in this thesis. These are:

1. Is it possible to repeat the experiments described in Kolaczkowski and Kim (2006) and to obtain the same form of KK leaf structure that they had observed? This is an important question, as their discovery was only by chance, and they did not have the time to pursue it further.
2. From the literature (see Table 2.1), in some of the freeze-drying processes, the sol-gel formed comes into contact first with the liquid nitrogen before it is freeze-dried, and in other instances it does not (but is placed directly into the freeze-drier). In Ma *et al*. (2003), freeze-drying produced TiO_2 microtubes which were about 1 μm in diameter (with lengths ranging from several to over 100 μm), and some sheets were also formed. In work on vanadium-molybdenum oxynitrides, El-Himri *et al.* (1999) report that freeze-drying resulted in the formation of solid precursors in the form of amorphous loose powders. Besides the work of Kolaczkowski and Kim (2006), the formation of KK leaf-like structures does not appear to have been reported in any other work seen so far. So what are the important factors affecting the formation of the KK leaf structures formed in the freeze-drying process? How do the variables in that coating and freeze-drying process affect the structure of the KK leaves? For example, what is the effect of temperature and vacuum?
3. The discussion in Nishihara *et al.* (2006), on the use of an 'ice-templating method', for the preparation of macroporous foam-like structures, and then using freeze-drying to create the walls was interesting. This stimulates many questions about the way in

which the KK leaves are formed. For example, does the way (orientation) in which the gel-coated support is immersed into the liquid N_2 affect the arrangement of the KK leaves on the support? Will the KK leaf structure form on other types of support materials? In Kolaczkowski and Kim (2006), these aspects were not studied, yet they could have very important implications for the way in which such systems are coated and freeze-dried in a commercial process, and then how they are subsequently used (e.g. in a reactor).

4. From the literature review, there is evidence (Osaki *et al.* (2007)) that a Pt-Al_2O_3 sol-gel freeze-dried catalyst system can be formed, and in a catalytic combustion application, that catalyst showed a higher thermal stability of the platinum (than the corresponding xeroel, or impregnation catalysts). So could a Pt catalyst be incorporated into the KK leaves, and will this lead to an improvement in the performance of that catalyst system?
5. From the literature, there is evidence (Vergust *et al. (*2001)) that in a catalyst preparation step involving drying, then to reduce the transport of catalyst precursors to the exterior of a support, freeze-drying was one of the three preferred methods of catalyst formulation. So could this also be a benefit in the way in which KK leaf structures could be used to support a catalyst?

Within the scope of this MPhil thesis, it will not be possible to answer all of these questions; however, some are explored further in the chapters that follow.

Materials	**Sol-gel formed**	**Immersing in liquid N_2**	**Freeze drying**	**Condition of calcination**	**Structure formed**	**References**
TiO_2	Yes	no	yes	700 ^{o}C, 8h	Nanoparticles	Chen and Wang (2007)
TiO_2	yes	no	yes	300 ^{o}C, 6h 600 ^{o}C, 6h	Nanoparticles	Izutsu*et al.* (1997)
TiO_2	yes	no	yes	no	Nanoparticles	Boiadjieva *et al.* (2003)
TiO_2	yes	no	yes	600 ^{o}C, 6h	Microtubes	Ma *et al.* (2003)
Al_2O_3- TiO_2	yes	no	yes	no	Nanoparticles	Vargas *et al.* (2004)
Al_2O_3	no	no	yes	no	Particles	Mamchik*et al.* (1998)
Carbon	no	yes	yes	550 ^{o}C, 40 min	Nanotubes	Kim *et al.* (2005)
Fe/Mo/ Al_2O_3	yes	no	yes	no	Nanotubes	Mehn*et al.* (2004)
ZrO_2	no	no	yes	no	Particles	Su *et al.* (2001)
V-Mo oxynitrides	no	yes	yes	no	Amorphous loose powders	El-Himri*et al.* (1999)
Pt- Al_2O_3	yes	no	yes	600 ^{o}C	Nanoparticles	Osaki *et al.* 92007)
SiO_2- Al_2O_3	yes	no	yes	no	Macroporous foam	Nishihara *et al.* (2006)
Silica	yes	no	yes	no	Particles	Choi *et al.* (2004)
Pt- Al_2O_3	yes	yes	yes	500-800 ^{o}C	Coated monoliths	Osaki *et al.* 92007)
Al_2O_3	yes	no	no	450^{o}C	Coated monoliths	Nijhuis*et al.* (2001)
Al_2O_3	yes	yes	yes	550 ^{o}C	Coated monoliths	Kolaczkowski and Kim (2006)

Table 2.1 Summary of applications reviewed in Chapter 2.

REFERENCES

1. Boiadjieva, T., Cappelletti, G., Ardizzone, S., Rondinini, S., and Vertova, A., 2003. Nanocrystalline titanium oxide by sol-gel method. The role of the solvent removal step. *Physical chemistry and chemical physics,* Vol. 5, pp. 1689-1694.
2. Chen, G., and Wang, W., 2007. Role of freeze drying in nanotechnology. *Drying technology,* Vol. 25, pp. 29-35.
3. El-Himri, A., Cairols, M., Alconchel, S., Sapina, F., Ibanez, R., Beltran, D., and Beltran, A., 1999. Freeze-dried precursor-based synthesis of new vanadium-molybdenum oxynitrides. *Journal of materials chemistry,* Vol. 9, pp. 3167-3171.
4. EI-Himri, A., Sapina, F., Ibanez, R., and Beltran, A., 2000. Synthesis of new vanadium-chromium and chromium-molybdenum oxynitrides by direct ammonolysis of freeze-dried precursors. *Journal of materials chemistry*, Vol. 10, pp. 2537-2541.
5. Hayes, R.E., and Kolaczkowski, S.T., 1997. Introduction to Catalytic Combustion, Gordon & Breach Science Publishers (now assigned to Taylor & Francis Books Ltd).
6. Izutsu, H., Nair, P. K., and Mizukami, F., 1997. Physical stabilization of anatase (TiO_2) by freeze-drying. *Journal of material chemistry,* Vol. 7, pp. 855-856.
7. Kim, D.Y., Yoo, J.B., Berdinsky, A.S., Park, C.Y., Han, I.T., Jung, J.E., Jin, Y.W., Kim, J.M., 2005. Preparation of uniformly dispersed iron-acetate nanoparticles using freeze-drying method for the growth of carbon nanotubes. *Diamond & related materials,* Vol. 14, pp. 810-814.
8. Klein, L.C., 1991. *Thin film processes II,* p.502. New Jersey: Academic Press. Inc.

9. Kolaczkowski, S. T., Kim, S., 2006. Novel alumina 'KK Leaf Structures' as catalyst supports. *Catalysis Today,* Vol.117, pp. 554-558.

10. Lzutsu, H., Nair, P.K., and Mizukami, F., 1997. Physical stabilization of anatase (TiO_2) by freeze-drying. *Journal of material chemistry,* Vol. 7, pp. 855-856.

11. Ma, D., Schadler, L.S., Siegel, R.W., and Hong, J., 2003. Preparation and structure investigation of nanoparticle-assembled titanium dioxide microtubes. *Applied physics letters,* Vol. 83, pp. 1839-1841.

12. Mamchik, A.I., Kalinin, S.V., and Vertegel, A.A., 1998. Cryosol synthesis of nanocrystalline alumina. *Chemistry of materials,* Vol. 10, pp. 3548-3554.

13. Mehn, D., Fonseca, A., Bister, G., Nagy, J.B., 2004. A comparison of different preparation methods of $Fe/Mo/Al_2O_3$ sol-gel catalyst for synthesis of single wall carbon nanotubes. *Chemical physics letters,* Vol. 393, pp.378-384.

14. Nastaj, J.F., Ambrozek, B., 2005. Modeling of vacuum desorption in freeze-drying process. *Dry technology* Vol. 23, Pp.1693-1709.

15. Nijhuis, T. A., Beer, E.W., Vergunst, T., Hoek, I., Kapteijin, F., Moulijn, J. A., 2001. Preparation of monolithic catalysis. *Catalysis review.* Vol.43 (4), pp.345-380.

16. Osaki, T., Nagashima, K., Watari, K., Tajiri, K., 2007. $Pt\text{-}Al_2O_3$ cryogel with high thermal stability for catalytic combustion, *Catalytic Letter* Vol. 119, pp.134-141.

17. Su, C., Li, J., He, D., Cheng, Z., Zhu, Q., 2000. Synthesis of isobutene from synthesis gas over nanosize zirconia catalysts. *Applied catalysis A: General,* Vol. 202, pp. 81-89.

18. Vargas, A., Montoya, J.A., Maldonado, C., Hernandez-Perez, I., Acosta, D.R., Morales, J., 2004. Textural properties of Al_2O_3-TiO_2 mixed oxides synthesized by the aqueous sol method. *Microporous and Mesoporous Material* Vol.74, pp. 1-10.

19. Vergunst, T., Kapteijin, F., Moulijin, J.A., 2001. Monolithic catalysts-non-uniform active phase distribution by impregnation. *Applied catalysis A: General,* Vol. 213, pp.179-187.

Chapter 3 Preparation of freeze dried structure

In this chapter, freeze-dried structures have been prepared, using a variety of different techniques, with a strong focus on the way in which such KK leaf structures had been made by Kolaczkowski and Kim (2006). By exploring different techniques, this helps to answer the questions: 'How *were these leaf-like structures formed?*' which was asked at the start of the thesis.

Freeze-dried structures are formed from:

- an alumina sol-gel (on glass dish, monoliths, and wire mesh rings), and
- a silica sol-gel (on monoliths).

3.1 Structures formed from an alumina sol-gel after calcination

Kolaczkowski and Kim (2006) formed KK leaf structures from alumina creating thin leaf-like structures that had a thickness of 0.2-0.8 μm, and these are illustrated in Figure 3.1. In their work, aluminium iso-propoxide was transformed into a sol-gel and then frozen at -195^{o}C. The sample was then placed in a freeze-drying unit at -60^{o}C (and 0.133 Pa) for 15 hours using phosphorous pentoxide as a drying agent to remove water, and a cryogel was formed. The sample was then dried at room temperature, and then it was calcined at 450^{o}C for about 5 hours. The structure formed was named KK leaves, as they resembled a loosely packed collection of thin curly leaves with fine ribs resembling leaf veins on trees and plants. The leaves had a surface area of about 282 m^2/g, and an average pore diameter of about 2.8 nm.

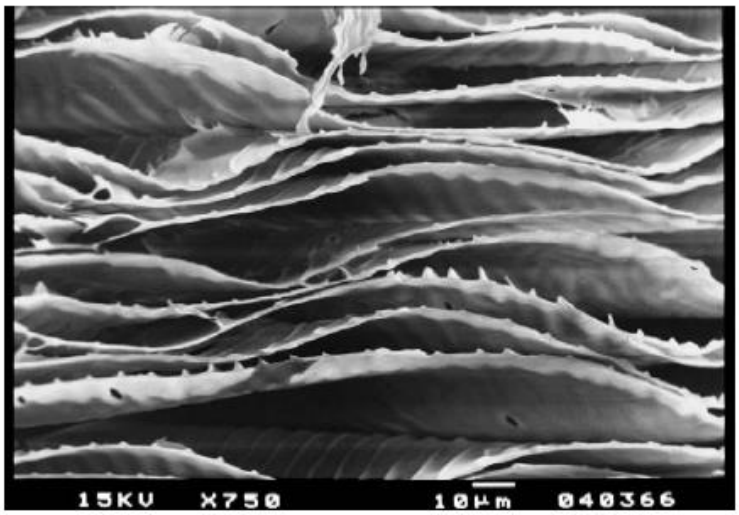

Figure 3.1(a) SEM image showing the loosely packed 'KK Leaves' on the surface of a sample that was formed in a glass dish (Kolaczkowski and Kim, 2006).

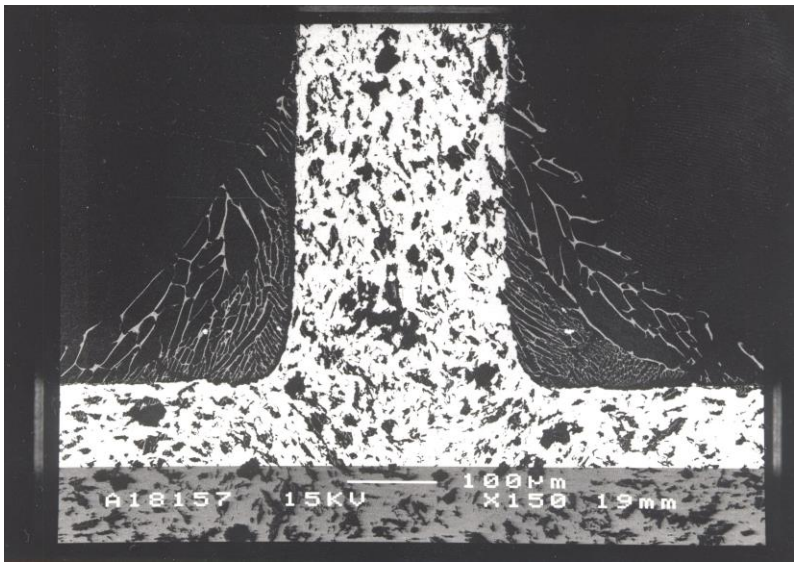

Figure 3.1(b) An SEM image used in Kolaczkowski and Kim (2006), showing the face of a coated monolith at the point of gas entry. The channels are 1 mm x 1 mm. The KK leaves appear as fine irregular lines that form a mesh that has voids between them. In this example: coating, freezing, freeze-drying and calcining processes, were repeated twice, so there are two distinct layers. A difference in compactness of the leaves indicates the presence of the interface between the two layers. Image supplied courtesy of Kolaczkowski, University of Bath.

3.1.1 Preparation of alumina sol-gel to form 'KK leaves'

Based on general descriptions of the sol-gel process in the literature, a 'sol' is a colloidal solution and this acts as the precursor for an integrated network of either discrete particles or a network of polymers. The term colloid is used to describe a broad range of solid-liquid (and/or liquid-liquid) mixtures, all of which contain distinct solid (and/or liquid) particles which are dispersed to various degrees in a liquid medium.

Typical precursors are metal alkoxides and metal salts (such as chlorides, nitrates and acetates), which undergo various forms of hydrolysis and poly-condensation reactions.

In this thesis, the alumina sol gel was prepared making use of explanations in Kolaczkowski and Kim (2006) who in turn made use of advice offered in Yoldas (1975).

In summary the procedure followed in this thesis consists of the following steps:

Step 1 - Hydrolysis: 50 g of aluminium iso-propoxide (98%) was put in a 2L flask, and 500 ml of distilled water was added. The mixture was stirred with a magnetic stirrer for 20 min at 75^{o}C. Then 0.012 mol of 35wt% HCl was added and the mixture was stirred for a further 30 min.

Step 2 - Peptization: the mixture was stirred at about 80^{o}C for 1hour to remove the residual group.

Step 3 - Aging: a water-cooled condenser was mounted on top of the flask (see Figure 3.3, and the mixture was maintained at about 80^{o}C while stirring for 36 hours.

A comparison of procedures followed in this thesis, and how they compare with the procedure followed in Kolaczkowski and Kim (2006) is shown in Table 3.1 and the following more detailed comments are made:

In **Step 1**, the hydrolysis of aluminium iso-propoxide in water produces iso-propanol, this reaction can be represented as:

$$Al(OC_3H_7)_3 + H_2O \rightarrow Al(OC_3H_7)_2OH + C_3H_7OH \qquad (3.1)$$

This step is faster than in Kolaczkowski and Kim (2006), because more water is added and this helps to push the forward reactions to make the alcohol and isopropanol. During hydrolysis, the pH was maintained below pH = 3. By increasing the pH, $[Al(OH_2)_6]^{3+}$ can be hydrolyzed extensively as show below:

$$[Al(OH_2)_6]^{3+} + h\,H_2O \longrightarrow [Al(OH)_h(OH_2)_{6-h}]^{(3-h)+} + h\,H_3O^+ \qquad (3.3)$$

$$h\,H_3O^+ + hOH^- \longrightarrow 2h\,H_2O \qquad (3.4)$$

where: h is defined as the molar ratio of hydrolysis which is equivalent to the OH:Al ratio.

Subsequent condensation results in polynuclear hydroxides or oxo-hydroxide, which can re-dissolve slowly, the species distribution being sensitive to the precise conditions of the hydrolysis procedure. In the method used the reaction takes a shorter time to complete than that described in Yoldas (1975).

In **Step 2 (peptization)**, the reaction is an acid catalyzed reaction, and this can be described as:

$$Al\,(OC_3H_7)_2OH + H_2O \rightarrow C_3H_7O\,[(OH)\,Al\text{-}O\text{-}Al\,(OH)]_nOC_3H_7 + C_3H_7OH \qquad (3.2)$$

By adding 0.5 mol of HCl per mol of aluminium isopropoxide the HCl (which acts as a catalyst) has significantly enhanced the peptization stage. In the procedure described in Yoldas (1975), this required 5 to 6 hours while evaporating the mixture at 80^{o}C to reach approximately 10 wt% alumina. In the method followed in this thesis, the procedure took about 30 minutes, to reach a value of 12.5 wt% alumina in the sol-gel.

In **Step 3 (aging)** the same operating time of 48 h was used as in Kolaczkowski and Kim (2006).

According to Yoldas (1975), the aging step is also crucial as the degree of crystalline order, particle size, and the chemical composition of the gelatinous alumina depends critically on temperature, rate of precipitation, final pH, ionic composition, concentration of starting solutions, and time of aging.

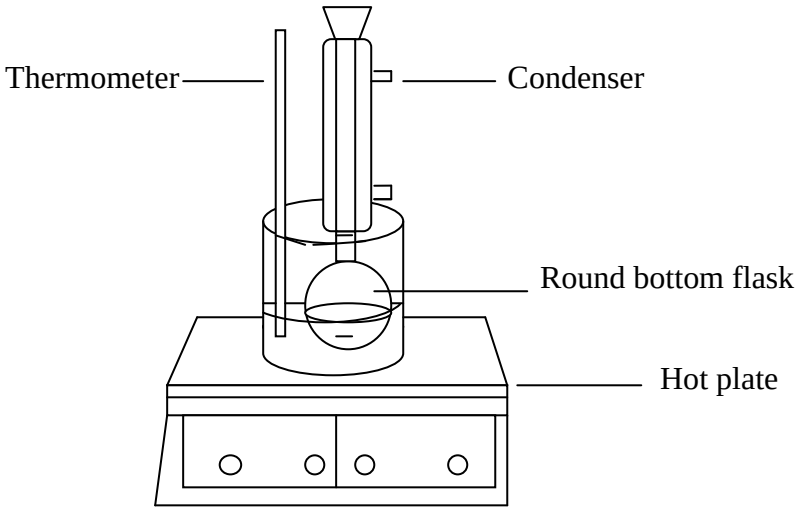

Figure 3.2 Apparatus used to prepare the sol-gel.

Table 3.1: Comparing the two methods of preparing the alumina sol-gel.

Method	**Step 1** **Hydrolysis**	**Step 2** **Peptization**	**Step 3** **Aging**	**Freeze-drying**
Kolaczkowski and Kim (2006)	1kg aluminium iso-propoxide + 5 litre of distilled water. [≡1g per 5 ml] T = 80 ºC	1) 0.05 mol of HCl per mol of aluminium iso-propoxide. 2) Zirconium nitrate was added. 3) Needs to be evaporated into half of the volume to produce 10 wt % alumina. Duration: 5-6 h T = 90 ºC	Duration: 48 h T = 80 ºC	Duration: 15 h T=-60 ºC
Current method in this thesis.	50 g aluminium iso-propoxide + 500 ml of distilled water. [≡1g per 10 ml] T = 80 ºC	1) 0.5 mol of HCl per mol of aluminium iso-propoxide 2) Half an hour of evaporation to produce 12.5 wt% alumina. T = 90 ºC	Duration: 48 h T = 90 ºC	Duration: 24 h T = -60 ºC

3.1.2 Sample coating

Having made the sol-gel, the sample to be coated was then:

(a) Dipped in the sol-gel for one minute.

(b) The sampled was dropped into liquid nitrogen for about 5 min and then removed and put in a round-bottom flask.

(c) The flask was then connected to a freeze drying unit for a duration of 24hours (see Figure 3.3.

(d) The sample was then calcined at 450^{o}C for about 5h.

A summary of the procedure followed is illustrated in Figure 3.4.

An example of what such a calcined sample looked like is shown in Figure 3.5 and this has a close similarity with the sample in Figure 3.1.

Figure 3.3 Photograph of freeze-drying unit.

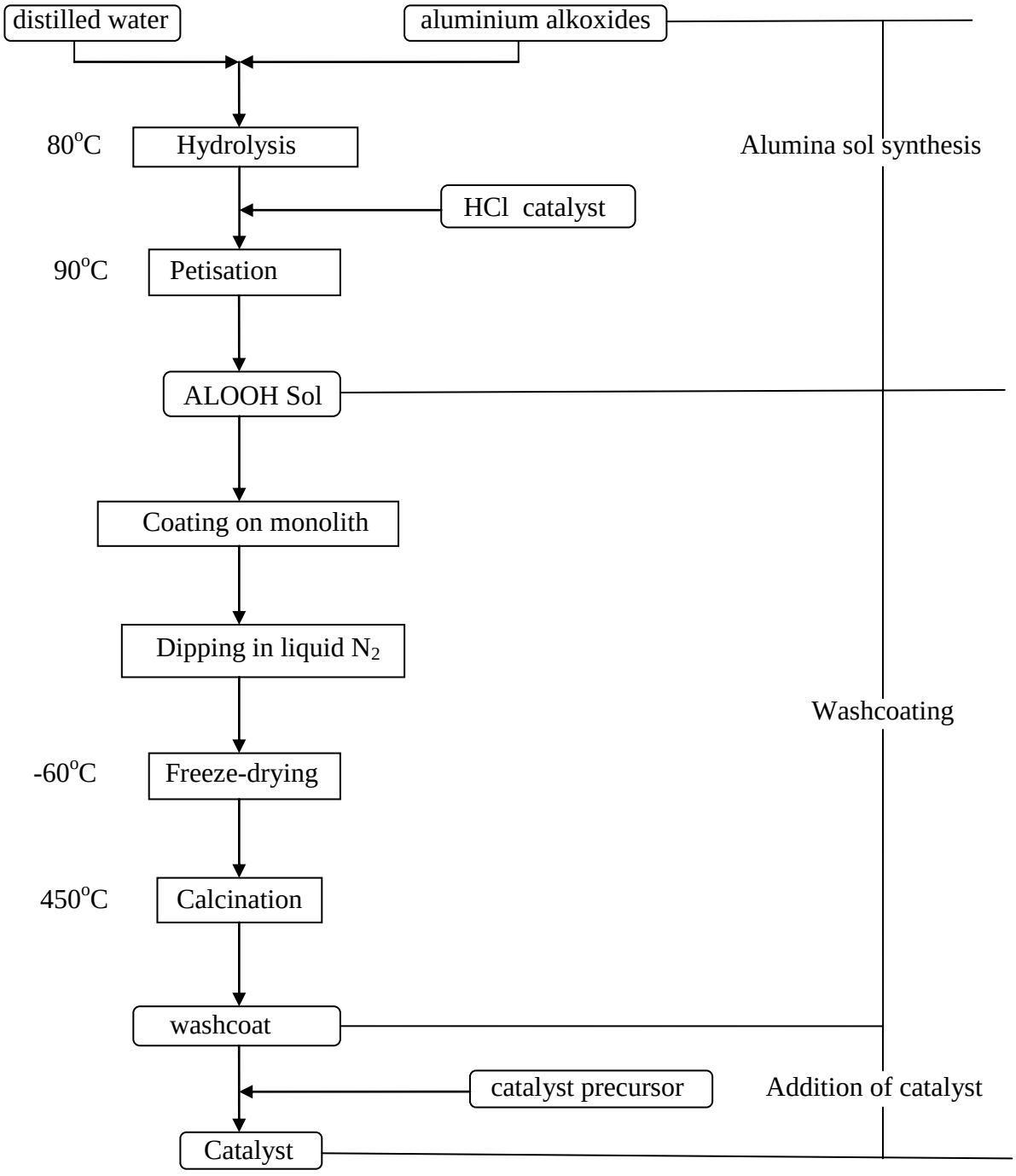

Figure 3.4 A summary of the procedure in this thesis.

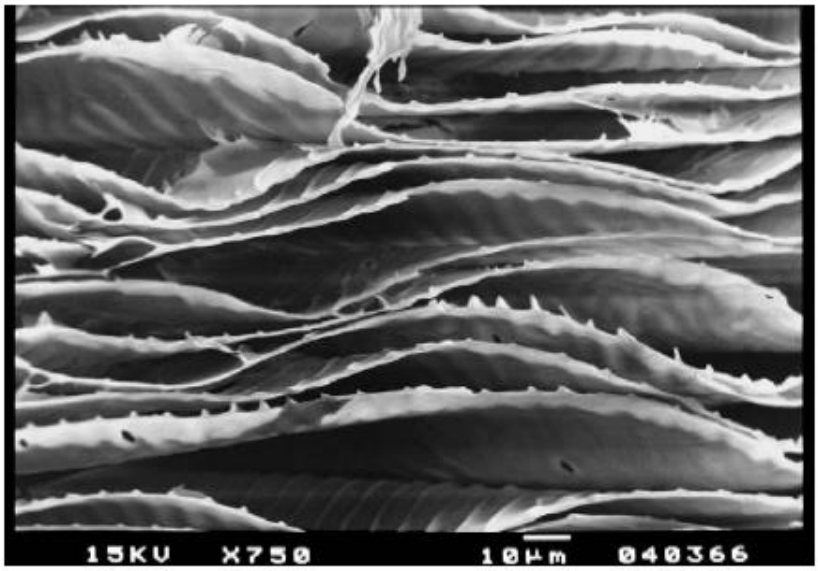

Figure 3.1(a) Extra copy of SEM image showing the loosely packed 'KK Leaves' on the surface of a sample that was formed in a glass dish (Kolaczkowski and Kim, 2006).

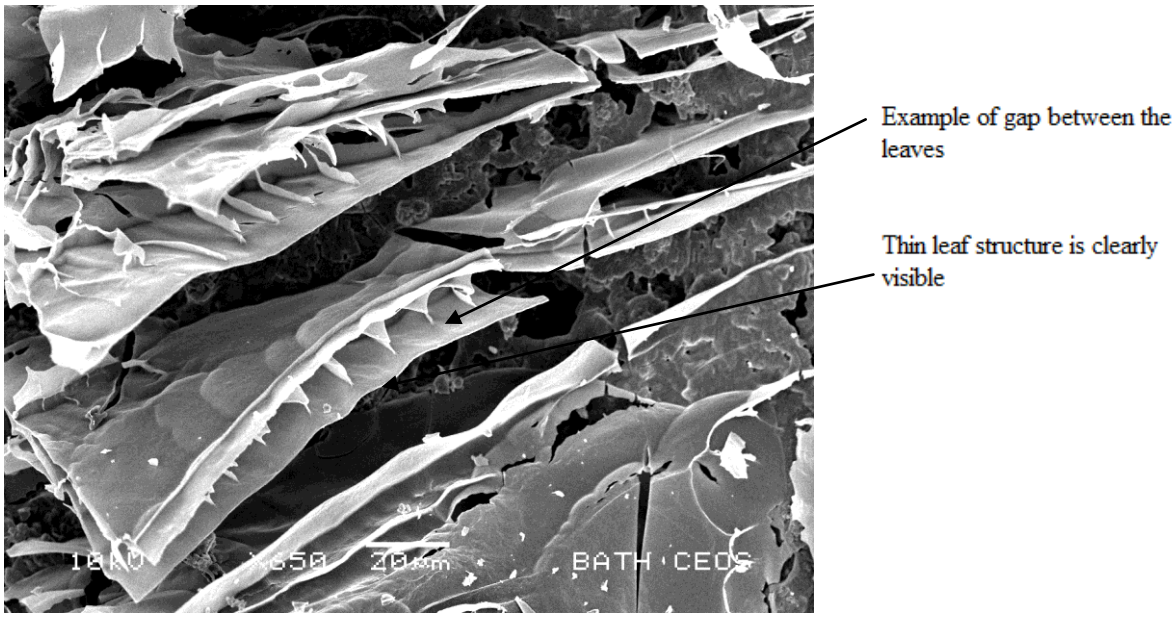

Figure 3.5 SEM image showing the leaf-like structures formed on a monolith in this thesis (sample dip-direction into liquid nitrogen was random).

Key observation No 1: ***This is very important as one of the questions on reproducibility of the results set at the start of this thesis has now been answered.***

In Kolaczkowski and Kim, a small quantity of zirconium nitrate had been added at the peptization stage (giving 1 wt% zirconia content in the KK leaves). The purpose of adding zirconia was to explore if the temperature to which the γ-alumina could be exposed could be increased without the occurrence of a phase change to forms that have a lower surface area. In the sample illustrated in Figure 3.5, zirconia was not used, so it was interesting to see that leaf-like structures could still be formed.

Key observation No 2: ***Zirconia is not necessary to create the leaf-like structures.***

Additional images of the structure formed in this thesis, and their attachment to a ceramic (cordierite) monolith support are presented in Figure 3.6. When the sol-gel coated monolith was dipped into the liquid nitrogen, the orientation of the channels relative to the liquid nitrogen surface as the sample was immersed was unknown (random).

From Figure 3.6, looking at the SEM images of the calcined sample:

- the layers tend to look more flat rather than having a curly leaf-like appearance;
- each leaf has a thickness of about 0.5-0.8μm;
- some of the leaves have pointed edges, while others have a flat side;
- the gaps between the layers are different, with the width between a pair of leaves ranging from about 10 to 30 μm.

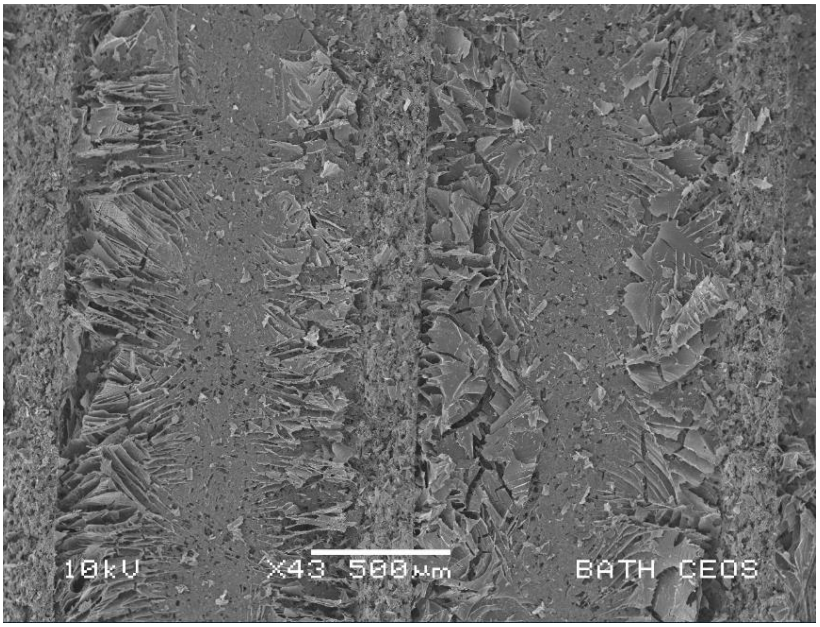

(a) View showing the leaves attached to the surface of the ceramic monolith wall.

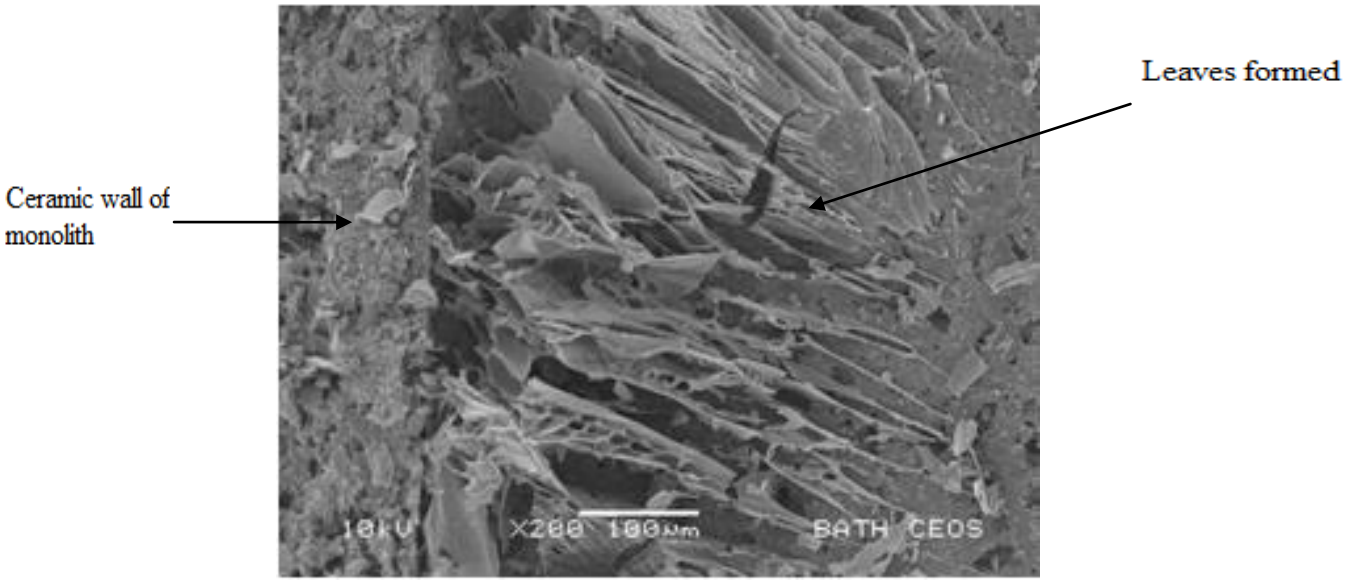

(b) Magnified view showing the leaves attached to the surface.

Figure 3.6 SEM images showing the loosely packed leaf-like structures in this thesis.

3.1.3 Sol-gel freezing in liquid nitrogen effect of dipping method

In order to explore if the way in which the sample was immersed in liquid nitrogen had an effect on the physical appearance of the structure formed, the following two different dipping methods were tested:

Method A: The sample was immersed with the axial direction of the channels parallel with the surface of the fluid (see Figure 3.7).

Method B: The sample was immersed with the axial direction of the channel perpendicular to the surface of the fluid (see Figure 3.7).

The sol-gel was prepared following the Standard Procedure as follows:

(a) 50 g of aluminium iso-propoxide (98wt%) was put in a 2L flask and 500 ml distilled water was added.

(b) The mixture was stirred (magnetic stir) for 20 min at 75^{o}C.

(c) 0.012 mol of 35 wt% HCl was added and the mixture was kept stirred for a further 30 min.

(d) The contents in the flask were stirred for a further 1 h at about 80^{o}C, to remove the residual group.

(e) A water cooled cold condenser was mounted on top of the flask, and the mixture was maintained at about 80^{o}C while stirring for 36 hours.

Sample coating: A piece of monolith was cut from a cordierite monolith block, and this had the following dimensions: length = 30 mm; width = 10 mm; and depth = 10 mm.

The monolith sample to be coated was then:

(a) Dipped in the sol-gel for one minute.

(b) Immersed into liquid nitrogen from the direction indicated in

- Figure 3.7 (a) for **Method A**, and
- Figure 3.7 (b) for **Method B**.

The sample was immersed for about 5 min, and then removed and put in a round-bottom flask.

(c) The flask was then connected to a freeze drying unit for duration of 24 hours.

(d) The sample was then calcined at 450ºC for about 5 h.

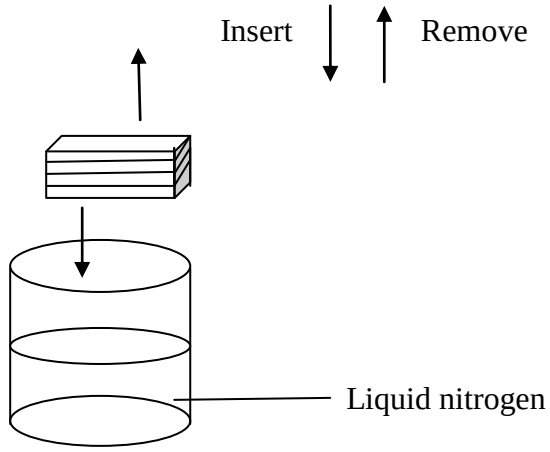

(a) Method A

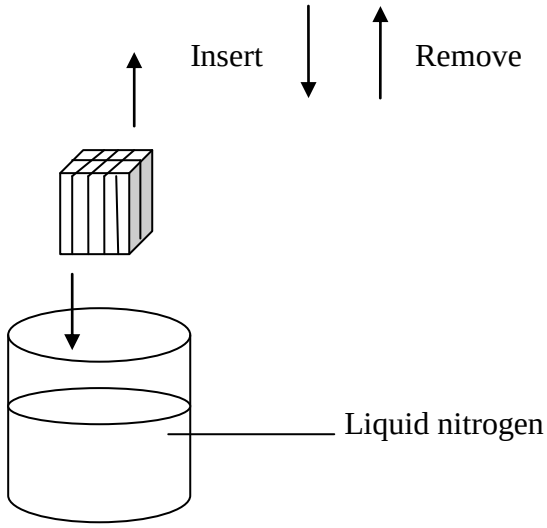

(b) Method B

Figure 3.6 Schematics illustrating the two different methods used to insert the sol-gel coated monolith sample into liquid nitrogen.

In the earlier experiments shown in Figure 3.5, the leaves consist of one dimensional nano-layer with a thickness of about 0.5-0. 8μm. The sample was place in the liquid nitrogen in a random manner**.**

However, when using **Method A**, the results show that a slightly different form of structure has been formed (see Figure 3.8). The leaf-like layers look more crumpled, and the enlarged image in Figure 3.8 (d) shows the structure formed in the more porous layer.

In **Method B**, the method of dipping made it easier for the liquid nitrogen to enter the channels as the sample was immersed, and then to drain from the channels when the sample was removed. Most interestingly, the resulting SEM images in Figure 3.9 show a different form of structure, which contains cracks that are about 20 μm in width.

Key observation No 3: ***This demonstrates that the way in which the sample is dipped into the liquid nitrogen and is then removed, affects the shape of the structures formed.***

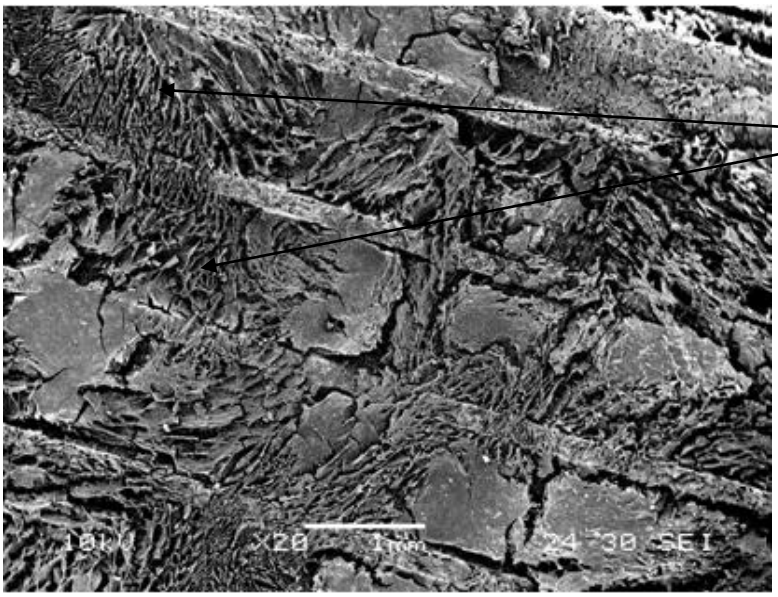

(a) View of the surface at low magnification (cordierite wall of the channels are clearly visable).

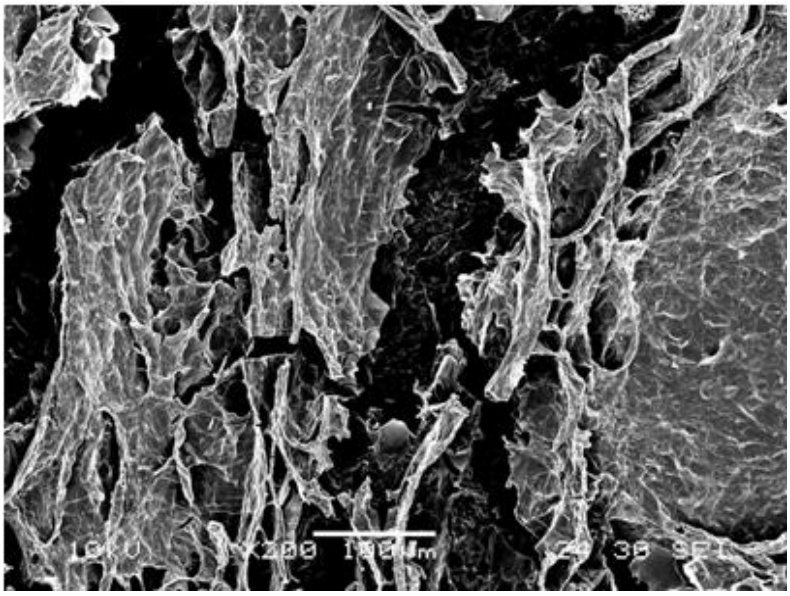

(b) View of the surface at higher magnification

Figure 3.8 SEM images of a sol-gel monolith after it had been dipped in liquid nitrogen using **Method A**, and then dried and calcined (cont.).

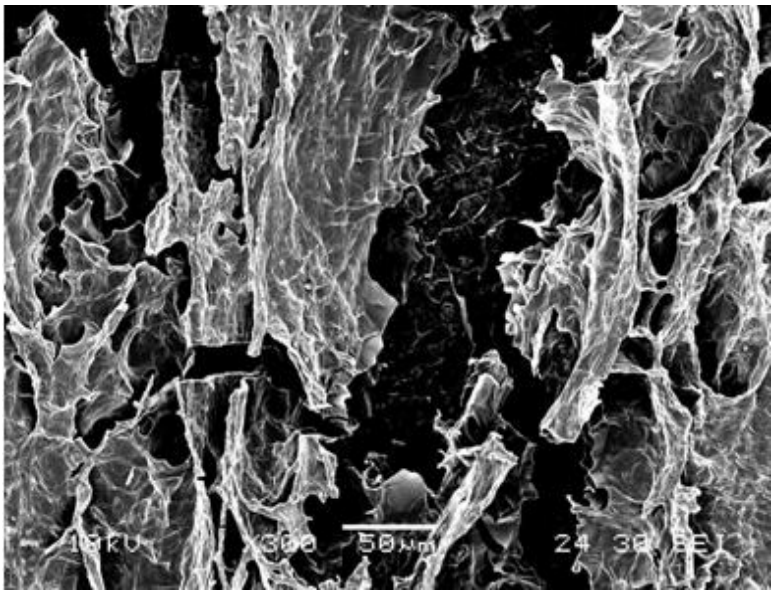

(c) View of the surface shows the crack width at about 50 µm

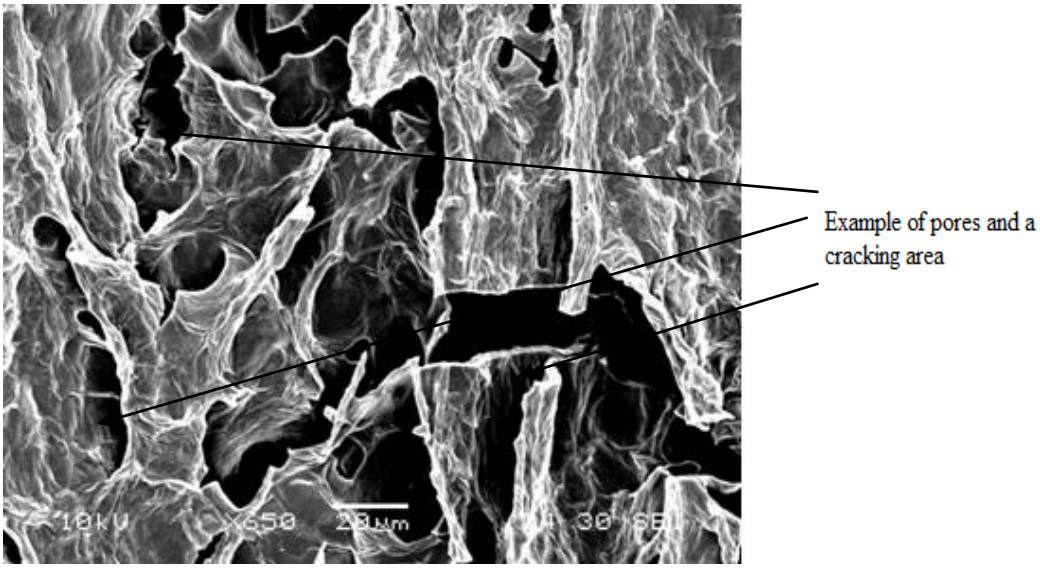

(d) Magnified view of a surface which is more porous (this shows surface cracking, and the size and shape of pores).

Figure 3.8 (cont.) SEM images of a sol-gel monolith after it had been dipped in liquid nitrogen using **Method A**, and then dried and calcined.

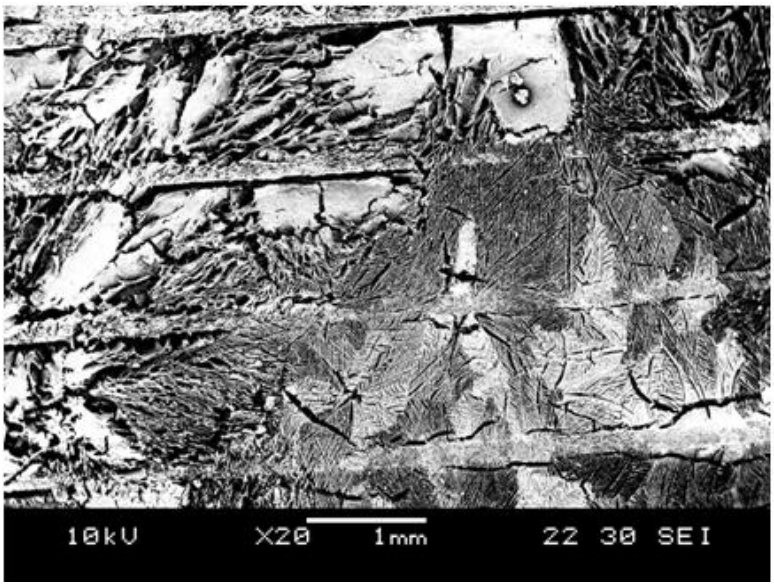

(a) View of the washcoated monolith at low magnification

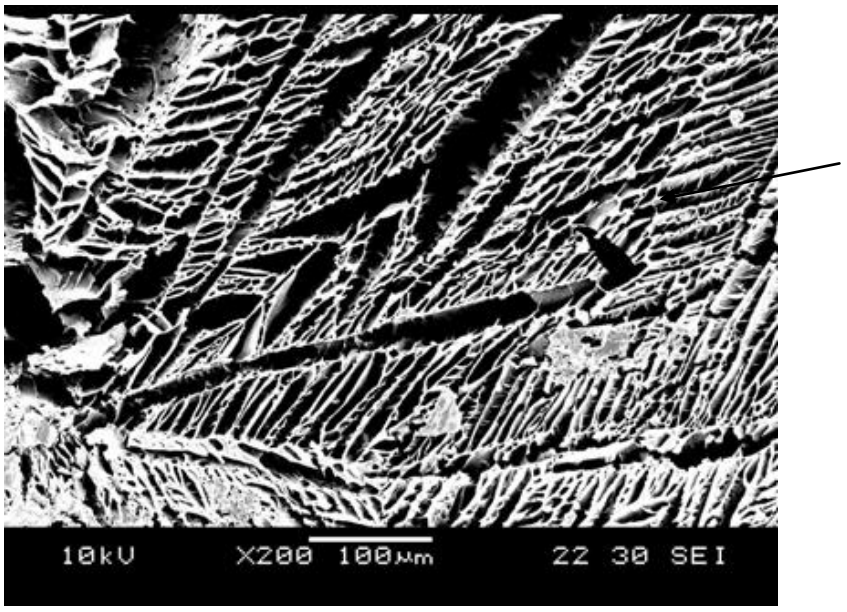

(b) View of a honeycomb like structure

Figure 3.9 SEM images of a sol-gel monolith after it had been dipped in liquid nitrogen using **Method B**, and then dried and calcined (cont.).

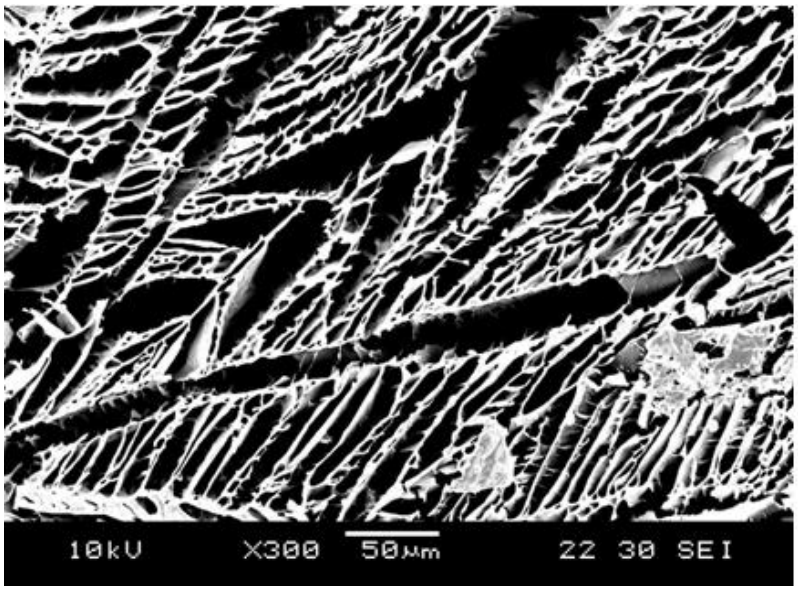

(c) View of a coated monolith at higher magnification

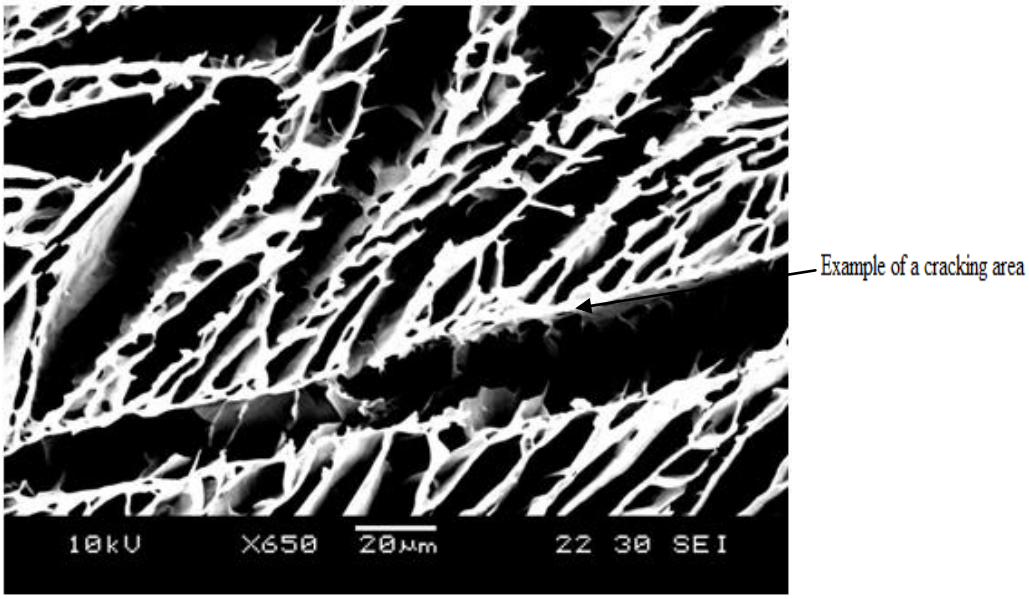

(d) Magnified view of the surface

Figure 3.9 (cont.) SEM images of a sol-gel monolith after it had been dipped in liquid nitrogen using **Method B**, and then dried and calcined.

3.1.4 Using a commercial form of sol-gel

In Nijhuis *et al.*, (2001) an alumina sol was prepared from:

- Alumina sol (DISPAL 14N4-25),
- urea, and
- 0.3M HNO_3 solution,

in a weight ratio of 2:1:5. It was decided to follow this procedure.

These chemicals were mixed using a high-shear mixer. The formation of large three dimensional alumina networks was prevented by the addition of a polar acid, which created positive charged agglomerates. The mixture was stirred for 10 minutes, and the pH was 1.2 at the end of the reaction.

It is interesting to note, that by using this method the sol-gel was formed within 10 minutes. The sol-gel was used to coat a monolith which was freeze-dried and then calcined. SEMs of the final calcined samples are illustrated in Figure 3.10, and these do not show any evidence of the KK leaf structures. Instead, the material looks more like a paste with fine cracks.

Key observation No 4: ***This demonstrates that the way in which the alumina sol is formed affects the shape of the structures formed.***

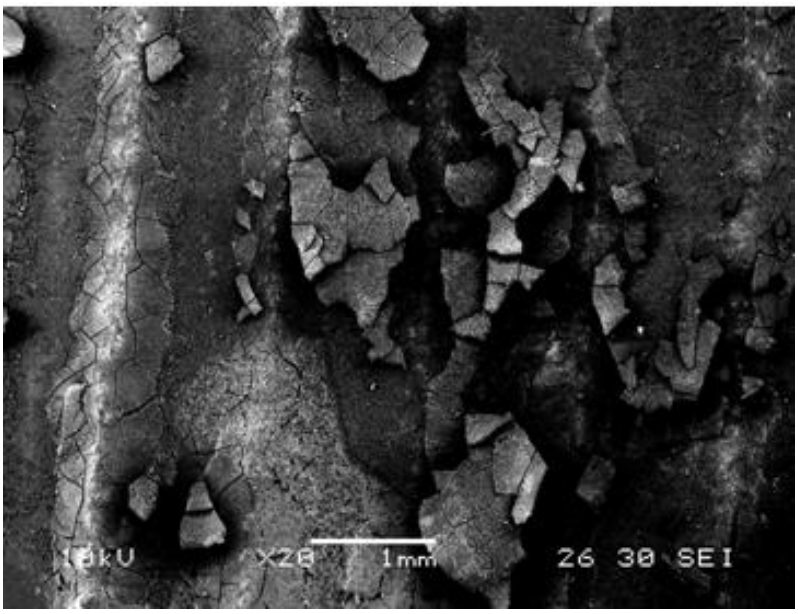

(a) View showing the wash coated monolith.

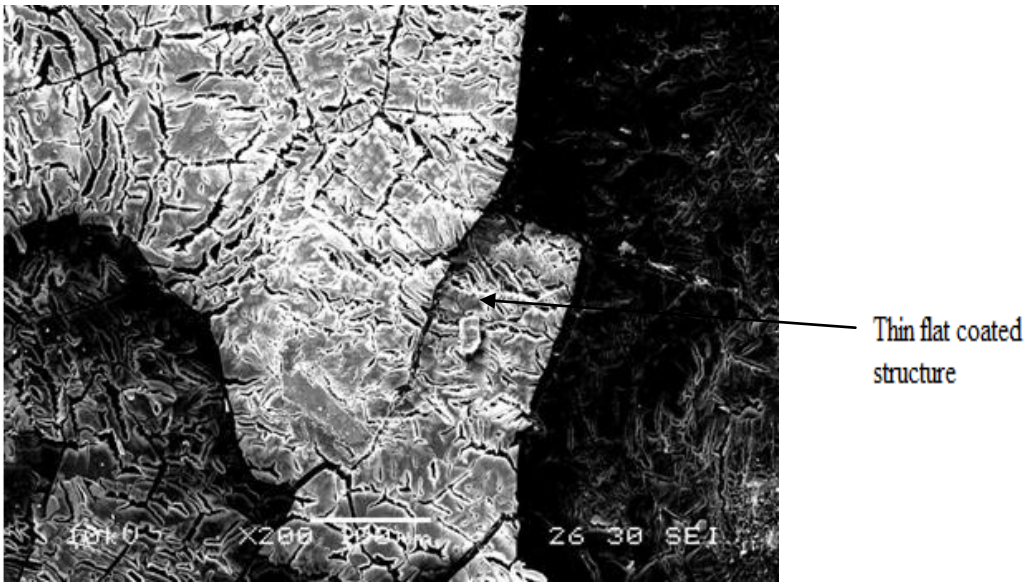

(b) View showing the flat wash coating attached to the surface of the ceramic monolith wall.

Figure 3.10 SEM images showing the structure of washcoated monoliths formed using a commercial ready made alumina sol (cont.).

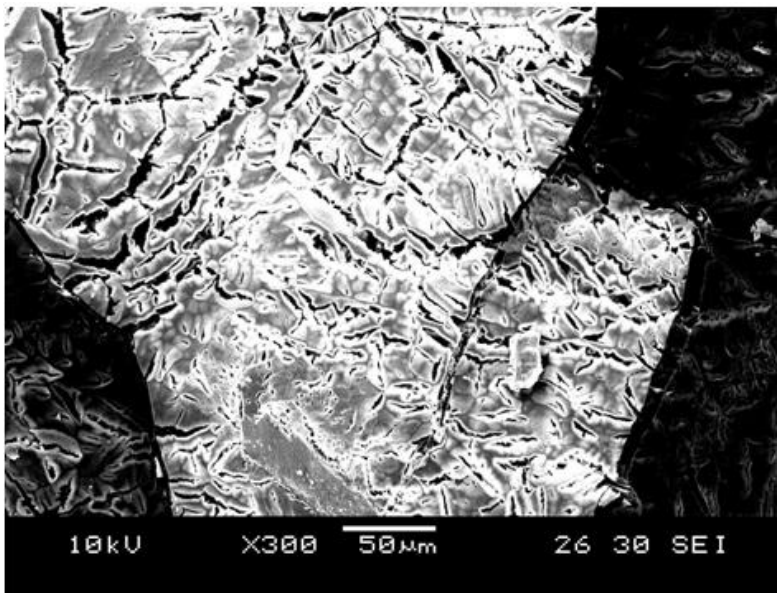

(c) Magnified view of coated monolith.

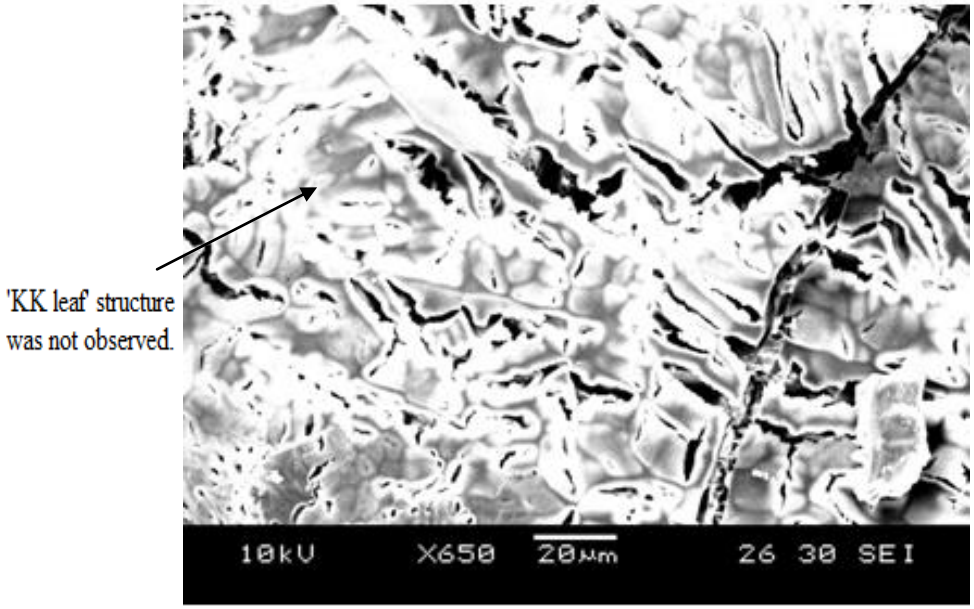

(d) Magnified view of surface.

Figure 3.10 (cont.) SEM images showing the structure of washcoated monoliths formed using a commercial ready made alumina sol.

3.1.5 Dipping the sample into liquid nitrogen and then drying and calcining without using the freeze-drying unit

In this set of experiments, it was decided to explore what the structures may look like if the sample as it is withdrawn from the liquid nitrogen is just dried and calcined (without using the freeze-drying unit). The sol gel was prepared following the Standard Procedure as follows:

(a) 50 g of aluminium iso-propoxide (98wt%) was put in a 2L flask and 500 ml distilled water was added.

(b) The mixture was stirred (magnetic stir) for 20 min at 75^{o}C.

(c) 0.012 mol of 35 wt% HCl was added while stirring for a further 30 min.

(d) The contents in the flask were stirred for a further 1 h at about 80^{o}C, to remove the residual group.

(e) A water cooled cold condenser was mounted on top of the flask, and the mixture was maintained at about 80^{o}C while stirring for 36 hours.

Sample coating: Two pieces of monolith were cut from a cordierite monolith block, and these had the following approximate dimensions: length = 30 mm; width = 10 mm; and depth = 10 mm. The samples to be coated were then:

(a) dipped in the sol-gel for 1 min, and then

(b) completely immersed into liquid nitrogen for 5 min.

(c) These two samples were then put into the fume cupboard to dry for 24 h (a freeze-drying unit was not used).

(d) The samples were then calcined at 450^{o}C for 5 h**.**

Figure 3.11 shows the SEM images of alumina wash coated monolith produced under these conditions, and it is clear that the surface looks very flat.

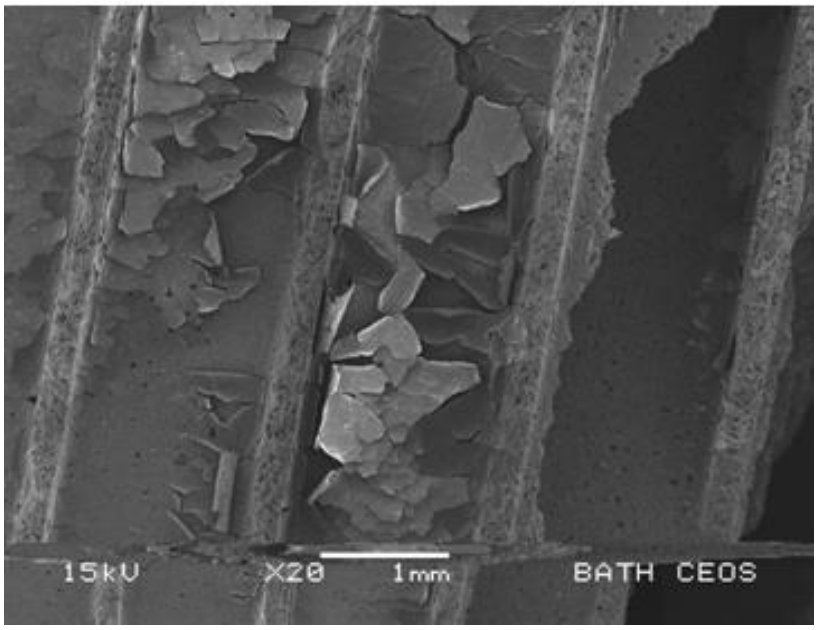

(a) View showing the surface of the coated monolith without using a freeze drying unit.

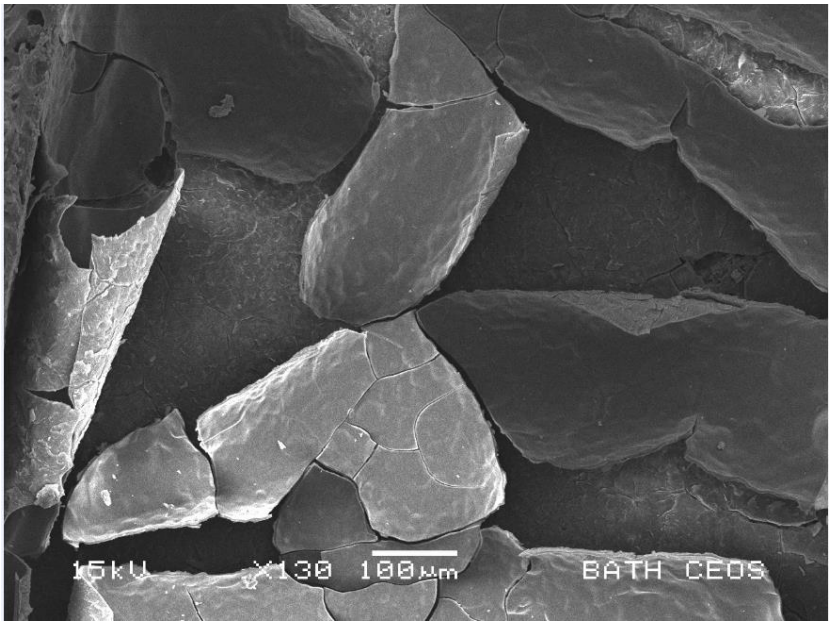

(b) View showing a single layer of coated surface without using a freeze drying unit.

Figure 3.11 SEM images showing a single flat layer of the surface of a sample that was prepared on a ceramic monolith without using the freeze-drying unit (cont.).

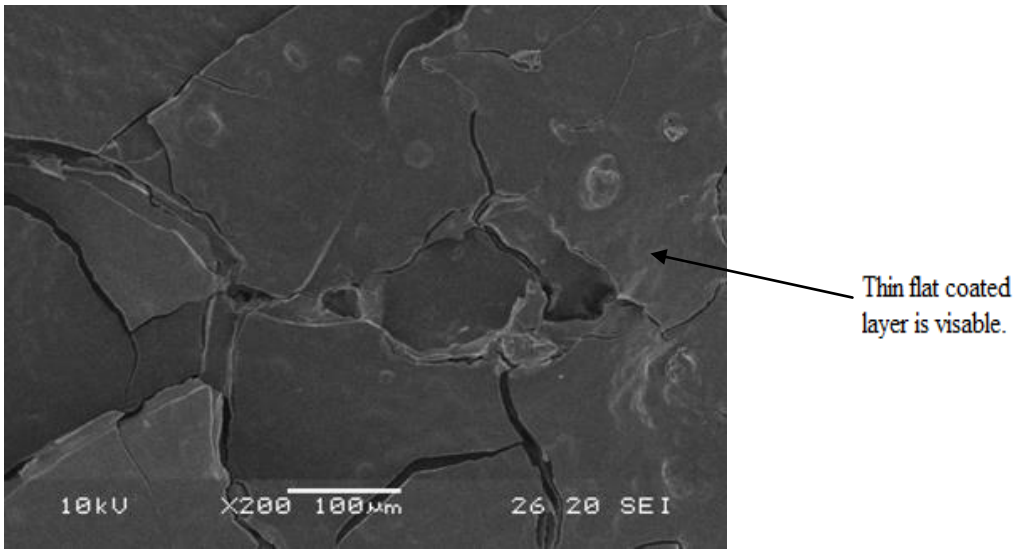

(c) View showing the surface of the coated structure without using a freeze drying unit.

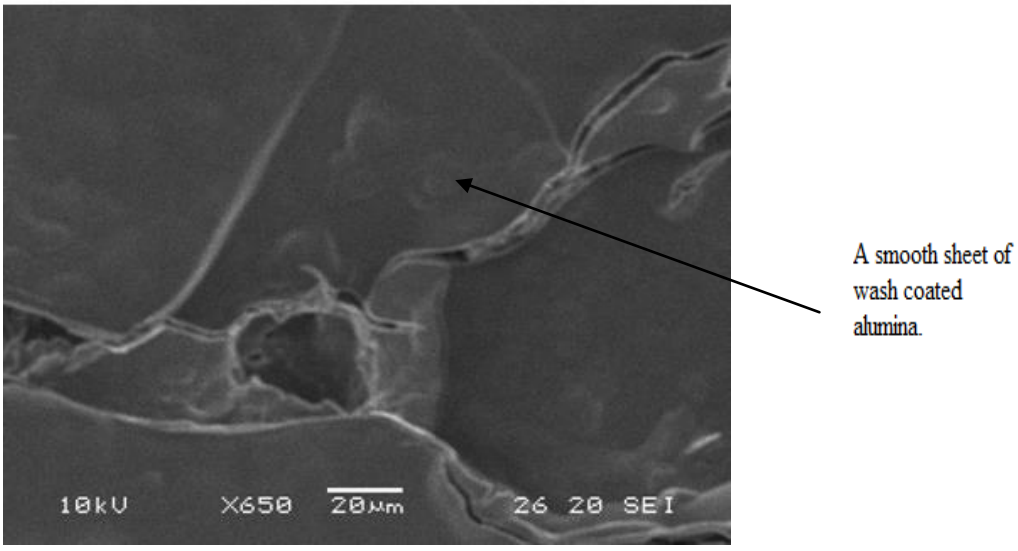

(d) Magnified view of surface.

Figure 3.11 (cont.) SEM images showing a single flat layer of the surface of a sample that was prepared on a ceramic monolith without using the freeze-drying unit.

It was found, that after calcination, the alumina layer peeled-off easily and no leaf-like structures could be observed. It can therefore be concluded, that the freeze-drying method is very likely to play a key role in the formation of the KK leaves. Based on information in Freeze-drying (Oetjen and Haseley, *2004)*, the following explanation is offered. Water molecules normally surround ions in a liquid phase, however, some water molecules are clusters and consist of approximately 10 water molecules in a tetrahedral geometry surrounded by O-H-O groups. The clusters are not stable units (they do not remain with the same molecules) they constantly exchange molecules with their surroundings and have an average lifetime of between 10^{-10} and 10^{-1} s. The number of clusters decreases as the temperature is lowered until freezing occurs. In water which is very well cleared of all foreign particles, the clusters begin to crystallize in the subcooled water at -39^{o}C – and this is called homogeneous nucleation. Foreign, un-dissolved particles in water act as nuclei for the crystallization of ice and this is called heterogeneous nucleation (Oetjen and Haseley, 2004, p.14). When water is frozen into ice at -18^{o}C, it forms icy crystals. The alumina in the sol-gel probably acts as nuclei for the crystallization of ice and produces the KK leaf-like structures observed.

<u>Key observation No 5:</u> ***This demonstrates that the freeze-drying step is an essential part of the process to aid the formation of KK leaves.***

3.1.6 Formation of a double-coated alumina washcoat layer on a monolith

In Kolaczkowski and Kim (2006), they presented the results of work in which a double-layer of KK leaves had been formed on a monolith. In this section, an attempt is made to apply such a double layer, using the slightly modified sol-gel preparation procedure described in this thesis.

The sol-gel was prepared following the Standard Procedure:

(a) 50 g of aluminium iso-propoxide (98wt%) was put in a 2L flask and 500 ml distilled water was added.

(b) The mixture was stirred (magnetic stir) for 20 min at 75^{o}C.

(f) 0.012 mol of 35 wt% HCl was added and the mixture was kept stirred for a further 30 min.

(g) The contents in the flask were stirred for a further 1 h at about 80^{o}C, to remove the residual group.

(h) A water cooled cold condenser was mounted on top of the flask, and the mixture was maintained at about 80^{o}C while stirring for 36 hours.

Sample coating: A piece of monolith was cut from a cordierite monolith block, and this had the following approximate dimensions: length = 30 mm; width = 10 mm; and depth = 10 mm. The sample to be coated was then:

(a) dipped in the sol-gel for 1 min, and then

(b) completely immersed using method B into liquid nitrogen for 5 min

(c) freeze-dried, and

(d) calcined at 450^{o}C for 5 h.

The procedure in (a) to (d) was then repeated to obtain a double coating. The direction of dipping into the bath of liquid nitrogen was the same as the first coating (method B used).

The SEM images of a double coated monolith are shown in Figure 3.12. The magnified image reveals that the layers consist of one layer above another layer of multi-leaves.

<u>Key observation No 6:</u> ***This demonstrates that double-layers of alumina can be deposited using the freeze-drying method.***

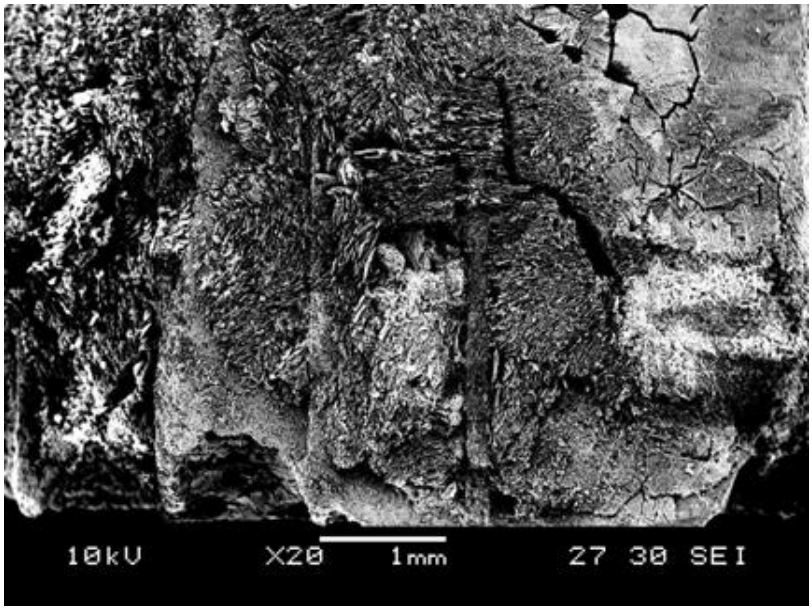

(a) View showing a freeze-dried double coated monolith.

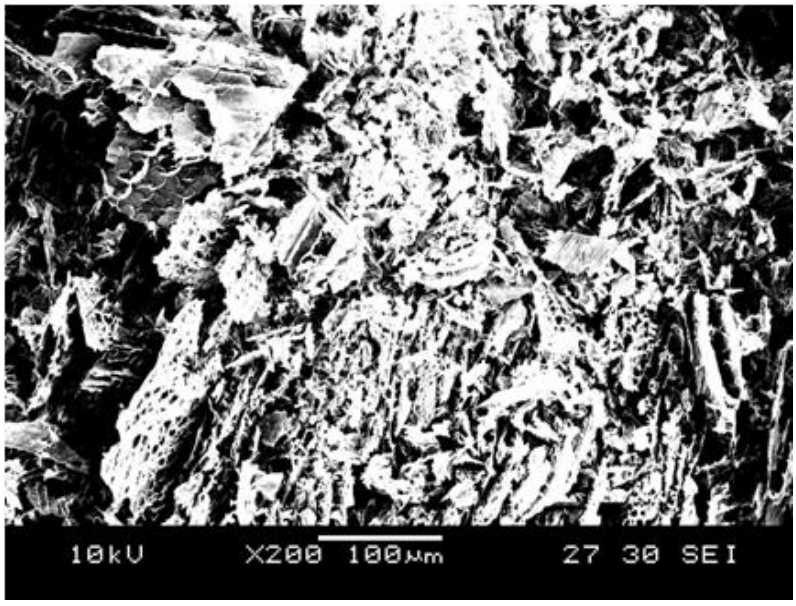

(b) View showing a freeze-dried double coated monolith surface.

Figure 3.12 SEM images showing a double-layered alumina coated monolith (cont.).

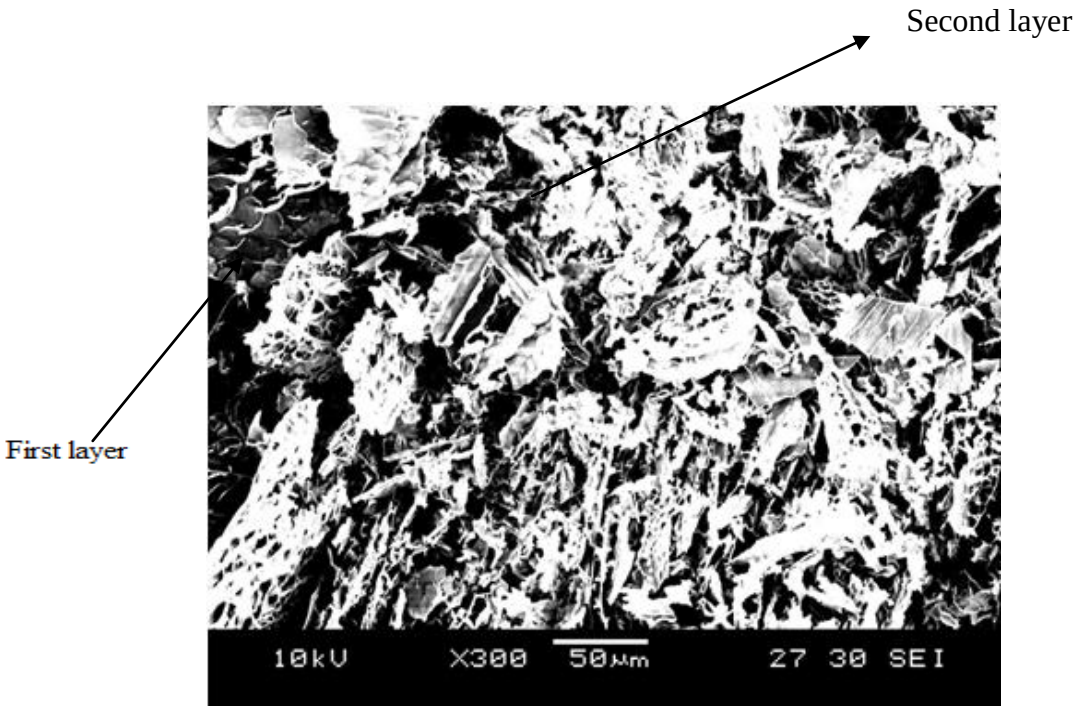

(c) Magnified view of double coated surface.

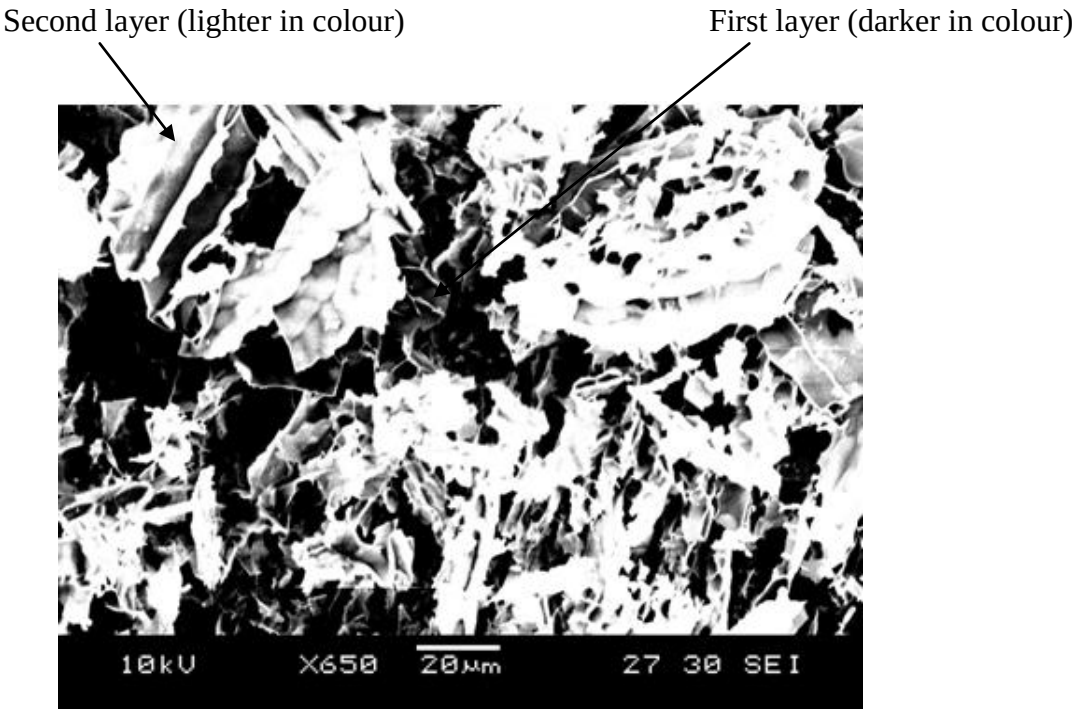

(d) Magnified view of surface.

Figure 3.12 (cont.) SEM images showing a double-layered alumina coated monolith.

3.1.7 Alumina-sol washcoating of wire meshes with freeze-drying and calcining

The motivation for exploring the coating of wire meshes, arose from:

- the ability to examine what the structure looked like more easily (easier to see than inside a channel in a monolith),
- an interest in how the structure would form in the interstitial gaps between the wire mesh,
- an interest in the potential use of these wire mesh supports as catalyst supports.

The particular type of wire structure that was studied in this section is known as a Dixon ring, and one of these is illustrated in Figure 3.13. These were developed (Alford *et al.*, 2011) as packing material which could be used in distillation columns. More recently, there has been renewed interest in the use of this packing in compact gas scrubbers (Alford *et al.*, 2011), and there was also an interest expressed by a catalyst supplier in the use of these Dixon rings as catalyst supports (Kolaczkowski 2001).

Based on earlier work at the University of Bath, experience had been gained with the use of a high efficiency form of column packing material known as Dixon rings (Dixon (1948 & 1949)), so these were selected for the experiments in which the use of water as a gas scrubbing fluid was used in a packed column (Nuckols *et al.* (2011)). Although the existence of Dixon rings has been known for more than 60 years, it is only relatively recently (over the last 2 years), that manufacturing techniques have improved, and the price of Dixon rings enables them to be considered for many more applications (Kolaczkowski (2011)).

The Dixon rings used had the following properties:

Size:	length = 4 mm; o.d. = 3.175 mm
Wire diameter:	0.02 mm
Aperture:	0.05 mm x 0.05 mm
Material:	stainless steel

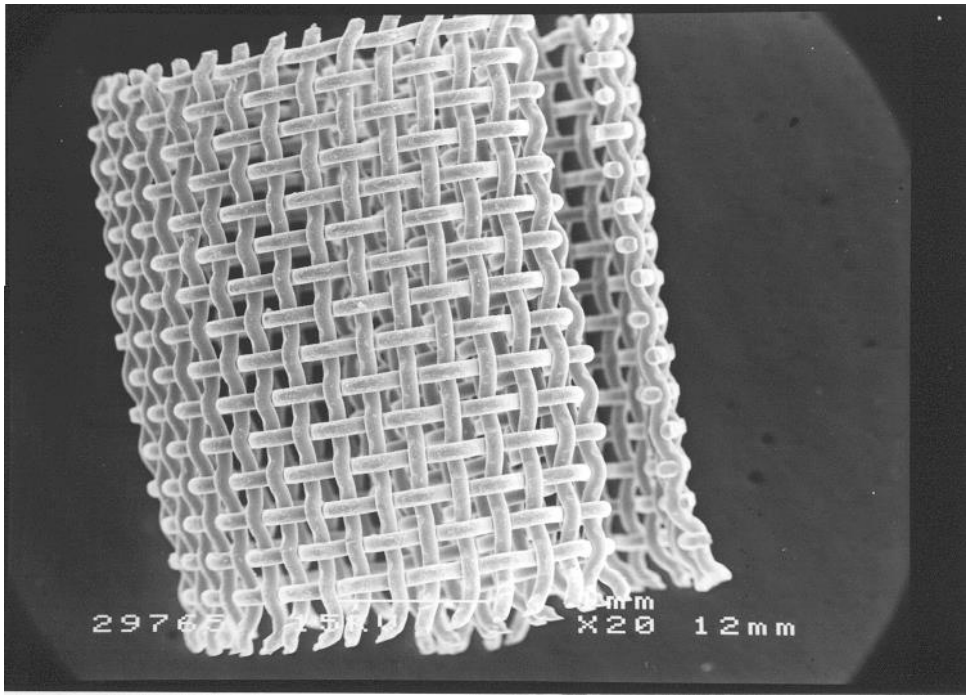

(a)

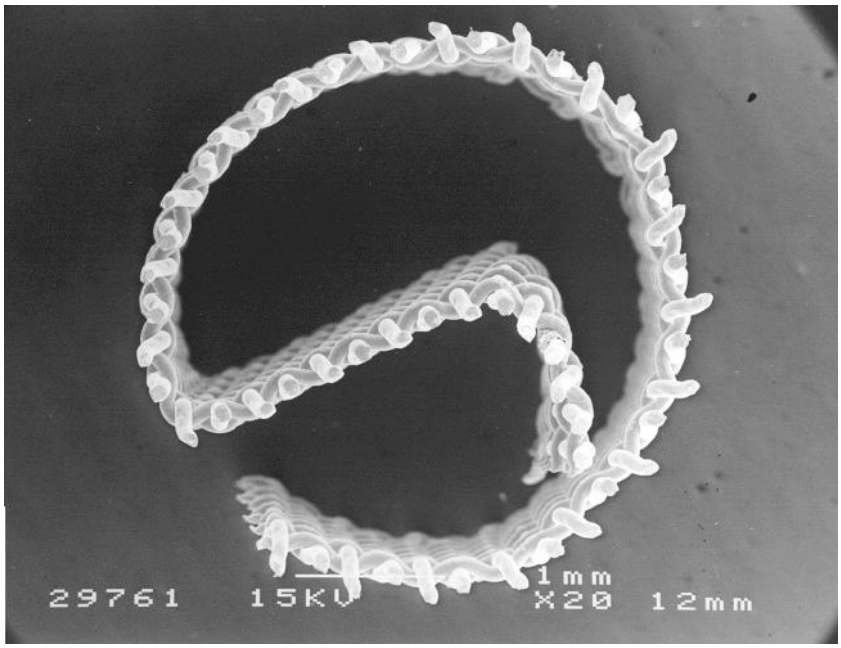

(b)

Figure 3. 13 Example of a 3 mm Dixon ring (a) side view, (b) top view (with permission Kolaczkowski, University of Bath).

These rings were coated using an alumina sol-gel that had been prepared following the Standard Procedure. The wire meshes were coated in the same manner as the monoliths had been.

After calcining at 450^{o}C, there were signs that some of the washcoat had peeled off the Dixon rings. However, the SEM images presented in Figure 3.14, do show that some interesting structures had been formed. It is clear that micro-sized flakes and also nano-sized flakes had been formed on the surface of the wire mesh.

Key observation No 7: ***This demonstrates that Dixon rings could be used to support an alumina structure, which has micro- and nano-sized flakes which could act as suitable catalyst supports.***

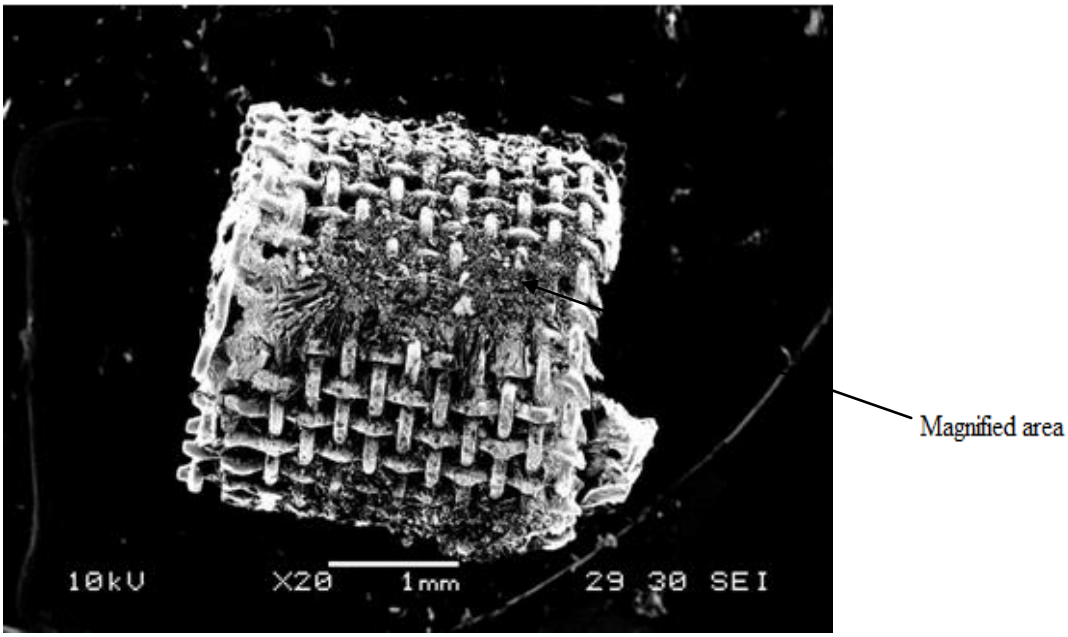

(a) View showing the coated wire mesh.

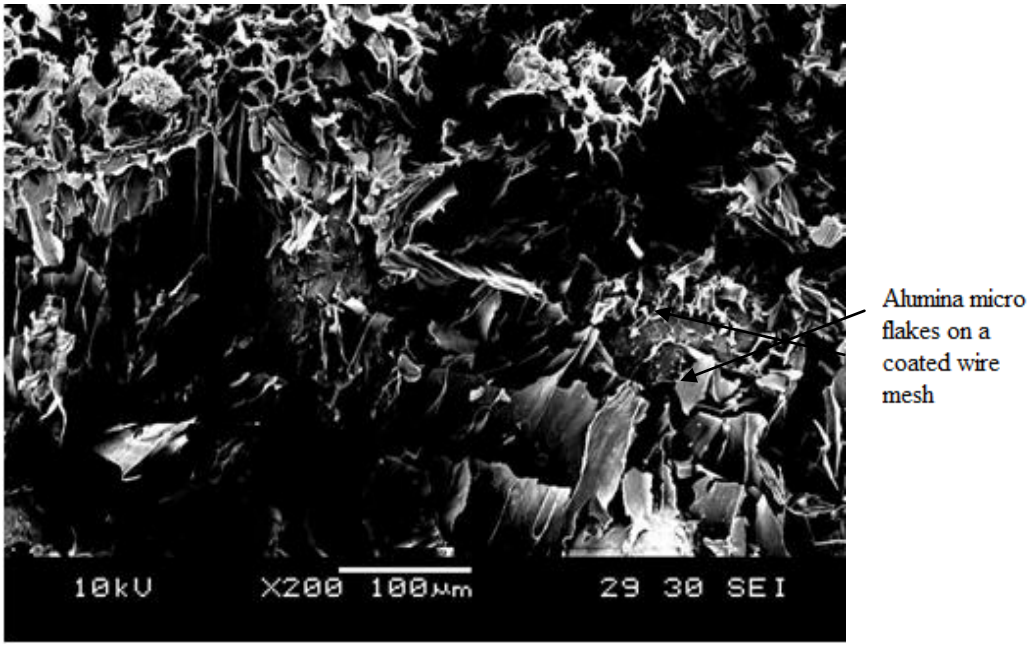

(b) Magnified view showing alumina flakes on the coated wire mesh.

Figure 3.14 SEM images showing the structure of a sample that was formed on a wire mesh (Dixon ring) (cont.).

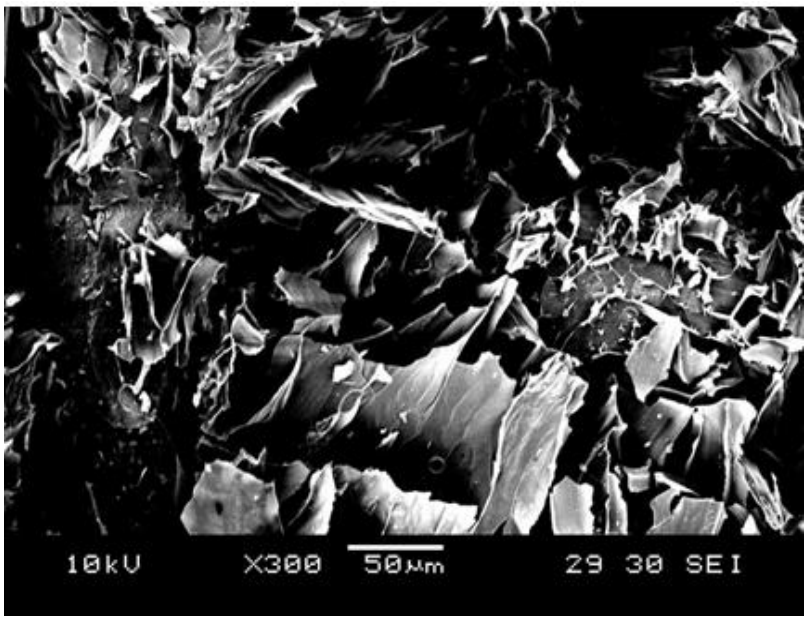

(c) Magnified view showing alumina flakes on coated wire meshes.

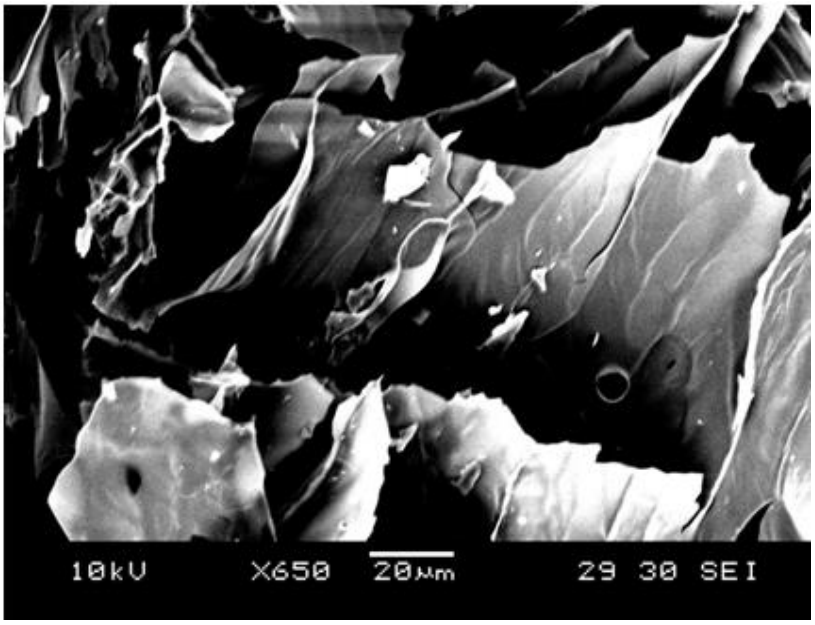

(d) Magnified view of structure formed.

Figure 3.14 (cont.) SEM images showing the structure of a sample that was formed on a wire mesh (Dixon ring).

3.2 Structures formed using a silica sol-gel with freeze-drying and calcining

Silica can also be used as a catalyst support, and hence it was decided to explore what structures could be formed if the sol-gel technique was combined with freeze-drying and calcining.

3.2.1 Preparing the silica sol-gel

Based on information in Brinker and Schere (1990), silicate gels are usually synthesized by hydrolyzing precursors and the most common tetra alkoxysilanes used in the sol-gel process are:

- tetraethoxysilane ($Si(OC_2H_5)_4$) abbreviated as TEOS, and
- tetramethoxysilane ($Si(OCH_3)_4$) abbreviated as TMOS.

The tetraalkoxysilanes are prepared by reacting tetrachlorosilane with alcohol.

$$SiCl_4 + EtOH \longrightarrow Si(OEt)_4 + 4HCl \qquad (3.5)$$

The three reactions which are generally used to describe the sol-gel process are:

Hydrolysis

$$Si\text{-}OR + H_2O \longrightarrow Si\text{-}OH + ROH \qquad (3.6)$$

Alcohol condensation

$$Si\text{-}OR + HO\text{-}Si \longrightarrow Si\text{-}O\text{-}Si + ROH \qquad (3.7)$$

Water condensation

$$Si\text{-}OH + HO\text{-}Si \longrightarrow Si\text{-}O\text{-}Si + H_2O \qquad (3.8)$$

where R is an alkyl group, C_XH_{2X+1}.

The hydrolysis reaction (3.6) replaces alkoxide group (OR) with hydroxyl groups (OH). The subsequent condensation reaction involving the silanol groups produce siloxane bonds (Si-O-Si) plus the by–products alcohol (ROH) reaction (3.7) or water in reaction (3.8). Under most conditions, condensation commences with reactions (3.7 and 3.8) before the hydrolysis reation (3.6) is complete. Gels can be prepared from a silicon alkoxide water mixture, without adding solvent since the alcohol is produced as a by-product of the hydrolysis reaction. Alcohol is not simply a solvent, it can participate in esterification or alcoholysis reactions (3.7 and 3.8).

Gelation: this results in the formation of a solid network from the whole volume of the original sol. A rapid increase in sol viscosity signals the outcome of gelation, which must be achieved in such a way that the particles join together and neighbouring aggregates are in contact to form a solid network. For the preparation of silica gels the tetraethyl orthosilicate (TEOS) is the common used alkoxides. Alcohols are used as the solvents, but may also be involved in the reactions. Ammonia or mineral acids are the frequently used as catalysts.

The silica sol-gel was prepared as follows:

(a) Tetraethyl orthosilicate $Si(OEt)_4$ (TEOS, 98wt%, Aldrich) was the starting alkoxide.

(b) Ethanol was used as the solvent.

(c) Aqueous ammonia NH_4OH (28wt%) was used as the catalyst.

(d) Distilled water was used.

(e) The molar ratios used were as follows:

- TEOS = 0.2,
- distilled water = 22
- ethanol = 1.6

- aqueous ammonia = 0.7.

(f) 30.44g of TEOS was put into a 2 litre flask and 400 ml distilled water and 73.6 g ethanol was added. The mixture was stirred with a magnetic stir for 20 min at 35^{o}C.

(g) 24.5g of 35wt% aqueous ammonia was added and the mixture was kept stirred for a further 2 h.

(h) Aging: Gelation is the first stage to produce a continuous solid network in the sol; the reaction does not stop but instead continues to develop the structures. There are four possible processes, polycondensation, syneresis, and coarsening and phase formation. A number of parameters can affect the aging process, temperature; pH and time are considered as the main factors. In the current experiments, aging is carried out at room temperature for 6 h.

3.2.2 Dipping into liquid nitrogen then freeze-drying and calcination

A similar coating procedure was followed, using samples of ceramic monolith. Having made the sol-gel, the sample to be coated was then:

(a) Dipped in the sol-gel for 1 min.

(b) The sample was dropped into liquid nitrogen for about 10 min and then removed and put in a round-bottom flask.

(c) The flask was then connected to a freeze drying unit for duration of 24 hours.

(d) The sample was then calcined at 450^{o}C for about 5 h.

An example of what such a calcined sample looked like is shown in Figure 3.15. This structure:

- consists of a variety of leaf-shaped nano-thin walled structures, which have tunnel in their walls - these are most interesting, and
- although they have some similarity they are different in form from the KK leaves.

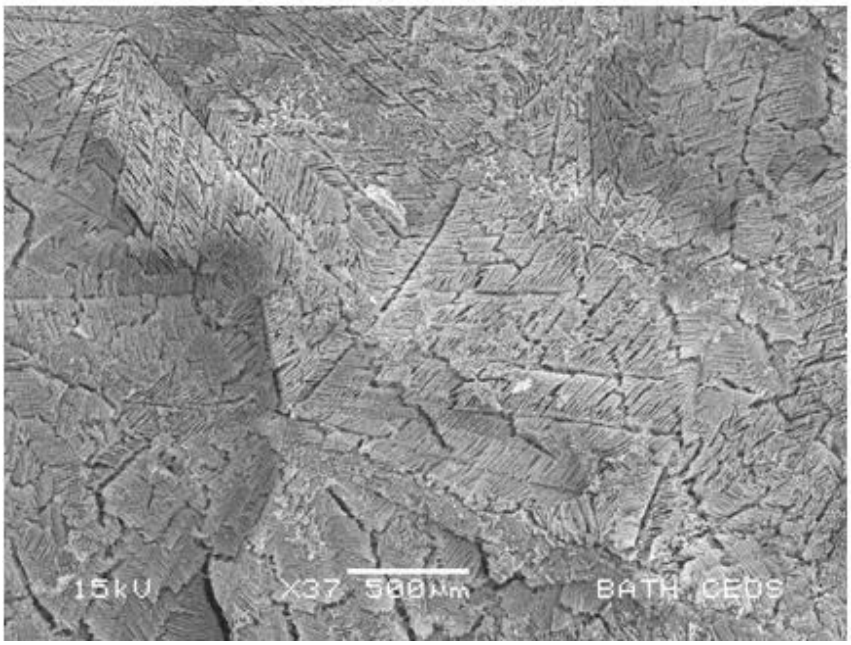

(a) Structures formed starting with a silica sol-gel.

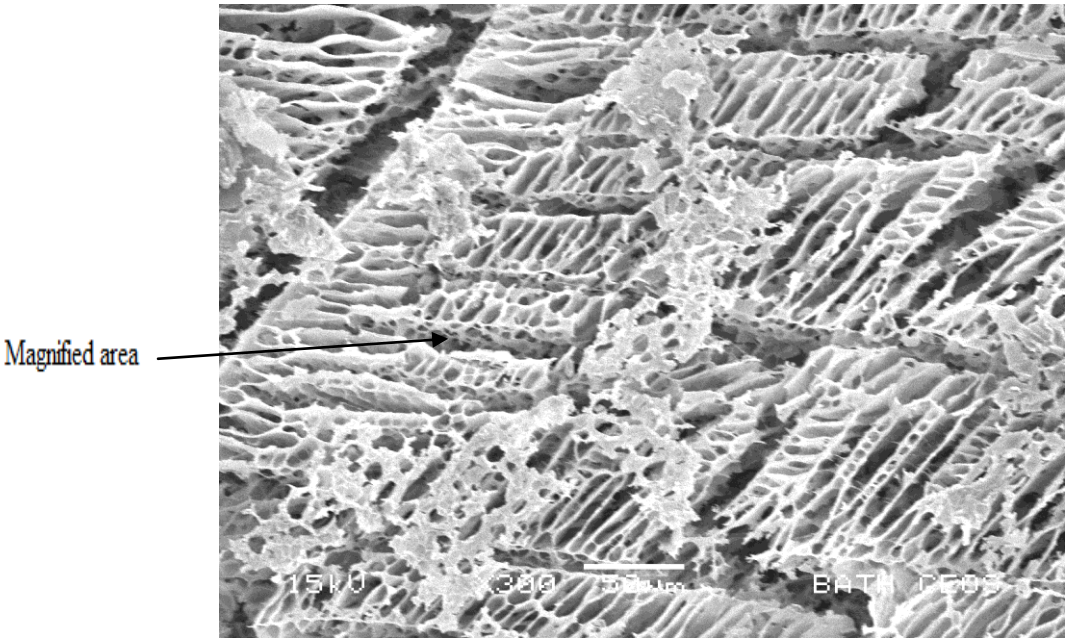

(b) Magnified view of coated monolith.

Figure 3.15 SEM images showing the structure formed starting with a silica sol-gel (cont.).

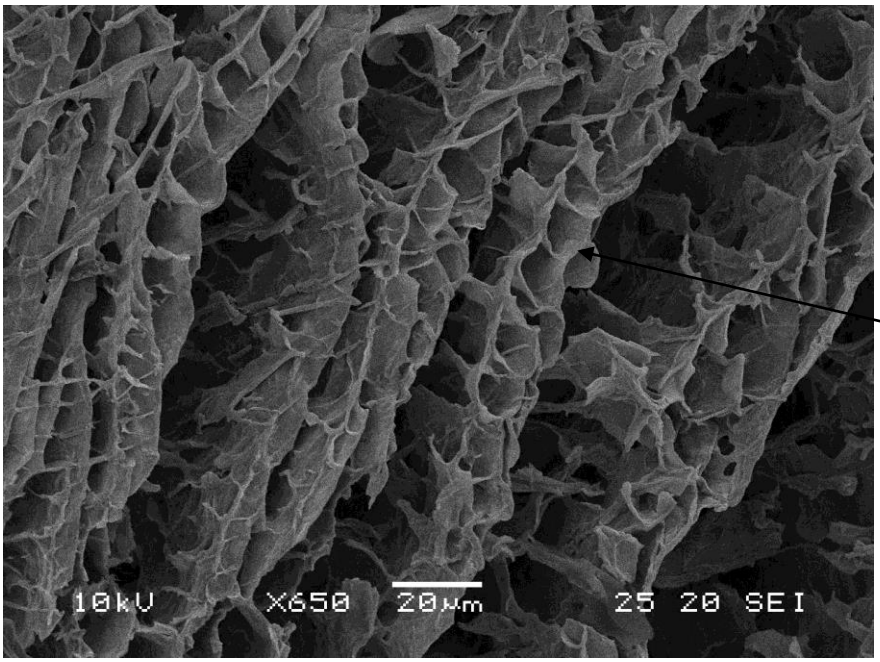

(c) Magnified view of surface in Figure 3.15(b).

Figure 3.15 (cont.) SEM images showing the structure formed starting with a silica sol-gel.

Looking more closely at Figure 3.15(b), the:

- average width of each pore is about 15μm, and
- leaves have a thickness of about 0.5-0.8 μm.

Obviously, the major difference in morphology is caused by the different characteristics of alumina and silica. The larger magnification image reveals that there are many pores and channels on the silica coated surface and all of the channels appear to be very accessible as the cracked lines provide the opening entries.

In some practical applications, when silica is coated onto the surface of a porous support, it could act as an interface, or a support for a membrane.

Key observation No 8: ***This demonstrates that novel shaped structures consisting of leaves and tunnels can be formed using a silica sol-gel as the starting material.***

3.3 Conclusions

KK leaf structures from alumina sol-gel:

(a) It was shown that similar structures could be formed to the ones described in Kolaczkowski and Kim (2006), however, they were not identical and maybe the absence of zirconia, or the physical way in which the samples had been immersed in liquid nitrogen was different.

(b) Trials on two different ways of inserting sol-gel coated monolith into the liquid nitrogen confirmed that this affected the characteristics of structures formed.

(c) Zirconia was not necessary to form leaf-like structures.

(d) The structures formed from a commercially available alumina sol (i.e. DISPSL 14N4-25) did not form KK leaf-like structures.

(e) To form leaf-like structures, the samples need to be freeze-dried.

(f) A double layer of leaf-like structures can be formed by repeating the coating, freeze-drying and calcining steps - thereby building a 2^{nd} layer on top of the 1^{st} on the support.

Wire mesh Dixon rings:

(g) The coating of the wire mesh Dixon rings with the alumina sol-gel produced some interesting structures, which could have commercial applications.

Structures formed from silica sol-gel:

(h) The coating of cordierite monoliths with a silica sol-gel produced some novel structures, consisting of plates, leaves and tunnels with nano-thin walls, and which could have commercial applications.

References

1. Alford, R., Burns, M., and Burns, N., 2011. Dixon rings-A revolutionary random colum packing. *Filtration*, Vol. 11(4), pp. 218-223.
2. Brinker, C.J., and Schere, G. W., 1990. Sol-Gel Science The physics and chemistry of sol-gel processing Academic *Press. INC*.
3. Dixon, O. G., 1949. High efficiency laboratory fractionation. I. Gauze ring packing and flooding techniques for laboratory columns. J.S.C.I., Vol. 68, March, PP.88-91.
4. Dixon, O. G., 1948. Improvements in and relating to the treatment of gases or vapours with liquids. British Patent Specification No 578,309, Accepted June 24, 1946.
5. Nishihara, H., Mukai, S.R., Fujii, Y., Tago, T., Masuda, T., Tamon, H., 2006. Preparation of monolithic SiO_2-Al_2O_3 cryogels with inter-connected macropores through ice templating. *Journal of materials Chemistry*, Vol.16, pp. 3231-3236.
6. Nuckols, M. L., Kolaczkowski, S., Awdry, S., Le, C.D., Smith, T., and Thomas, D., 2011. An initial assessment for the use of seawater as a method to remove metabolically-produced carbon dioxide from a submersible atmosphere. OCEANS 11, MTS/IEEE KONA, September 19-22, ISBN 978-0-933957-39-8.
7. Oetjen, G.W., Aseley, P.H., 2004. *Freeze –Drying, Wenham*: WILEY-VCH Veriag GmbH & Co. KGaA.
8. Kolaczkowski, S.T., Kim, S., 2006. Novel alumina 'KK Leaf Structures' as catalyst supports. *Catalysis Today*, Vol.117, pp. 554-558.
9. Kolaczkowski, S.T., 2001, University of Bath, UK, Private communication with a catalyst supplier.
10. Kolaczkowski S.T. 2011, Private communication based on work in a related project. Department of Chemical Engineering, University of Bath, UK.

11. Yoldas B.E., 1975. Alumina sol preparation from alkoxides. *Am. Ceram. Soc. Bull.* 54, 286-290.

Chapter 4 Enzyme immobilization on Dixon rings

Making use of the techniques described earlier in Sections 3.1.7 and 3.2 (see Chapter 3), an enzyme known as carbonic anhydrase, is incorporated into a silica sol-gel mixture which is then used to coat wire mesh Dixon rings. A freeze-drying technique was then applied, with the intention of trying to immobilize the enzyme on the wire mesh support.

This chapter consists of the following parts:

- An explanation of the motivation for the work.
- A description of the preliminary trials on the coating technique and what the freeze-dried structure looked liked.
- An explanation of how the carbonic anhydrase enzyme works.
- A description of improvements to the enzyme immobilization technique.
- Explanations of how the carbonic anhydrase enzyme worked in a CO_2 gas scrubbing experiment.

4.1 Motivation for the work

In a completely different project (but in the same research group at the University of Bath), there was an interest in the use of water as a gas scrubbing fluid, to remove carbon dioxide (CO_2), from a submersible habitat in which a person would live/operate for a period of time below the sea. In that study, experiments had been performed in a packed column in which the liquid flowed in a downward direction, and the gas flowed upwards. The column was packed with $1/8^{th}$ inch (3.2 mm) wire mesh Dixon Rings. As the CO_2 is soluble in water, then it was possible to transfer some of the CO_2 from the gas phase into the liquid phase. However, it was noticed in the literature that an enzyme known as carbonic anhydrase could increase the rate of one of the individual steps in the overall transfer process, namely the hydration of

CO_2 to form bicarbonate ions, which may be removed as either a solid carbonate, or in bicarbonate-enriched brine.

So the question posed was: could this enzyme be used to increase the overall rate of the transfer process, and thereby reduce the size of the gas scrubbing column?

Having gained experience in Section (3.1.7) in Chapter 3, of coating wire mesh Dixon rings with a silica washcoat layer (*via* the sol-gel freeze drying technique), it was decided to build on that experience, and to try to immobilize the enzyme:

- first on the surface of a cordierite monolith, then
- on wire mesh Dixon rings.

4.2 Immobilization of the enzyme

According to a review by Sheldon (2007), bio-catalysis has much to offer in the drive towards green and sustainable methodologies for chemicals manufacture, and the use of enzymes allows synthetic routes which are:

- shorter, and
- generate less waste.

Hence they are both environmentally and economically more attractive than traditional organic synthesis. However, Sheldon states that industrial application is often hampered:

- by a lack of long term operational stability,
- difficult recovery, and
- difficult re-use of these enzymes.

Sheldon concludes that these drawbacks can often be overcome by immobilization, and

states that there are three traditional methods of enzyme immobilization:

(1) Support binding: this can be physical, ionic, or covalent in nature. However, the physical bonding is generally too weak to keep the enzyme fixed to the carrier under industrial conditions.

(2) Entrapment: this occurs *via* inclusion of an enzyme in a polymer network such as an organic polymer or a silica sol-gel, or a membrane device such as a hollow fibber or a microcapsule. The physical restraints are generally too weak, however, to prevent enzyme leakage entirely; then additional covalent attachment is often required.

(3) Cross-linking: of enzyme aggregates or crystals using a bi-functional reagent, to prepare carrier-less macro-particles.

According to Tischer and Kascher (1999), the use of a carrier inevitably leads to dilution of activity, owing to the introduction of a large portion of non-catalytic ballast, ranging from 90% to larger than 99%, which results in lower space-time yield and productivity.

As mentioned in Yan *et al.* (2006), a two step procedure to encapsulate a single bovine carbonic anhydrase (BCA) molecule into a spherical nanogel was proposed. The encapsulated BCA maintained 70% of the activity of its free counterpart, but exhibited an increase in the molten temperature from 64 to 81^{o}C and an extension of the half-life from less than 3 to over 90 min at 75^{o}C.

According to Zhou and Hartmann (2012), mesoporous materials have been explored as supports for immobilization of enzymes. Increased stability and activity of immobilized enzymes in mesoporous materials may be achieved through well designed supports, suitable immobilization method and optimized immobilization conditions. However, with respect to

their scale- up and applications in industrial processes, continuous and intensive research is still required.

Zhang *et al.* (2013) studied the catalytic behaviours of carbonic anhydrase enzyme immobilized onto nonporous silica nanoparticles for enhancing CO_2 absorption into carbonate solution. They found that nonporous, nano-sized silica particles offered a large external surface area for enzyme immobilization and improved the activity of the immobilized enzyme by eliminating internal diffusion of a substrate. The enzyme's thermal stability also was improved by the immobilization, compared to its free enzyme counterpart, the half-life time of the immobilized enzyme was increased by up to 4.4 times over a 30-day test period at 50^oC.

Vinoba *et al.* (2010) studied biomimetric sequestration of CO_2 and its reformation to $CaCO_3$ using bovine carbonic anhydrase on a mesoporous silica based support. Various immobilization techniques were explored such as: covalent attachment, adsorption and cross-linked enzyme aggregation. The biocatalytic capture of CO_2 using bovine carbonic anhydrase immobilized on a silica support was considered to be tunable, reusable and promising.

Finally, as stated in Bryjak and Kolarz (1998), because of the use of a carrier, the immobilization of an enzyme resulted in a 50% loss in activity. So another approach could involve cross-link the enzyme crystals and to cross-link enzyme aggregates, thereby creating a carrier-free immobilized enzyme which would have a high activity. However, this approach was not explored in this thesis, as the plan was to make use of the wire mesh Dixon rings as the support for the enzyme, and for them also to act as the packing in the gas scrubbing column.

4.2.1 Immobilization on a cordierite monolith – Preliminary trials

The carbonic anhydrase enzyme used in this thesis was of the following form:

Supplied by: Sigma-Aldrich Company Ltd.

Catalogue number: C3934-100mg

Price: £124.00 (23.05.2013)

Description: white powder

Properties: Lyophilized powder

Storage temperature: 2-8^{o}C

Figure 4.1 shows images of a monolith which has been washcoated with a mixture of enzyme (carbonic anhydrase) in silica sol-gel. As the carbonic anhydrase will not survive temperatures > 55 ºC (Smith *et al.*, 1999), this washcoated monolith cannot be calcined. The sample was prepared by:

(a) Immersing a cordierite monolith for about 2 min into a sol-gel made from a mixture of enzyme in silica sol-gel.

(b) The coated monolith was then immersed in liquid nitrogen.

(c) The sample was then placed in a freeze-drying unit at -60^{o}C for about 8 hrs.

The SEM images in Figure 4.1, show that the surface is in general flat with numerous white patches which represent the enzyme. As the sample had not been calcined, leaf-like structure were not observed.

Out of curiosity (as the enzyme would not have survived in an active form), the sample was calcined at 200^{o}C for 30 min. As illustrated in Figure 4.2, the structure of the washcoated surface changed rather dramatically, and interestingly, a porous structure started to form on that surface.

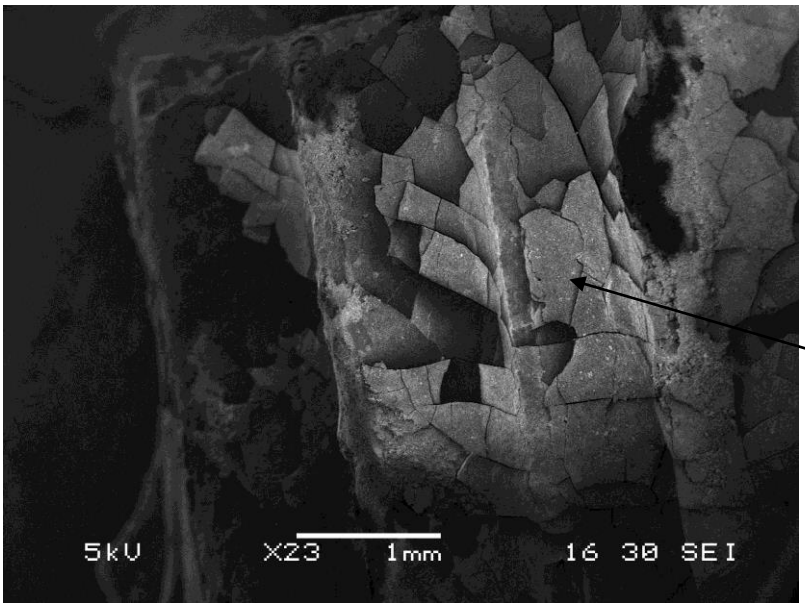

(a) View showing the coated surface of the monolith.

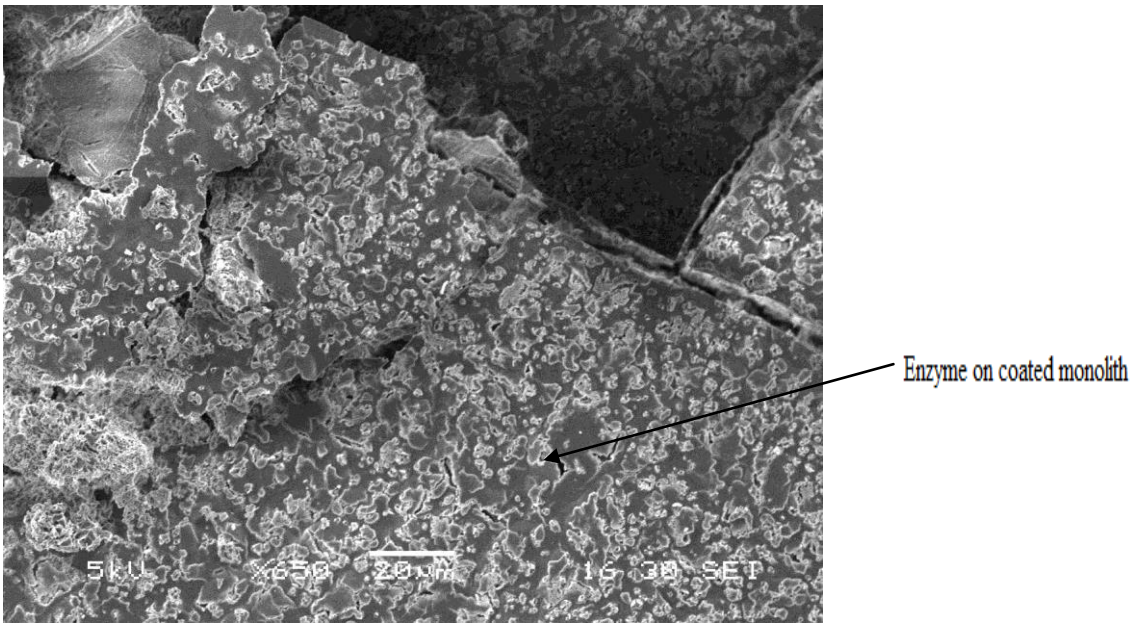

(b) Magnified view showing the enzyme (carbonic anhydrase) white patches on the surface.

Figure 4.1 SEM images of a washcoated monolith which had been coated with an enzyme & silica sol-gel mixture, then freeze-dried.

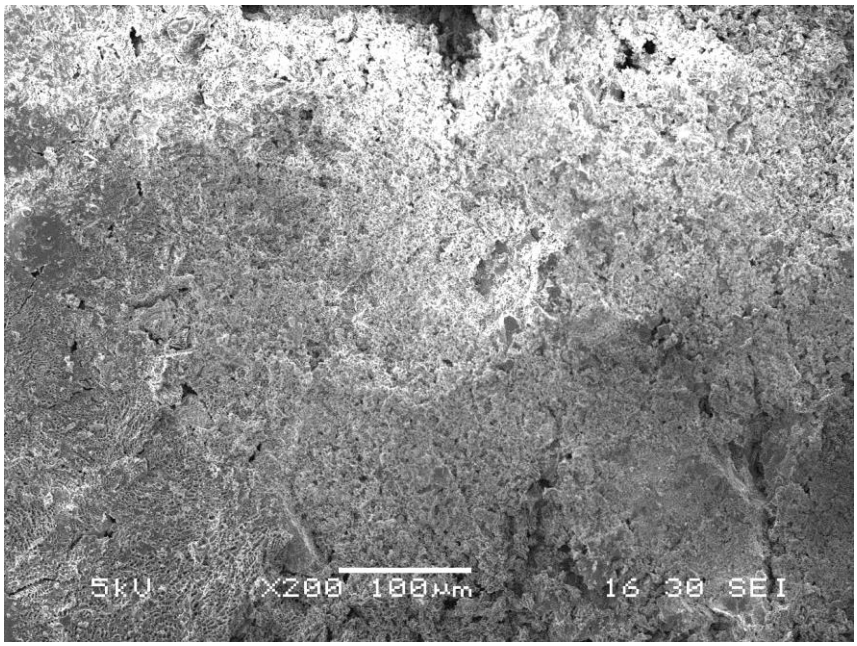

(a) View of the surface.

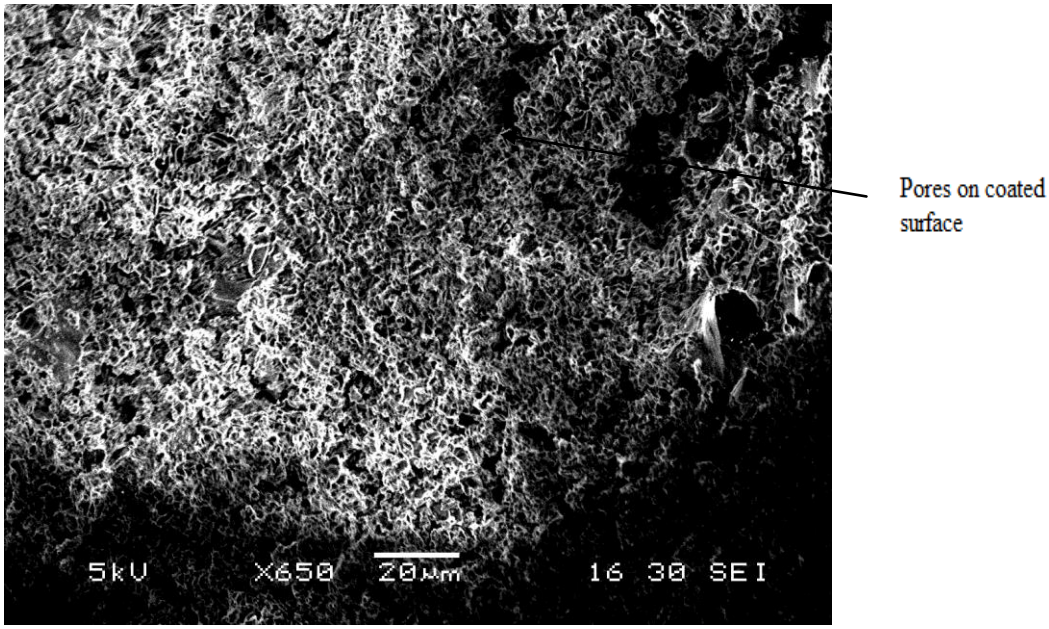

(b) Magnified view of the surface showing the porous structure.

Figure 4.2 SEM image of the surface of a monolith coated with an enzyme & silica sol-gel mixture, which had been freeze-dried and then calcined at 200ºC.

4.2.2 Enzyme immobilization on wire mesh Dixon rings – Preliminary trials

As a reminder, this freeze-dried sample could not be calcined as the carbonic anhydrase (enzyme) would not survive above a temperature of 55^{o}C.

In Figure 4.3, SEM images are shown of the wire mesh 3.2 mm Dixon rings which had been coated with the enzyme & silica sol-gel mixture, using the freeze drying method. The image shows:

- that in general, the coating has adhered extremely well to the rings, and has filled the gaps between the wire mesh,
- on some of the edges small pieces had cracked and become dislodged,
- white patches of the enzyme are also visible on the surface,
- the surface in Figure 4.3(b) looks similar to that formed on the monolith (see Figure 4.1(b)).

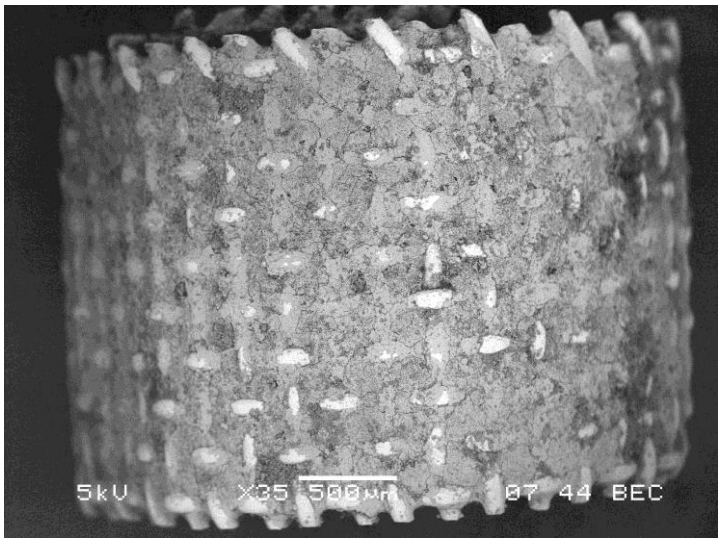

(a) View of surface of coated Dixon ring.

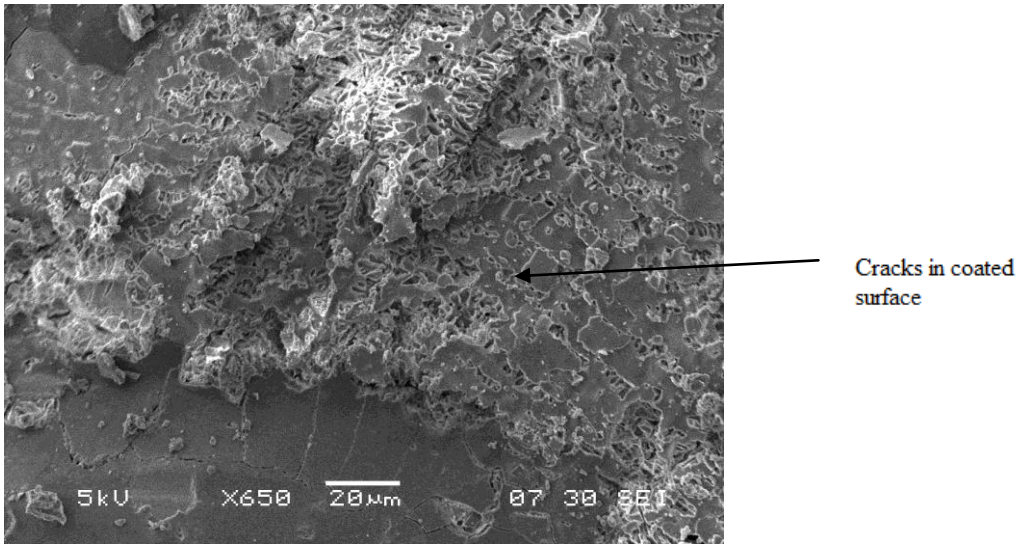

(b) Magnified view.

Figure 4.3 SEM images of coated wire mesh Dixon Rings using the carbonic anhydrase & silica sol-gel mixture, which was freeze-dried.

4.3 The hydration of carbon dioxide and use of carbonic anhydrase

In this section the way in which the carbonic anhydrase enzyme could work is considered in more detail.

As illustrated in Figure 4.4, it is well known that gaseous CO_2 dissolves rapidly in water to produce a loosely hydrated aqueous form, and that this reaction is rapid. The aqueous CO_2 may react either with water or at high pH, with hydroxyl ions. Once bicarbonate ions are present in solution, they will dissociate to form carbonate ions to an extent dependent on pH.

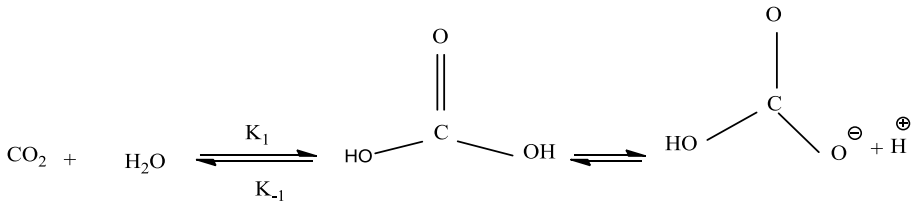

Figure 4.4 The hydration of carbon dioxide (adapted from Berg *et al.*, 2012, p.274).

As described in (Berg *et al.(*2012) and Ozdemir (2009)), in the presence of the enzyme carbonic anhydrase (which acts as a catalyst), the speed at which CO_2 is hydrated can be increased. Carbonic anhydrase consists of a group of zinc metallo-enzymes, and examples of different structures are shown in Figure 4.5. These enzymes are among the fastest enzymes known. For example according to Khalifah (1971) (as reported in Ozdemir (2009)), each molecule of 'isozyme C' from the human body can catalyze 1.4×10^6 molecules of CO_2 per second.

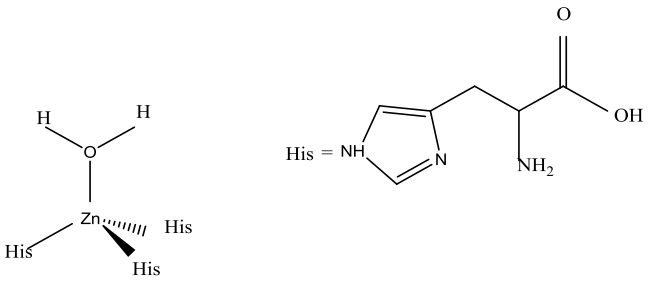

(A) (B)

Figure 4.5 Two examples of carbonic anhydrase. (A) The structure of human carbonic anhydrase II and its zinc site. (B) An organic compound, capable of binding zinc, was synthesized for carbonic anhydrase (adapted from Berg *et al.*, 2012, p. 275).

According to Berg *et al.(*2012, p.274), the reaction mechanism for the hydration of carbon dioxide can be explained as illustrated in Figure 4.6, for which the following comments apply:

(a) Zinc facilitates the release of a proton from a water molecule, which generates a hydroxide ion.

(b) The carbon dioxide substrate binds to the enzyme's active site and is positioned to react with the hydroxide ion.

(c) The hydroxide ion attacks the carbon dioxide, converting it into a bicarbonate ion.

(d) The catalytic site is regenerated with the release of the bicarbonate ion and the binding of another water molecule.

Several groups have attempted to produce synthetic analogues of the zinc containing metallo-enzymes, and one example is illustrated in Figure 4.7.

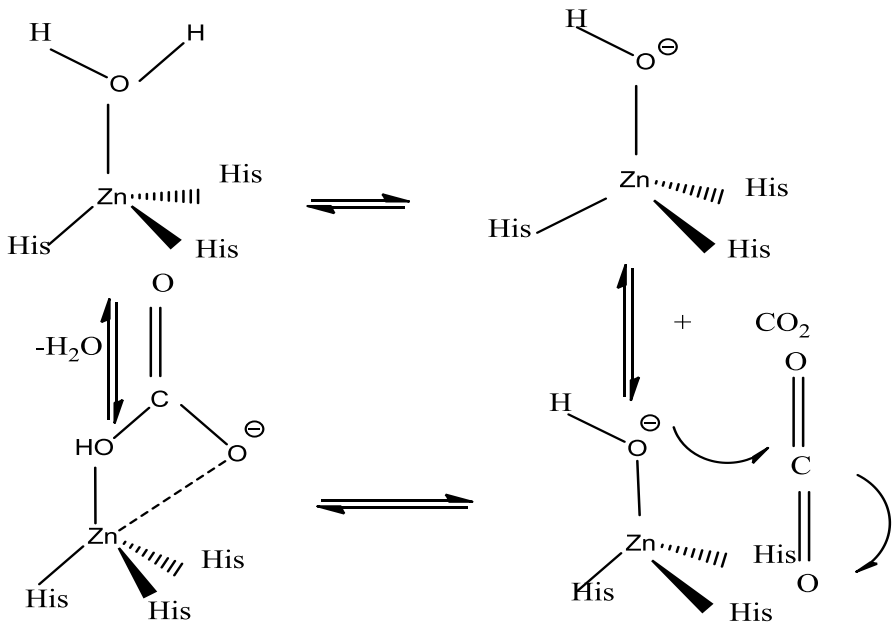

Figure 4.6 The reaction mechanism for the hydration of carbon dioxide (adapted from Berg *et al.*, 2012. p.277).

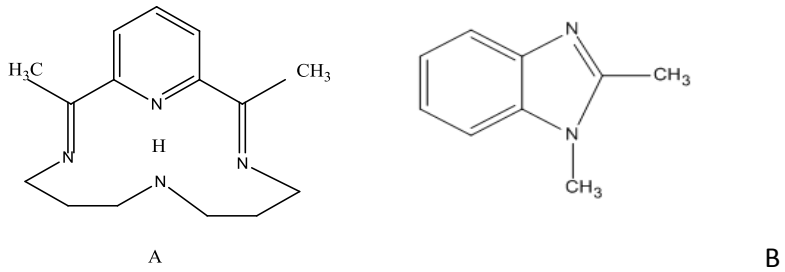

A B

Figure 4.7 Previous attempts at a synthetic analogue. (A) An organic compound, capable of binding zinc, was synthesized as a model for carbonic anhydrase. The zinc complex of this ligand accelerates the hydration of carbon dioxide more than 100-fold under appropriate conditions. (B) The buffer 1,2-Dimethylbenzimidazole (adapted from Berg *et al.*, 2012, p.277).

According to Berg *et al.(*2012), when ligand A (see Figure 4.7) is bound to zinc at pH of 9.2, this acts as a catalyst and can accelerate the hydration of carbon dioxide up to 100 times that of the non-catalysed system. The rate of carbon dioxide hydration increases with the concentration of the buffer 1,2-Dimethylbenzimidazole (B).

According to Mirjafari *et al.* (2007), the enzyme enhanced the hydration of CO_2 and the rate of hydration reaction increased with both the enzyme concentration and temperature. The enzyme activity was not influenced by the pH of the reaction mixture.

Bond *et al.* (2001), described a CO_2 scrubber which uses an enzyme that can be used to reduce CO_2 emissions from, for example, fossil-fuel burning power plants. In that system, the enzyme worked as a catalyst to accelerate the rate of CO_2 hydration for subsequent fixation into stable mineral carbonates (the counterions for which may be supplied from such sources as brines from saline aquifers, waste brines from desalination operations, or seawater). Their results showed high enzyme activity in the presence of low levels of SO_X and NO_x and also in a solution representative of seawater. Further more, the same research group (Liu *et al.,* 2005) also studied carbonate precipitation from synthetic brines corresponding to a range of compositions of produced waters from the Permian and San Juan basins, their results showed that carbonic anhydrase CO_2 sequestration capacities were estimated to be 0.49 to 1.85 $\times 10^3$ tonnes CO_2/year and 1.28-2.80$\times 10^3$ tonnes CO_2/year for the San Juan and Permian basins, respectively.

4.4 Enhancements to the enzyme immobilization technique

4.4.1 Enhanced procedure based on use of alumina sol-gel

Following the preliminary coating trials described in Section 4.2, the coating technique was modified, and the procedure consisted of two key steps as follows:

Step 1: Coating the Dixon rings with alumina

(a) The wire-mesh Dixon rings were soaked in an alumina sol-gel for 5 min.

(b) They were then dipped into liquid nitrogen for about 10 min.

(c) The coated Dixon rings were then put into a freeze-drying unit for 24 h, and this removed and residual water.

(d) The coated Dixon rings were then calcined at 450°C for 5h in air.

The results of this coating process are shown in the SEMs in Figure 4.8, from which it is clear that leaf-like structures have been formed, providing a large surface area support .

Step 2: Impregnating with the enzyme

(e) A measured quantity (0.0336 g) of the enzyme was dissolved in 10.2 g of phosphate buffer solution.

(f) This enzyme solution was then poured onto 27 g of the alumina coated Dixon rings.

(g) The enzyme loaded Dixon rings were then immersed in liquid nitrogen for 10 min.

(h) Then they were placed into the freeze-drying unit for 3h.

As a reminder, the enzyme cannot be exposed to temperatures > 55 ºC, so it cannot be calcined. SEM images showing the enzyme coated structure are presented in Figure 4.9. In these, the white patches represent the enzyme and these are clearly visible on the surface. By using this two-step procedure, it was now possible to calcine the alumina and create the leaf-like structure which then acted as the support for the enzyme.

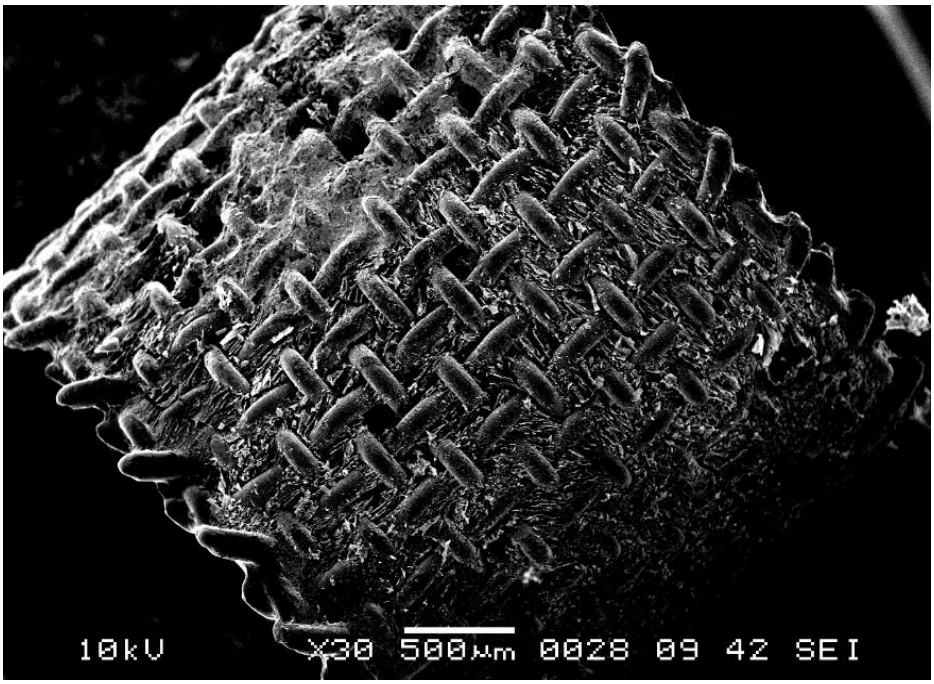

(a) Side view of a coated Dixon ring.

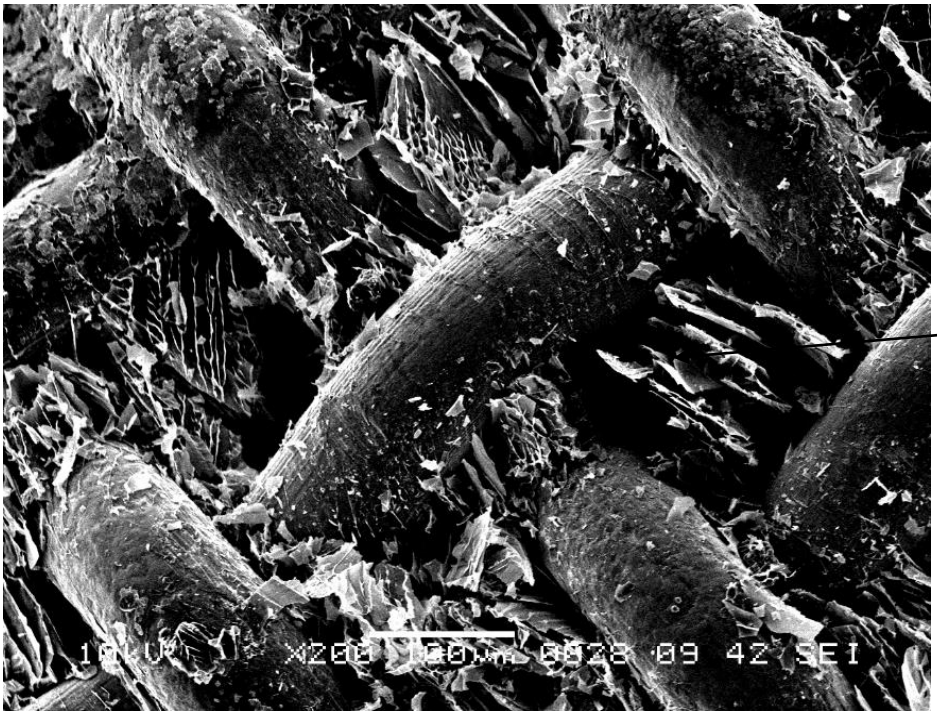

(b) Magnified view of coated wire mesh.

Figure 4.8 (cont.)

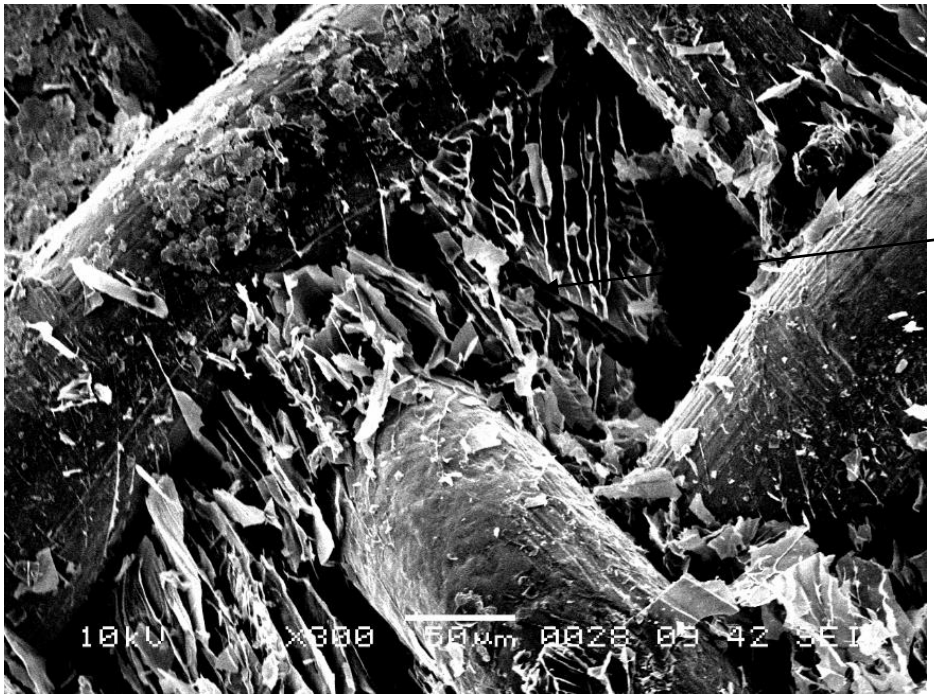

(c) Magnified view: showing the leaf-structures attached to the wire mesh.

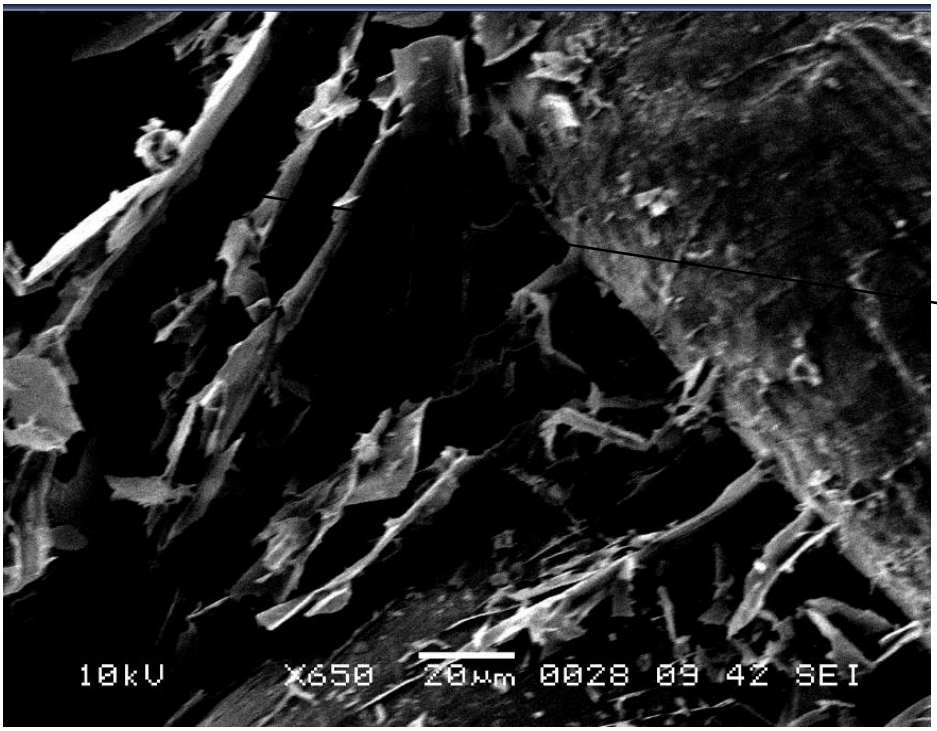

(d) Magnified view.

Figure 4.8 (cont.)

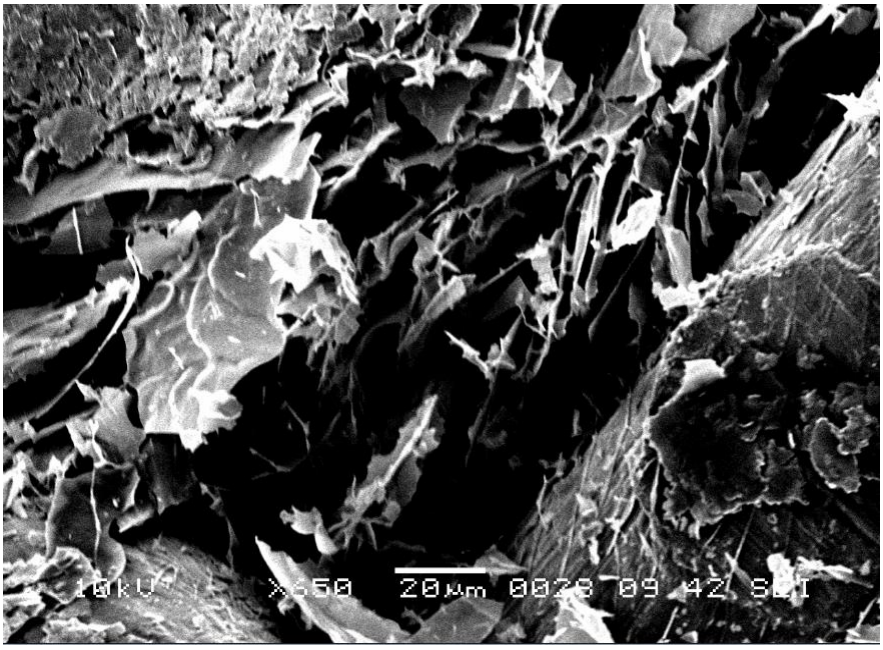

(e) Magnified view of filled gaps between the wires in the mesh.

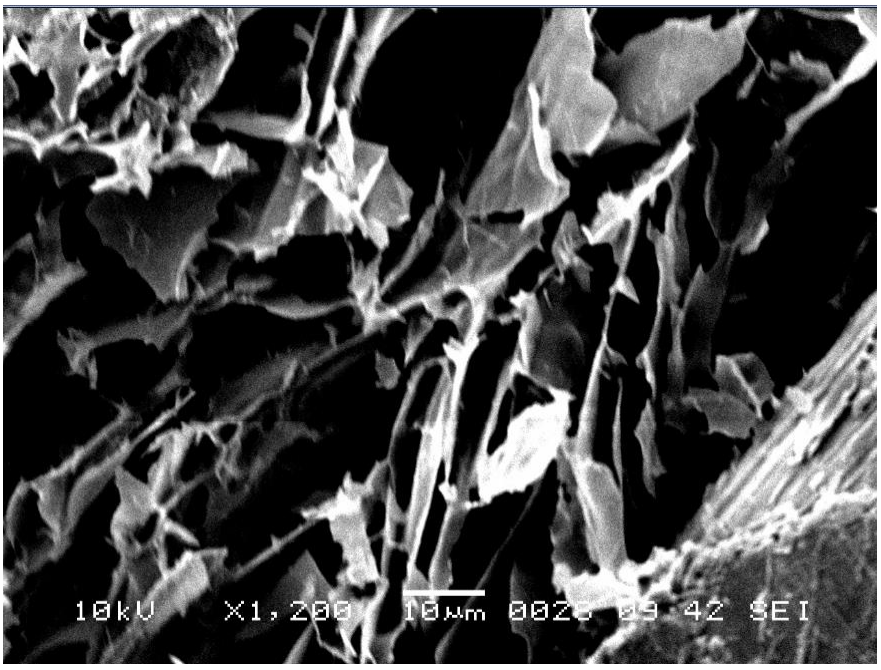

(f) Magnified view: leaf-like structure is clearly visible.

Figure 4.8 (cont) SEM images of wire-mesh Dixon rings: coated with alumina sol-gel, freeze-dried, and then calcined at 450 ºC.

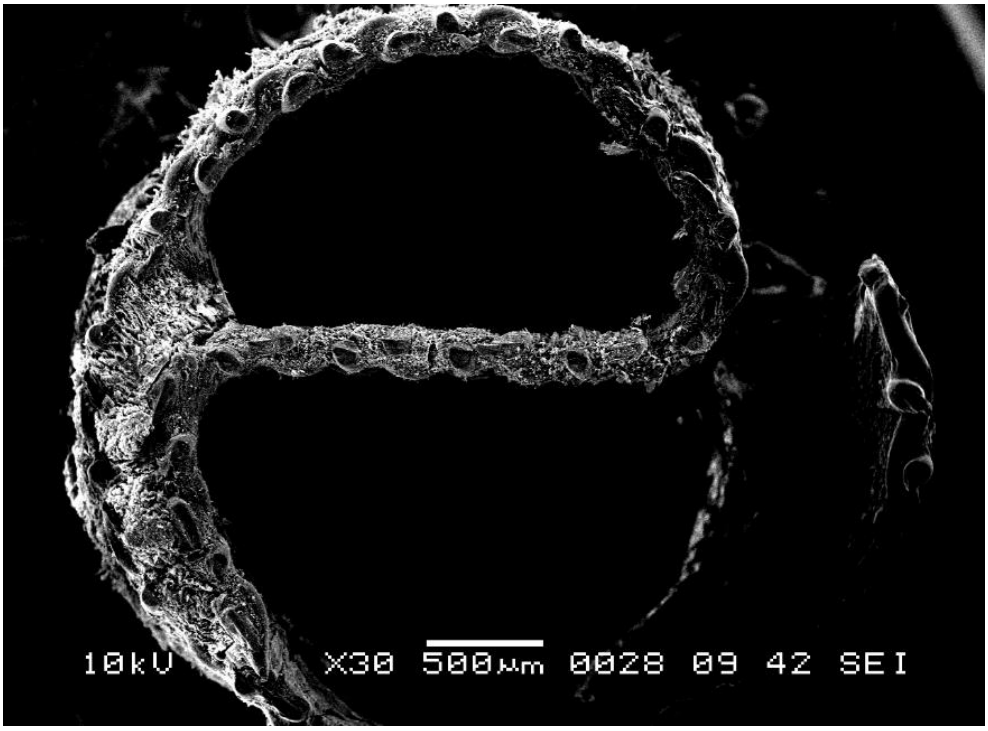

(a) Top view of a coated wire mesh Dixon ring.

(b) Magnified view of surface showing the white coverage of enzyme.

Figure 4.9 (cont.)

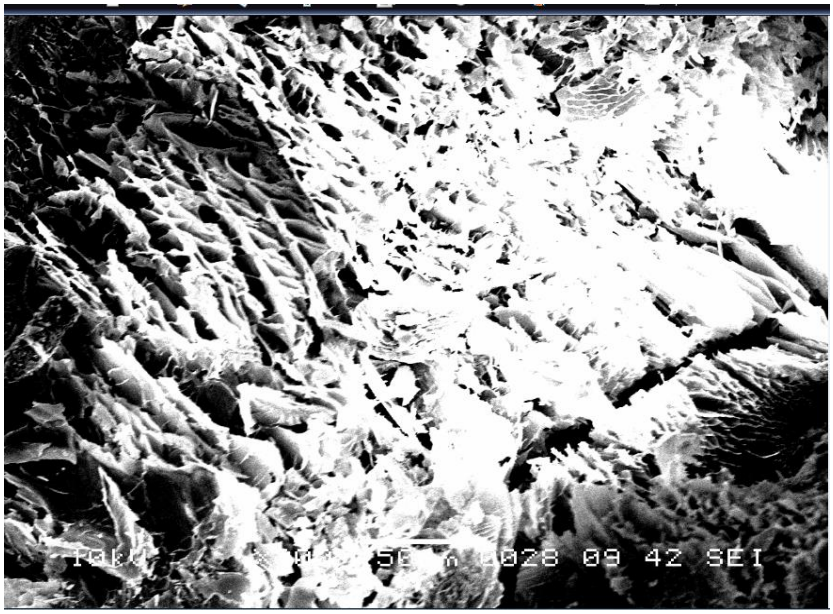

(c) Magnified view of surface.

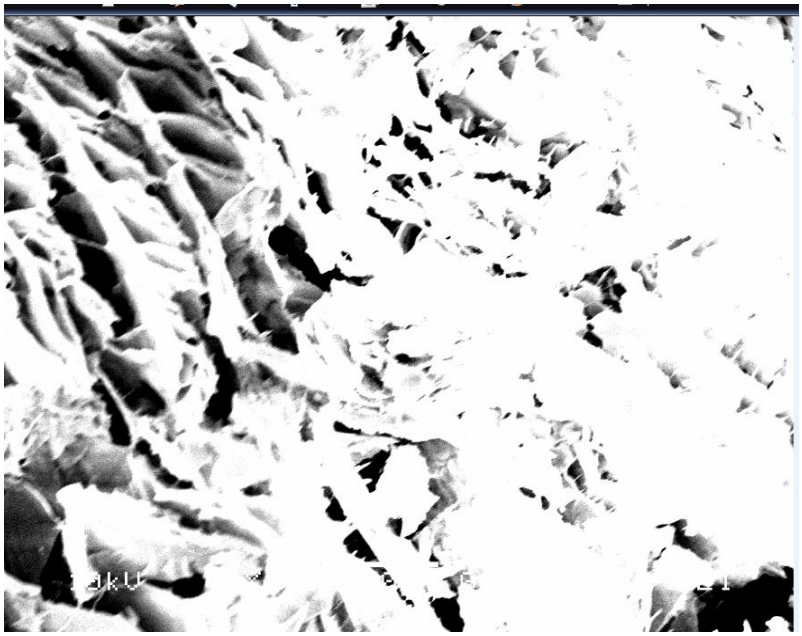

(d) Magnified view of surface.

Figure 4.9 (cont) SEM images of wire-mesh Dixon rings: coated with alumina sol-gel, freeze-dried, calcined at 450 ºC, and then impregnated with enzyme and freeze-dried.

4.4.2 Enhanced procedure based on use of a silica sol-gel

In this section, the enzyme is entrapped in a silica structure. According to Sheldon *et al.* (2007), entrapment is the inclusion of an enzyme in a polymer network (gel lattice) such as:

- an organic polymer, or
- a silica sol-gel, or
- a membrane device such as a hollow fibre, or a microcapsule.

As physical restraint is generally too weak on its own, additional covalent attachment is often required to prevent enzyme leakage. The difference between entrapment and support binding is often not clear. They define support binding as the binding of an enzyme to a prefabricated support (carrier) irrespective of whether the enzyme is situated on the external or internal surface. Entrapment requires the synthesis of the polymeric network in the presence of the enzyme. For example, when an enzyme is immobilized in prefabricated mesoporous silica, the enzyme may be situated largely in the mesopores, but this would not be entrapment.

In this thesis, Si $(OCH_3)_4$ was used to synthesise the silica sol-gel with an enzyme present during the synthesis. Thereby, the enzyme was entrapped in a polymer gel lattice. The sol-gel process was based on the method described in Badjic and Kostic (1999).

The silica sol was prepared as follows:

(a) A mixture of 15.25 g of $Si(OCH_3)_4$, 3.38 g of water, and 0.3g of 0.04 M HCl was placed in an ultra-sonic ice-bath for 30 min.

(b) A portion of sol (4.64 ml) was mixed with 5.64 ml of the phosphate buffer and kept in an ice bath.

(c) A stock solution of carbonic anhydrase containing 10 mg of the enzyme in 3.4 ml of the buffer solution was added to the sol.

(d) The wire-mesh Dixon rings were then dipped in the sol-gel.

(e) The sol-gel coated rings were then immersed into liquid nitrogen for about 10 min.

(f) The frozen rings were then placed into the freeze-drying unit for 24 h.

Using this method of coating, the coated support was not calcined. By inspecting the vessel used for freeze-drying, it was evident that much of the coating had dropped-off the wire mesh rings, as a loose white powder was visible in the container. This indicated that adhesion of the mixture to the rings was very poor. The SEM images in Figure 4.10 also show a low level of material adhering to the wire mesh, and the absence of any leaf-like structures.

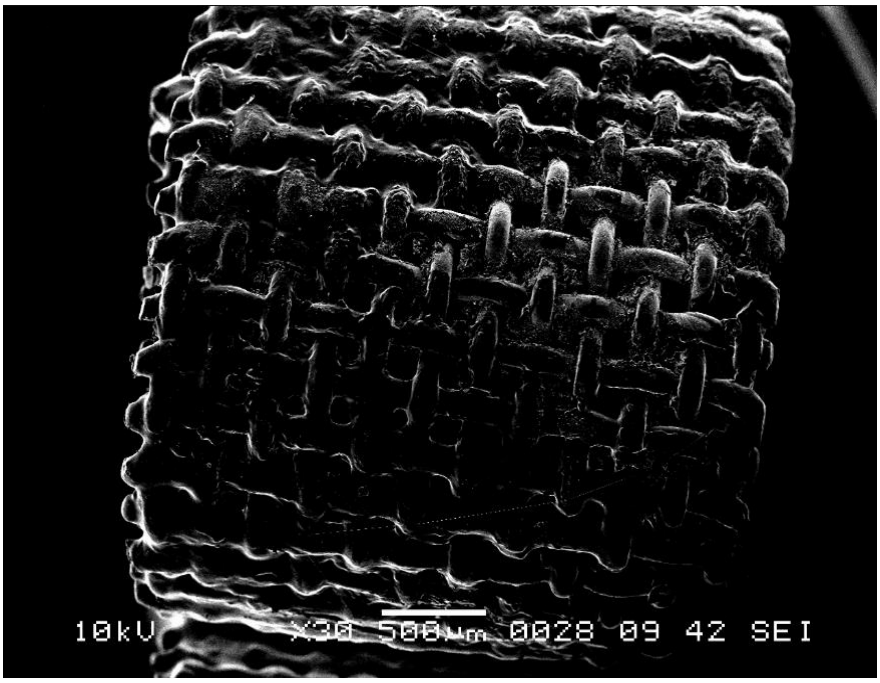

(a) Side view of a coated wire-mesh Dixon ring.

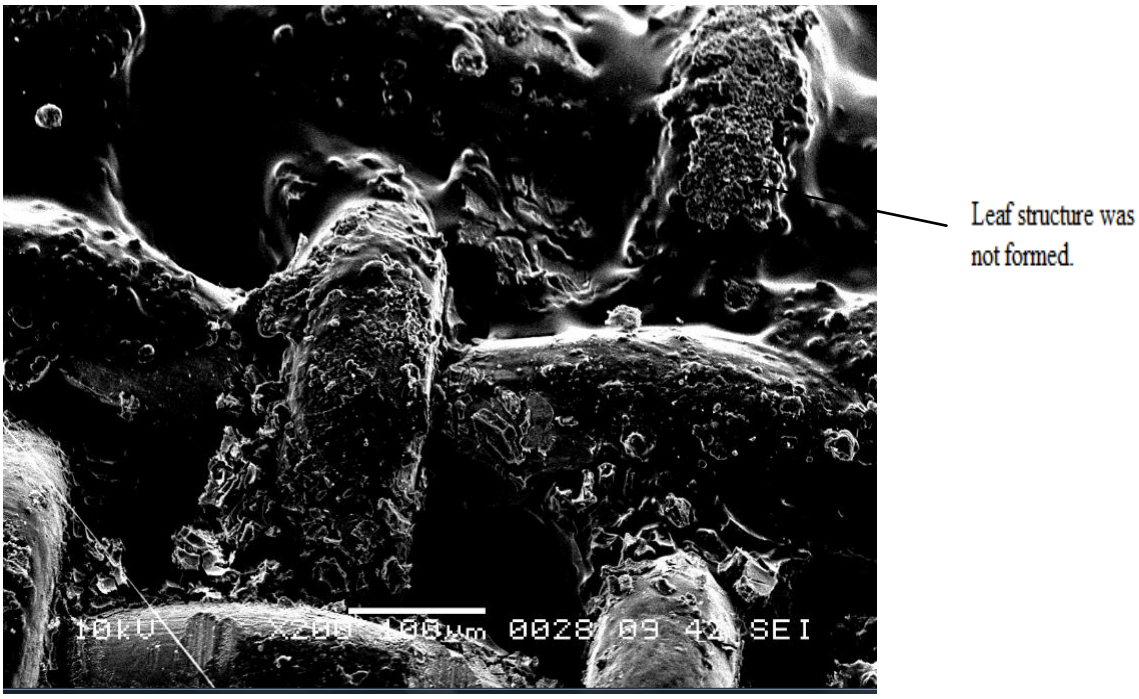

(b) Magnified view of the surface of the coated wire mesh.

Figure 4.10 (cont.)

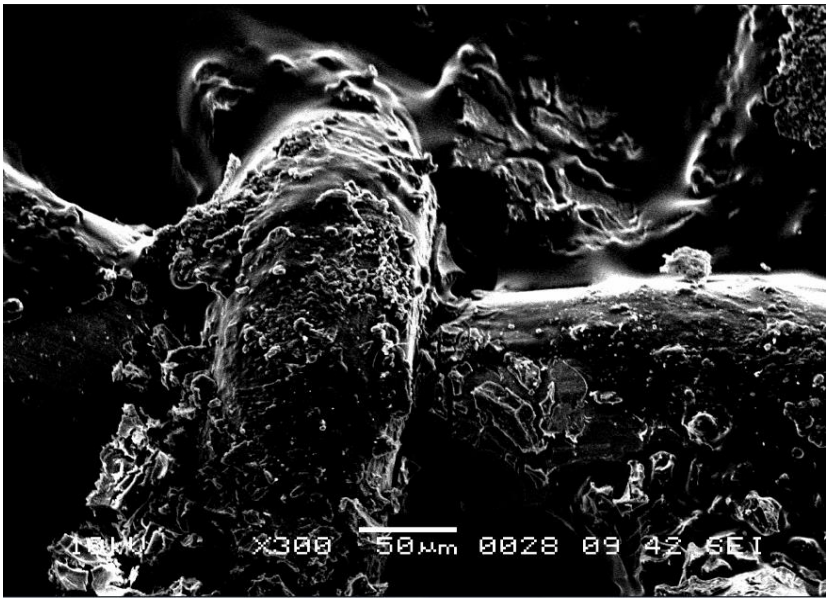

(c) Magnified view of coated wire.

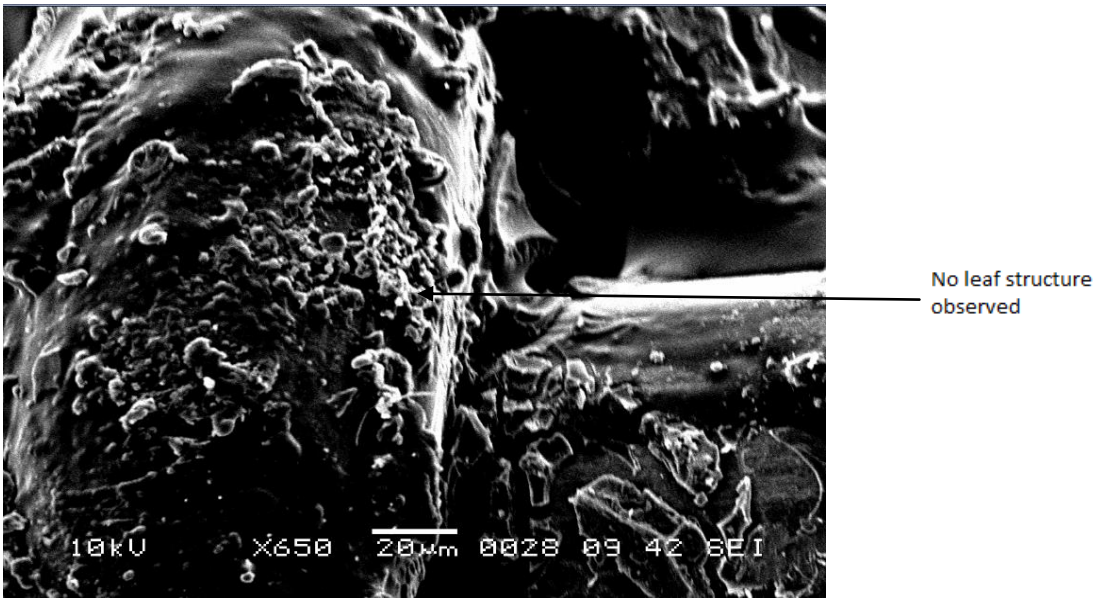

(d) Magnified view of surface of a wire.

Figure 4.10 (cont.) SEM images of the surface of a wire mesh Dixon ring: coated with a silica sol-gel and enzyme mixture, then freeze-dried.

4.4.3 Enhanced procedure based on use of a silica sol-gel and pre-treatment

According to Han *et al.* (2011), pre-treatment can increase the roughness of the metal surface and thereby improve washcoat adhesion. There are two ways to enhance the bonding force between the surface coating and the metallic carrier. One is to increase the specific surface area of the substrate, and the other is to promote chemical affinity. Thermal oxidation is a standard method used to enhance bonding with metal surfaces, as textured oxide layers are formed on the surface under high temperature.

Han et *al.* (2011) reported that an electro-deposited nickel substrate was effectively micro-roughened with an acidic bath containing 5 wt. % H_2SO_4 and 10 wt. % $(NH_4)_2SO_4$ at room temperature. The polished copper foils were immersed in the acid solution. The roughened surface was then either:

- dip-coated with a 10 wt% boehmite primer sol, dried at room temperature for 1h, and then calcined at 300°C for 2h, or
- dip-coated with a 30 wt% alumina slurry, dried at 120°C for 2h, and then calcined at 500°C for 2h.

A similar technique was applied, which consisted of the following.

<u>Step 1: Pre-treatment of the metal surface</u>

(a) Wire-mesh Dixon rings were immersed in 5 wt% H_2SO_4 at room temperature for 10 minutes. Small bubbles of gas were formed in the solution indicating that a reaction was taking place. The wire mesh had been micro-roughened by the acid.

Step 2: Preparation of silica sol

(b) A mixture of 15.25 g of $Si(OCH_3)_4$, 3.38 g of water, and 0.3g of 0.04 M HCl was placed in an ultra-sonic ice-bath for 30 min.

(c) A portion of sol (4.64 ml) was mixed with 5.64 ml of the phosphate buffer and kept in an ice bath.

(d) A stock solution of carbonic anhydrase containing 10 mg of the enzyme in 3.4 ml of the buffer solution was added to the sol.

(e) The wire-mesh pre-treated Dixon rings were then dipped in the sol-gel.

(f) The sol-gel coated rings were then immersed into liquid nitrogen for about 10 min.

(g) The frozen rings were then placed into the freeze-drying unit for 24 h.

However, after the freeze-drying stage, white powder was observed in the vessel, indicating poor adhesion to the metal rings.

4.4.4 Enhanced procedure: using calcined silica sol-gel then enzyme impregnation

In this section, the wire mesh Dixon rings are silica sol-gel coated, calcined, and then impregnated with the enzyme following a technique described in Mokoena (2005).

The procedure followed is summarized in Figure 4.11, and consists of the following key steps:

Step 1: Preparation of silica-sol

(a) Tetraethyl orthosilicate $Si(OEt)_4$ (TEOS, 98%, Aldrich) was the starting alkoxide, ethanol was used as the solvent, and aqueous ammonia NH_4OH (28%) as the catalyst.

(b) The molar ratios were:

TEOS = 0.2; water = 22; ethanol = 1.6; aqueous ammonia = 0.7.

(c) Using a 2 litre flask the following was added: 30.44 g of TEOS; 400 ml distilled water and 73.6 g ethanol. The mixture was stirred for 20 min at 35^{o}C.

(d) Then 24.5g of 35wt% aqueous ammonia was added, the mixture was kept stirred for a further 2h, and the sol-gel was formed.

Step 2: Coating the wire mesh Dixon rings

(e) The wire mesh rings were then dipped into this sol-gel.

(f) The sol-gel coated rings were immersed in liquid nitrogen for 5 min.

(g) The rings were then placed in the freeze-drying unit.

(h) The rings were then calcined at 450^{o}C for 3h in the presence of air.

Step 3: Enzyme impregnation

(i) A quantity (0.0336 g) of the enzyme was dissolved in 10.2 g of phosphate buffer solution.

(j) This enzyme solution was then poured onto 27 g of the coated rings.

(k) The enzyme impregnated rings were then immersed in liquid nitrogen for 10 min.

(l) The rings were then placed into the freeze-drying unit for 3h.

It was interesting to observe that the rings turned a darker colour after dipping in this silica sol-gel, and the SEM images in Figure 4.12 show that a better coating surface had been formed on the rings. This final coating procedure is summarized in Figure 4.11.

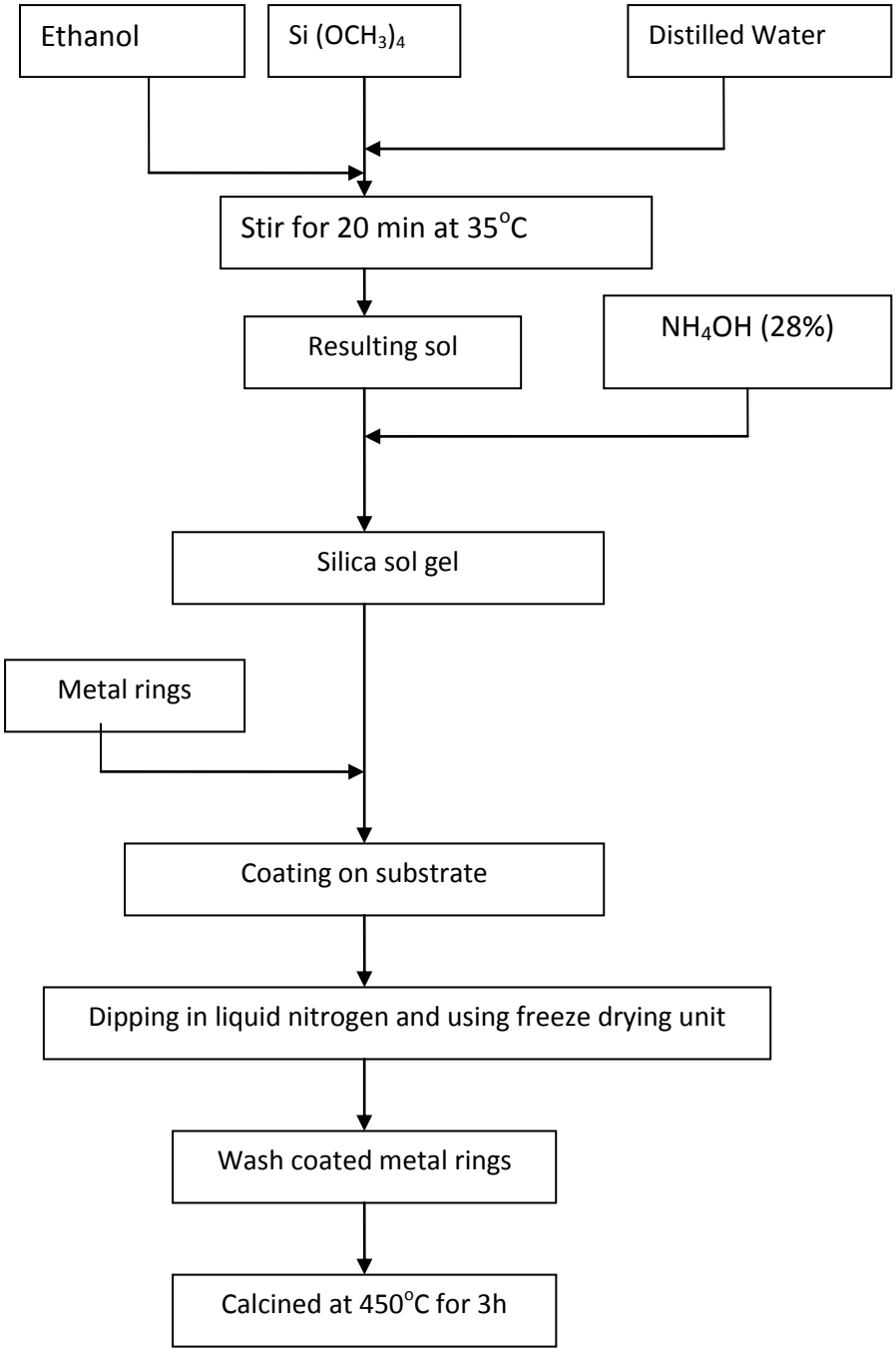

Figure 4.11 Flow diagram indicating the key steps in the final coating process used.

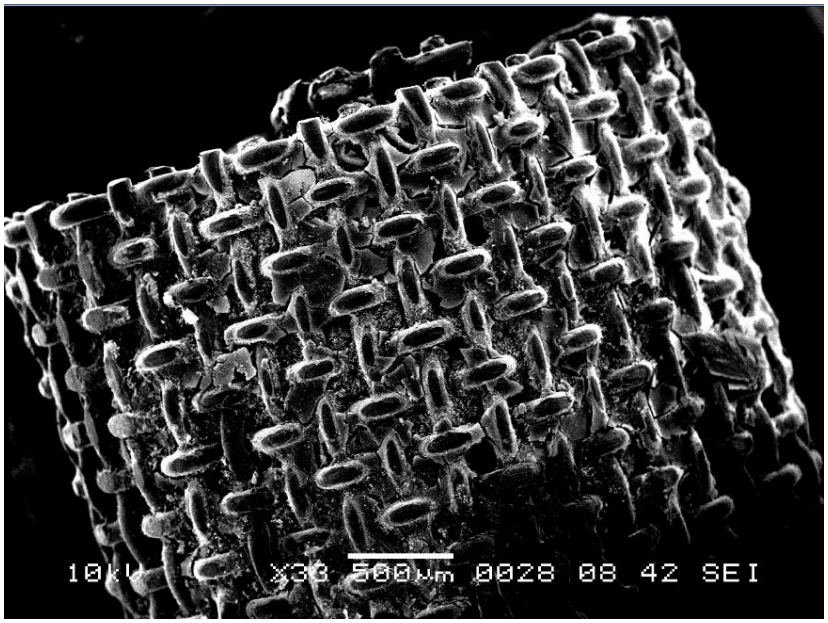

(a) Side view of a coated ring.

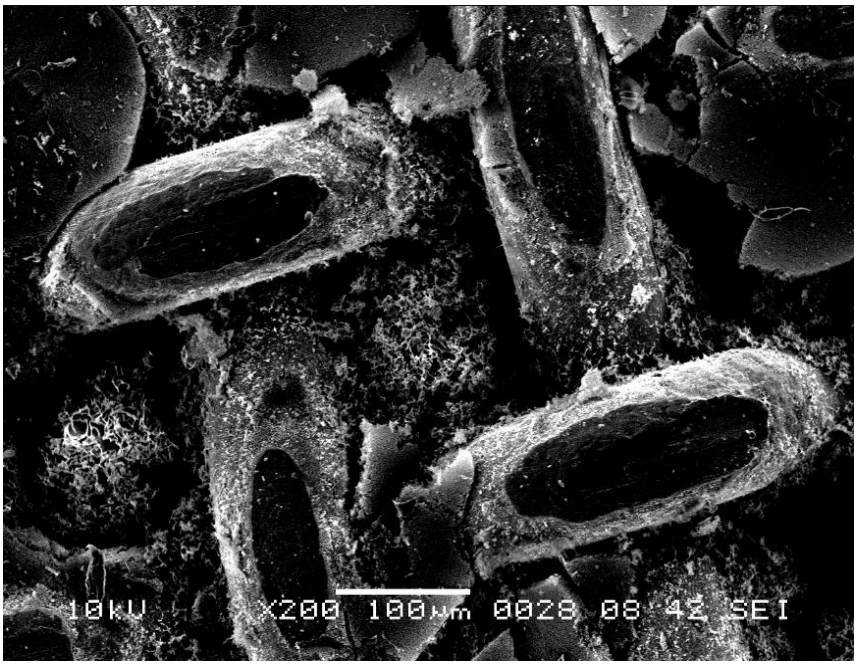

(b) Magnified side view of a coated ring.

Figure 4.12 (cont)

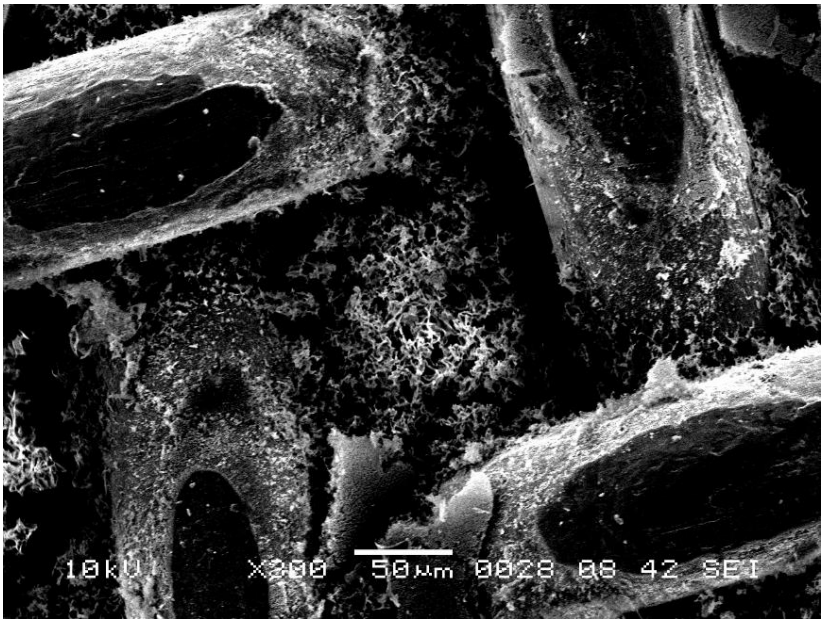

(c) Magnified side view of a coated ring.

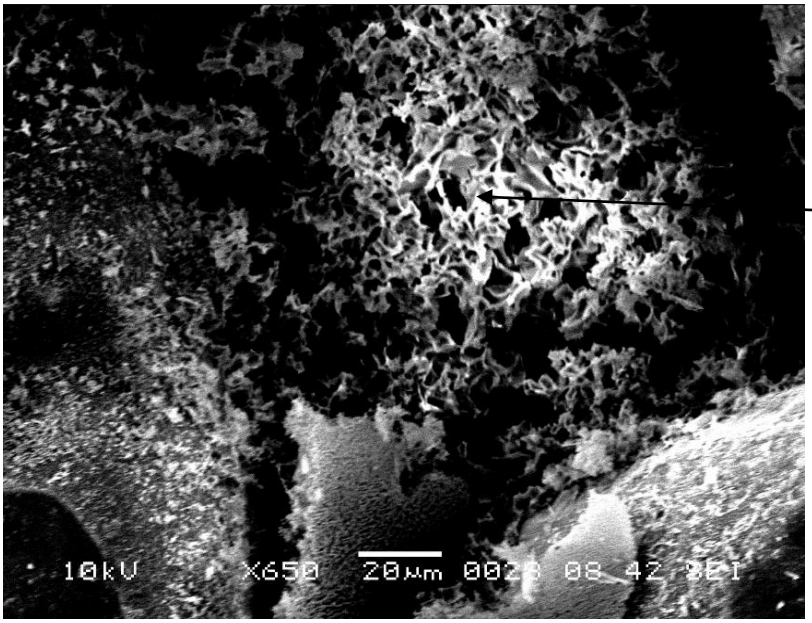

(d) Magnified view of the coating in the gap between the wires.

Figure 4.12 SEM images of a wire mesh Dixon ring coated with a silica sol-gel that was calcined and then impregnated with the enzyme and freeze-dried.

4.3 Assessing the performance of the enzyme coated rings

The enzyme coated rings were placed inside a mini-column as illustrated in Figure 4.13. Water was fed into the top of the packed column, and a gas stream with CO_2 was fed into the base of the column. As water flowed into the flask at the base of the column it was pumped out with a peristaltic pump. The concentration of the CO_2 leaving the top of the column was measured with a mass spectrometer (MS). The key dimensions and flow conditions are summarized:

Column i.d. = 30 mm; o.d. = 35mm

Column length = 470 mm; packed bed height with coated rings = 300 mm

Liquid flow = 0.22 L min^{-1}

Gas flow = 1.0 L min^{-1}

Concentration of CO_2 in the gas feed = 4 vol.%

From the samples that had been prepared in Section 4.2, a number were selected for trials in this apparatus and the results are presented as follows:

In Table 4.1, information is provided on the performance of the column with uncoated rings. This provides a useful base case with which to compare the rest of the data. From these results, the concentration of CO_2 in the gas exit is 3.63 vol%.

In Table 4.2, the performance of rings which had just been coated with alumina (no enzyme) is presented. The concentration of CO_2 is slightly higher, most probably because of the reduction in interfacial gas-liquid surface area, as the interstitial gaps between the wires on the rings have now been blocked by alumina.

In Table 4.3 the performance of the alumina coated rings impregnated with the enzyme are now presented. The performance of the column is just slightly better (3.57 vol % of CO_2), than in Table 4.2 (3.66 vol %), showing that maybe the enzyme is helping.

In Table 4.4 the performance of silica coated rings impregnated with the enzyme is presented. Again there is a very small improvement in performance (3.55 vol % of CO_2 versus 3.66 vol %).

Experimental errors could arise from a number of different sources:

(a) CO_2 gas inlet concentration: this was supplied from a premixed gas bottle, so the gas inlet concentration would have been the same in all of the runs.

(b) Gas flow: this was controlled by setting the flow on a rotameter. The same position was used for all of the runs.

(c) Liquid flow: this was controlled by setting the flow on a rotameter. The same position was used all of the runs.

(d) Mass spectrometer: this had been calibrated using the gas inlet concentration as reference.

Any systematic errors in the measurement in (a) to (d) would have been in the same direction in each of the comparative runs.

Random errors may have arisen as a result of small fluctuations in gas or liquid flow into the column. However, by looking at the data these are relatively small (i.e ± 0.015 vol % of CO_2 in the gas outlet for worst case in Table 4.3).

Finally, in Table 4.5, a summary table is provided which compares the performance of the different materials tested. Relative to possible experimental errors, this level of enhancement is very small.

However, the main thrust of this work was to show how the enzyme could be immobilized on the wire mesh Dixon rings, and to explore the surface structure that was formed on the rings when different coating techniques were investigated. This was achieved.

Further work is recommended, on exploring the viability of using this enzyme in the manner described, to enhance the rate of CO_2 gas scrubbing in a column.

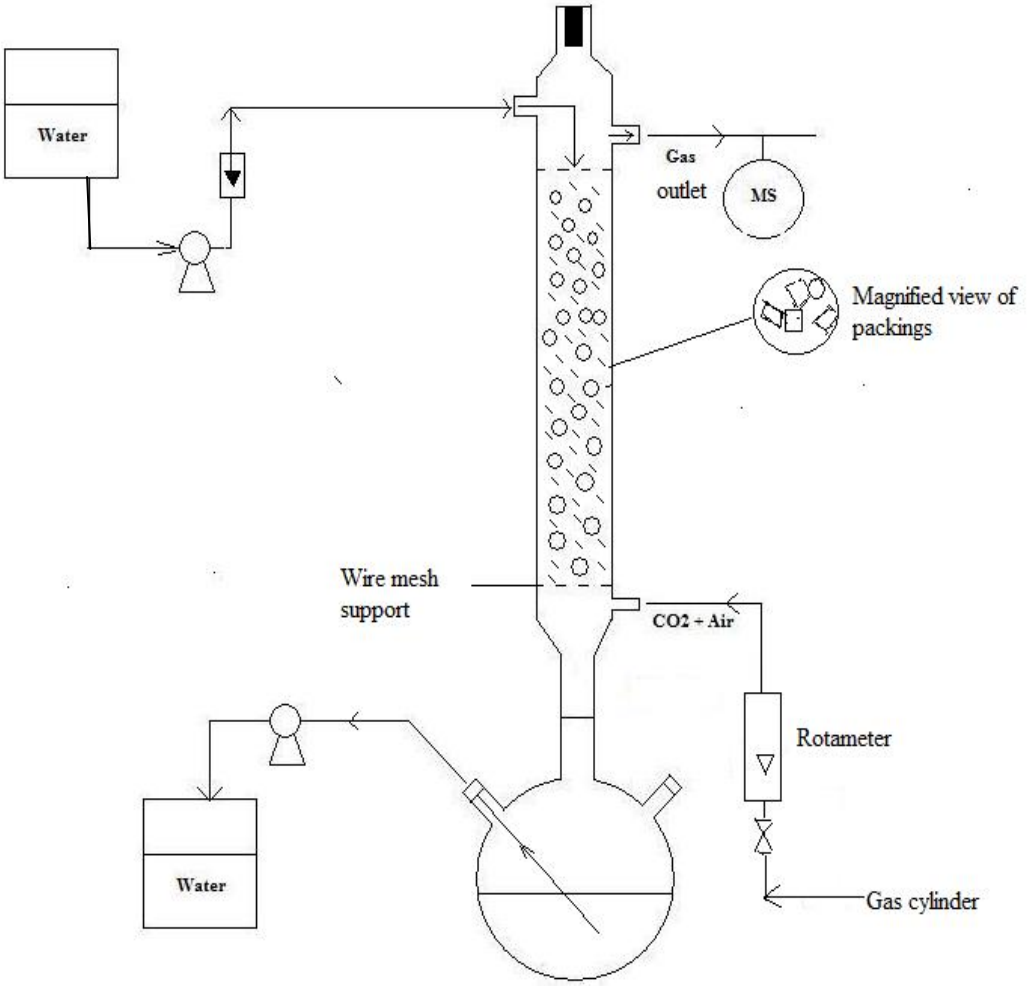

Figure 4.13 Schematic of the experimental apparatus that was constructed to test the performance of the enzyme coated rings in a mini-column.

Table 4.1 Performance of the column with uncoated rings (bare metal).

Time	N_2 vol.%	O_2 vol.%	Ar vol.%	CO_2 vol.%
1.40	74.3	21	1.07	3.63
1.45	74.2	21	1.07	3.63
1.50	74.3	21	1.07	3.63
1.55	74.2	21.1	1.07	3.63
2.01	74.2	21.1	1.07	3.63
2.47	74.2	21	1.07	3.64
2.57	74.1	21.1	1.07	3.63
3.02	74.2	21	1.07	3.64
3.13	74.2	21.1	1.07	3.63

Table 4.2 Performance of the column – rings alumina coated (but without enzyme)

Time	N_2 vol.%	O_2 vol.%	Ar vol.%	CO_2 vol.%
14.23	74.2	21.1	1.08	3.66
14.29	74.2	21.1	1.08	3.66
14.35	74.1	21.2	1.08	3.65
14.41	74.1	21.1	1.08	3.66
14.47	74.1	21.2	1.08	3.65
14.58	74.1	21.1	1.08	3.66
15.10	74.1	21.1	1.08	3.66
16.03	74.1	21.1	1.08	3.66
16.50	74.1	21.1	1.08	3.66

Table 4.3 Performance of the column – rings alumina coated with the enzyme.

Time	N_2 vol.%	O_2 vol.%	Ar vol.%	CO_2 vol.%
24.07	74.2	21.1	1.08	3.55
24.13	74.2	21.2	1.08	3.56
24.25	74.2	21.2	1.08	3.57
24.30	74.2	21.1	1.08	3.57
24.36	74.2	21.1	1.08	3.58
24.42	74.1	21.2	1.08	3.57
24.48	74.2	21.1	1.08	3.58
25.00	74.2	21.2	1.08	3.58
25.06	74.2	21.1	1.08	3.58

Table 4.4 Performance of the column – rings silica coated with the enzyme.

Time	N_2 vol.%	O_2 vol.%	Ar vol.%	CO_2 vol.%
3.13	74.4	20.9	1.08	3.55
3.30	74.4	21	1.08	3.55
3.42	74.4	21	1.08	3.55
4.11	74.3	21.1	1.08	3.55
4.29	74.3	21.1	1.08	3.54
4.35	74.3	21	1.08	3.54
5.22	74.4	21	1.08	3.55
5.40	74.3	21.1	1.08	3.54
5.45	74.3	21	1.08	3.55

Table 4.5 Summary table comparing the performance of different materials tested.

	Initial CO_2 vol.%	Column outlet CO_2 vol.%	Water flow $dm^3\ min^{-1}$	Gas flow $dm^3\ min^{-1}$	Enzyme loading on rings in column g
Bare uncoated rings	4.0	3.63	0.22	1.0	0
Alumina coated rings	4.0	3.66	0.22	1.0	0
Alumina +enzyme coated rings	4.0	3.57	0.22	1.0	0.0336
Silica + enzyme coated rings	4.0	3.55	0.22	1.0	0.0122

4.4 Concluding remarks

(a) By coating the rings with a sol-gel (made from alumina and also silica), immersing in liquid nitrogen, freeze-drying, and then calcining, it was possible to create a surface on the coated rings that was robust and had the visual appearance of a high surface area support.

(b) It was shown that a coated and calcined wire-mesh Dixon ring support (either with alumina or silica), could then be impregnated with the carbonic anhydrase enzyme. The enzyme had the appearance of white patches on the surface of the substrate.

(c) In experimental trials on the enhancement in performance of the mini-gas scrubbing column (for CO_2 removal), in the experiments on rings which were coated with the enzyme there was a very small improvement in performance observed. However, this clearly requires further work to investigate if this is real improvement, and how it could be enhanced further.

References

1. Alford, R., Burns, M., and Burns, N., 2011. Dixon rings-A revolutionary random colum packing. *Filtration,* Vol. 11(4), pp. 218-223.

2. Badjic, J. D., and Kostic, N. M., 1999. Effects of encapsulation in sol-gel silica glass on esterase activity, conformational stability, and unfolding of bovine carbonic anhydrase II. *Chemical materials,* Vol. 11, pp.3671-3679.

3. Berg, J. M., Tymoczko, J. L., and Stryer, L., 2012. *Biochemistry.* 7th ed. New York: W.H.Freeman and Company.

4. Bond, G. M., Stringer, J., Brandvold, D. K., Simsek, F. A., Medina, M. G., and Egeland, G., 2001. Development of integrated system for biomimetic CO_2 sequestration using the enzyme carbonic anhydrase. *Energy & Fuels,* Vol. 15, pp. 309-316.

5. Han, Y., Xu, D., Lu, C., Li, N., Zhou, J., 2011. Preparation of alumina coatings on metal nickel substrate using a room-temperature wet chemical pre-treatment method. *Materials chemistry and physics,* Vol. 127, pp.7-11.

6. Liu, N., Bond, G.M., Abel, A., McPherson, B. J., Stringer, J., 2005. Biomimetic sequestration of CO_2 in carbonate form: Role of produced waters and other brines. *Fuel processing technology,* Vol. 86 (14-15), pp. 1615-1625.

7. Mirjafari, P., Asghari, K., Mahinpey, N., 2007. Investigating the application of enzyme carbonic anhydrase for CO_2 sequestration purpose. *Ind. Eng. Chem. Res,* Vol. 46(3), pp. 921-928.

8. Mokoena, E. M., 2005. *Synthesis and use of silica materials as supports for the fischer-tropsch reaction.* Thesis (Ph.D.). University of Witwatersrand, Johannesburg.

9. Ozdemir, E., 2009. Biomimetic CO_2 sequestration: 1. Immobilization of carbonic anhydrase within polyurethane foam. *Energy fuels*, Vol. 23, pp. 5725-5730.

10. Sheldon, R. A., 2007. Enzyme immobilization: the quest for optimum performance. *Advanced synthetic catalyst,* Vol. 349, pp.1289-1307.

11. Smith, K. S., Jakubzick, c., and Whittam, T. S., 1999. Cabonic anhydrase is an ancient enzyme widespread in prokaryotes. *Microbiology*, Vol. 96, pp. 15184-15189.

12. Tisher, W., Kascher, V., 1999. Immobilized enzymes: crystals or carriers? *Trends in biotechnology*, Vol.17, pp.326-335.

13. Vinoba, M., Kim, D. H., Lim, K. S., Jeong, S. K., Lee, S. W., and Alagar, M., 2010. Biomimetic sequestration of CO_2 and reformation to $CaCO_3$ using bovine carbonic anhydrase immobilized on SBA-15. *Energy fuels,* Vol. 25, pp. 438-445.

14. Yan, M., Liu, Z., Lu, D., and Liu, Z., 2007. Fabrication of single carbonic anhydrase nanogel against denaturation and aggregation at high temperature. *Biomacromolecules,* Vol. 8, pp. 560-565.

15. Zhang, S., Lu, Y., Ye, X., 2013. Catalytic behaviour of carbonic anhydrase enzyme immobilized onto nonporous silica nanoparticles for enhancing CO_2 absorption into a carbonate solution. *International journal of greenhouse gas control,* Vol. 13, pp. 17-25.

16. Zhou, Z., Hartmann, M., 2012. Recent progress in biocatalysis with enzymes immobilized on mesoporous hosts. *Topics in catalysis*, Vol. 55(16-18), pp. 1081-1100.

Chapter 5 Conclusions & Recommendations

In this thesis, freeze-dried structures have been prepared, using a variety of different techniques, with a strong focus on the way in which such KK leaf structures had been made by Kolaczkowski and Kim (2006). By exploring different techniques, this helped to answer the question posed at the start of the thesis: How *were these leaf-like structures formed?*

Using a variety of different techniques, materials were prepared, and extensive studies were performed with the aid of scanning electron microscopy to see what the structures formed looked like.

5.1 Conclusions

5.1.1 KK leaf structures from alumina sol-gel

(i) It was shown that similar structures could be formed to the ones described in Kolaczkowski and Kim (2006), however, they were not identical and maybe the absence of zirconia, or the physical way in which the samples had been immersed in liquid nitrogen was different.

(j) Trials on two different ways of inserting sol-gel coated monolith into the liquid nitrogen confirmed that this affected the characteristics of structures formed.

(k) Zirconia was not necessary to form leaf-like structures.

(l) The structures formed from a commercially available alumina sol (i.e. DISPSL 14N4-25) did not form KK leaf like structures.

(m) To form leaf-like structures, the samples need to be freeze-dried.

(n) A double layer of leaf-like structures can be formed, by repeating the coating, freeze-drying and calcining steps - thereby building a 2nd layer on top of the 1st on the support.

5.1.2 Structures formed from silica sol-gel

(a) The coating of cordierite monoliths with a silica sol-gel produced some novel structures, consisting of plates, leaves and tunnels with nano-thin walls, which could have commercial applications.

5.1.3 Coating the wire-mesh Dixon rings

(a) By coating the wire-mesh Dixon rings with a sol-gel (made from alumina and also silica), immersing in liquid nitrogen, freeze-drying, and then calcining, it was possible to create a surface on the coated rings that was robust and had the physical visual appearance of a high surface area support.

(b) It was shown that a coated and calcined wire-mesh Dixon ring support (either with alumina or silica), could then be impregnated with the carbonic anhydrase enzyme. The enzyme had the appearance of white patches on the surface of the substrate.

(c) In experimental trials on the enhancement in performance of the mini-gas scrubbing column (for CO_2 removal), the performance of the rings which were coated with the enzyme, was slightly better. However, this clearly requires further work to investigate if this is real improvement, and how it could be enhanced further.

5.2 Recommendations for further work

(a) **Alumina & Silica structures:** It was shown that by starting with a sol-gel made from alumina (and also silica), then immersing it in liquid nitrogen, freeze-drying, and then calcining it, very interesting structures can be formed. It would be interesting to select such a system to act as a catalyst support for a reaction of commercial interest, and then to:

- impregnate the support with catalyst;
- characterize the catalyst (e.g. measure the surface area, pore size distribution, catalyst dispersion); and finally
- quantify its performance under reaction conditions.

(b) **Other sol-gels:** It would be worth performing further work with different mixtures that form a sol-gel and in which there is a commercial interest in the material acting as a catalyst support, or an adsorbent. This could ascertain whether the coated support when immersed in liquid nitrogen, freeze-dried, and then calcined, would provide interesting structures on the support. If they were produced, then their performance could be quantified in an application of commercial interest.

(c) **Carbonic anhydrase:** Further studies are recommended with the use of the carbonic anhydrase enzyme as a method of increasing the rate of CO_2 removal from gaseous streams. However, it should be recognized that in the gas scrubbing column application:

- The performance of this enzyme is very pH sensitive, and the requirement to control the pH of the water (scrubbing fluid) may be too restrictive in a commercial application.
- Extended experimental runs should be performed to quantify any loss of enzyme by leaching from the coated packing.
- Although the enzyme is known to increase the rate of the hydration of CO_2 to form the bicarbonate ions, this may not be the main rate limiting step in the gas scrubbing column. For example, from CO_2 absorption studies, it is well known (e.g. Danckwerts (1970)) that the transfer across the gas film is fast relative to that across the liquid film, and hence the liquid film resistance is considered to be the rate controlling step. So despite increasing the hydration of CO_2 to form the bicarbonate ions, the liquid film resistance may still be the overall rate controlling step.

To progress with the use of the enzyme as a means of increasing the rate of CO_2 removal a different type of device may be necessary, for example one that is similar to a membrane based separation device/reactor in which the enzyme would be immobilized in the walls of the membrane.

References

1. Danckwerts P.V., 1970. Gas-Liquid Reactions, McGraw-Hill Book Company, p.219.

2. Kolaczkowski, S.T., Kim, S., 2006. Novel alumina 'KK Leaf Structures' as catalyst supports. *Catalysis Today,* Vol.117, pp. 554-558.